Acta Universitatis Szegediensis

# Acta Biologica Szegediensis

Volume 61, Number 2, 2017

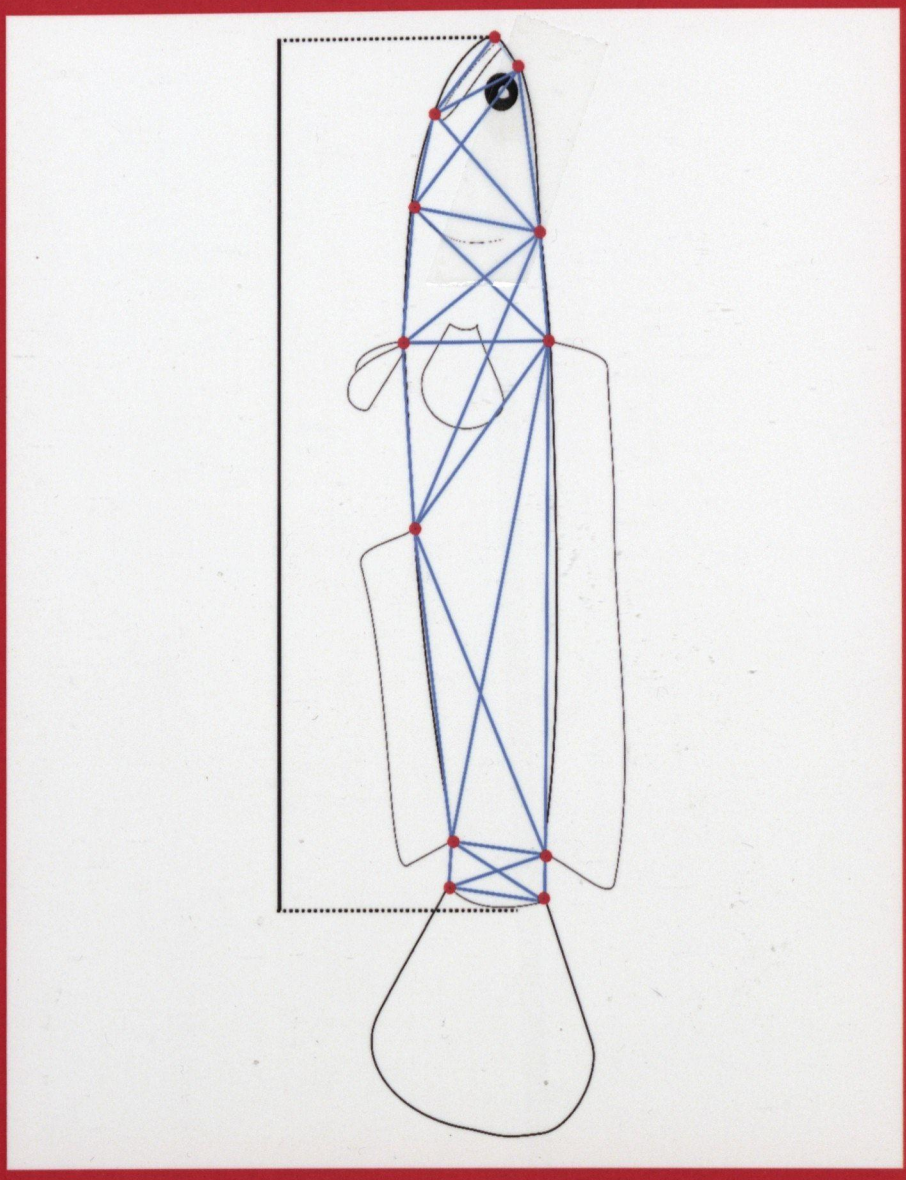

University of Szeged, Szeged, Hungary

Acta Biologica Szegediensis

*Acta Biologica Szegediensis* (ISSN 1588-385X print form; ISSN 1588-4082 online form) is an international peer-reviewed, open access journal published by the University of Szeged yearly, in two issues per volume.

*Acta Biologica Szegediensis* publishes novel findings in various fields of biology with special focus on innovative research in modern experimental life sciences. The journal publishes experimental and theoretical papers, reviews, short communications, and descriptions of new methods. Letters to the editor and conference proceedings may also be published, subject to the approval of the Editor-in-Chief.

*Acta Biologica Szegediensis* provides peer review by expert researchers, fast publication times, no page charge and free online accessibility. Table of contents and all issues of the journal are available at http://www2.sci.u-szeged.hu/ABS.
*Acta Biologica Szegediensis* is indexed in BIOSIS Database, CAB Abstracts, CABI - Review of Medical and Veterinary Mycology, EBSCO Databases, EMBASE, Excerpta Medica, Elsevier BIOBASE (Current Awareness in Biological Sciences), Enago, Google Scholar, KOBV, OCLC, Scopus, SCImago and Zoological Record.



Subscriptions

All subscriptions relate to the calendar year and must be pre-paid. The annual subscription rate is currently 100 USD and includes air mail delivery and handling.

Editor-in-Chief: Csaba Vágvölgyi
Department of Microbiology, Faculty of Science and Informatics
University of Szeged, Közép fasor 52., H-6726 Szeged, Hungary
Phone: 36 (62) 544-822, fax: 36 (62) 544-823
E-mail: csaba@bio.u-szeged.hu

Technical Editor: Tamás Mikola
Acta Biologica Szegediensis, Editorial Office
Közép fasor 52., H-6726 Szeged, Hungary
Phone: 36 (62) 544-822, fax: 36 (62) 544-823
E-mail: abs@bio.u-szeged.hu

# ACTA BIOLOGICA SZEGEDIENSIS

VOLUME 61(2), 2017


## Table of Contents

### Articles



On the cover: Truss and SL measurements on *Channa gachua* specimens. (see: Jearranaiprepame in this issue).

**Volume 61(2):119-128, 2017**
**Acta Biologica Szegediensis**
http://www2.sci.u-szeged.hu/ABS

**ARTICLE**

# Morphological differentiation among isolated populations of dwarf snakehead fish, *Channa gachua* (Hamilton, 1822) using truss network analysis

Pornpimol Jearranaiprepame*

Department of Biology, Faculty of Science, Khon Kaen University, Khon Kaen, 40002 Thailand

**ABSTRACT** Truss-network analysis was applied to examine morphological differences among distinct populations of *Channa gachua* (Hamilton 1822). Ninety-eight fish individuals were collected from three-isolated habitats in north-eastern Thailand. Twenty-six truss variables were measured and then subjected to Burnaby's size adjustment for removing size-dependent effect. The transformed data were processed for univariate and multivariate statistical analyses. The multivariate ANCOVA showed highly significant differences between populations (Pillai's trace = 1.561, $F = 10.102$, $p < 0.0001$). The univariate ANCOVA presented the significant differences between 20 out of 26 truss variables ($p < 0.05$) representing morphological characters of head, trunk and caudal peduncle areas. The variability in body shape among three populations obviously showed by the first three components of PCA accounting for 49.98% of total variances. In addition, five variables from head area and three variables from body were selected to stepwise discriminant analysis, representing the first two discriminant functions (DF1 and DF2) accounted for 72.95 and 27.95% of shape variability, respectively. A high rate of correct classification of *C. gachua* to actual sampling locations was at 93.88%. The results support the existence of local adaptation of *C. gachua* across the isolated geographical locations, and indicate the presence of three phenotypic stocks of *C. gachua* regarding their habitat locations.
**Acta Biol Szeged 61(2):119-128 (2017)**

**KEY WORDS**

body shape
*Channa gachua*
morphometrics
truss network analysis

## Introduction

Local adaptation within a species plays a fundamental role in the improvement of survival and reproductive success (Peterson et al. 2014), the generation and maintain of species diversity (Lenormand and Thomas 2012), the range of geographical distribution (Atkins and Travis 2012) as well as the ecological and evolutionary dynamics of species interaction (Bocedi et al. 2013). Local adaptation with environmentally induced phenotypic variation is commonly observed between fish populations (Lostrom et al. 2015; Bernatchez 2016; Seebacher et al. 2017). Such variation is influenced by an assortment of environmental conditions including physico-chemical parameters of water, habitat preferences and substrate types (Sajina et al. 2011; Drinan et al. 2012; Lostrom et al. 2015). In addition, biotic factors, such as food availability, competition and predation, are also contributed to morphological variability in fish (Scharnweber et al. 2013; Prado et al. 2016). The obtaining knowledge from the studies of morphological adaptation will lead to better understanding about ecology and evolution of the species (Agrawal 2001; Bijlsma and Loeschcke 2005; Lostrom et al. 2015), which potentially contributed to better management and conservation strategies of the fish (Schoenfuss et al. 2014).

Morphometric analysis is an integration of mathematical and statistical approaches to quantify the variation in morphological shape of an organism (Rohlf and Marcus 1993). Truss network system (TNS) is one of morphometric methods which relied on a series of measurements of across-body distances between two morphological landmarks, resulting in a uniform network covered entire body (Strauss and Bookstein 1982; Cadrin 2000). The TNS can overcome the inherent weakness of traditional measurement because of its high capability in capturing shape information with no restriction on the direction and localisation of variations (Cavalcanti et al 1999). The analysis is also applicable to characterise and determine a various level of groups of fish including populations, stocks and assemblages (Cheng et al 2005; Ferrito et al. 2007; McAdam et al. 2012; Mir et al. 2013; Siddik et al. 2016).

Submitted July 25, 2017; Accepted November 11, 2017
*Corresponding author. E-mail: address: porjea@kku.ac.th

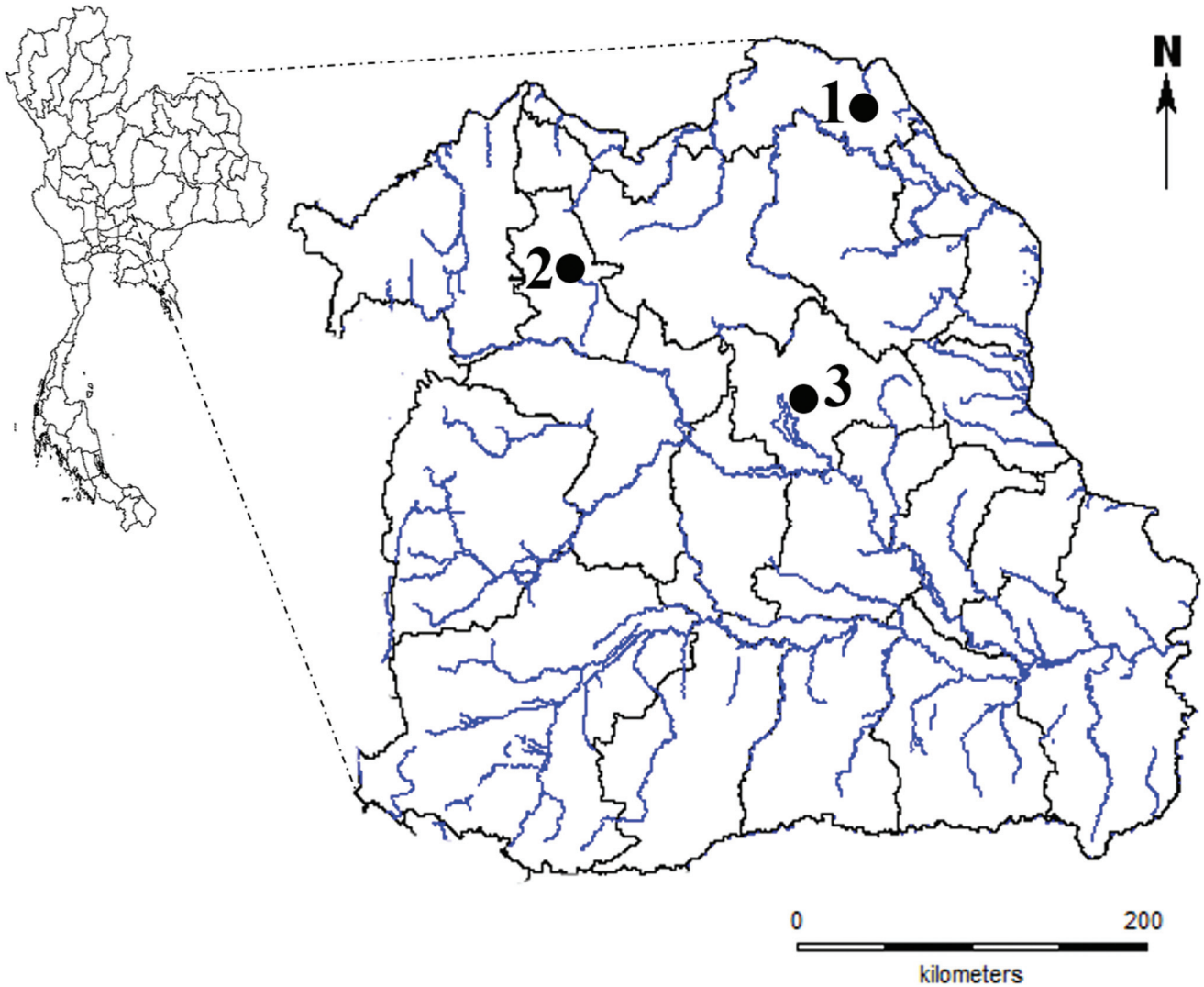


**Figure 1.** The locations of sampling sites. Populations: 1 = CG-BK; 2 = CG-NB; 3 = CG-KS.

Dwarf snakehead, *Channa gachua* (Hamilton 1822), is the smallest size and colourful fish species of family Channidae (Courternay and Williams 2003). The fish widely distributes in many parts of Asia from Afghanistan and Middle East Asia eastwards to Indonesia through South Asia (Ng and Lim 1990; Courternay and Williams, 2003). It can also occupy a broad range of habitat types so that it *Channa guchua* is sometimes considered as a species complex with the vast array of morphological variation (Ng and Lim 1990; Courternay and Williams 2003). Up to date very little information of morphological variability of *C. gachua* has been published. Hence, the present study aims to characterise the variation in morphometric characters of distinct *C. gachua* populations inhabiting in natural waters in northeast Thailand, using TNS analysis. The analysis will provide some useful information for taxonomic implication of this species.

## Materials and Methods

### *Study sites and sample collection*

A total of 98 specimens of *C. gachua* were collected from three geographical isolated populations in north-eastern Thailand (Fig. 1). Details of sample sizes, localities and habitat characteristics are showed in Table 1.

The fish samples were weighted, labelled and kept on ice to transport to laboratory in Department of Biology, Faculty of Science, Khon Kaen University. The fish were then stored at -20 °C prior to use, but did not stored for longer than 48 h. The precise species of the samples was identified based on Ng and Lim (1990) and Courtenay and Williams (2003).

**Table 1.** Details of, sample size (*N*), geographical locality, collecting date and ecological preferences of each sampling site.

| Population | *N* | Geographical coordinates | Collecting date | Environmental conditions |
|---|---|---|---|---|
| 1) CG-BK | 31 | 18° 12′ 41.7312″ N, 103° 29′ 48.4152″ E | February 2010 | A small and shallow waterway surrounded with rubber plantation and rice fields. Water level is less than 20 cm; habitat bottom contains small gravels and sand |
| 2) CG-NB | 31 | 17° 16′ 57.9432″ N 102° 28′ 00.3432″ E | February 2010 | A small and shallow waterway on the mountain surrounding Deciduous Dipterocarp Forest. Water level is less than 20 cm; habitat bottom contains rock bed and sand. |
| 3) CG-KS | 36 | 16° 47′ 11.0148″ N 103° 37′ 52.1256″ E | March 2010 | A small puddle in the rice filed which can connect to the reservoir in the raining season. Water level is around 50 cm; habitat bottom is sandy loam. |

### *Samples preparation and measurement*

Frozen fish were thawed by soaking in water and rubbed with a cotton cloth. Each specimen was then placed on polystyrene board with the right side down. The body posture and fins were pinned at distinctive landmarks to expose the outline of the fish form. Twelve landmarks determining 26 truss distances on the body and standard length (SL) were chosen and measured (Fig. 2) using digital calliper at ± 0.01 mm. All measurements were conducted on the left side of each fish.

The allometric Burnaby's size adjustment method (Burnaby 1966; Elliott et al. 1995) was primary performed using program PAST version 1.3 (Hammer et al. 2001) to remove size-dependent variation from raw data which can make misinterpretation of the body shape variations (Elliott et al. 1995; Hammer et al. 2001).

### *Statistical analyses*

The transformed data retrieved previously was subjected to test for the significance of correlations between each of 26 transformed truss variables and the SL measurement (Poulet et al. 2004). Multivariate analysis of covariance (MANCOVA) with SL adding as a covariate was performed to account for body size differences among populations. A principal component analysis (PCA) was applied to examine the patterns of morphometric variation among populations by reducing the redundancy in the morphometric variables and extracting some of independent variables for population differentiation (Samaee and Patzner 2011; Mir et al. 2013).

A stepwise discriminant analysis (SDA) was then conducted on the transformed data to investigate the integrity of the pre-defined groups. F value criterion was used for selecting the independent variables into a model. The differences were also tested with a forward manner approach using F = 3.84 for entering, and F = 2.71 for removal. The Mahalanobis distance which is based on generalised squared Euclidean distance that adjusted for unequal variances was used to estimate discriminate function. Accuracy of classification was evaluated using the jackknife cross-validation (Cheng et al. 2005).

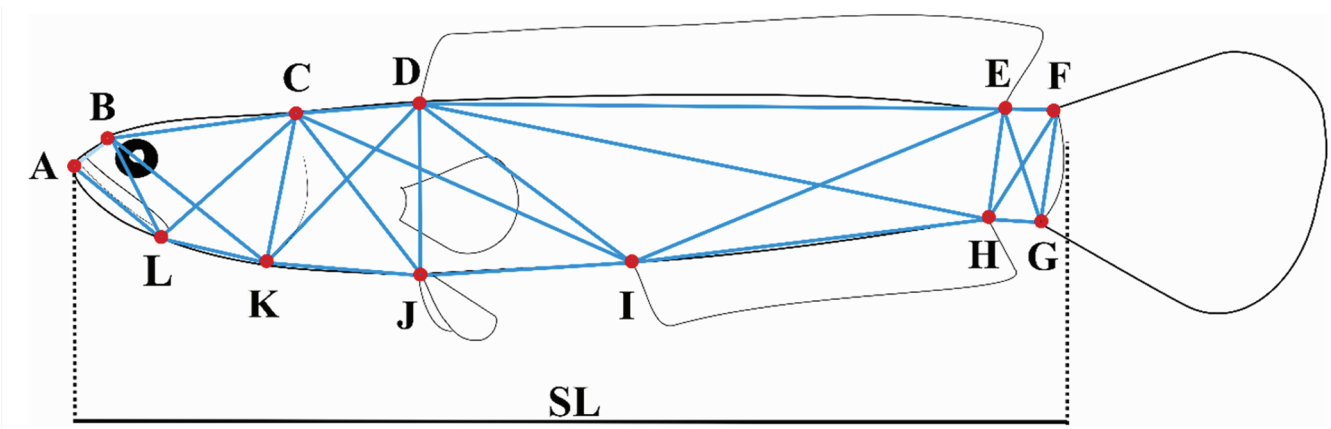


**Figure 2.** Truss and SL measurements on each *Channa gachua* specimens. A = anterior point of snout; B = posterior point of snout; C = upper-posterior point of head; D = start point of dorsal fin base; E = end point of dorsal fin base; F = upper point of caudal fin insertion; G = lower point of caudal fin insertion; H = end point of anal fin base; I = start point of anal fin base; J = point of pectoral fin insertion; K = lower posterior point of head; L = end point of mount.

**Table 2.** Descriptive statistic and univariate analyses of covariance (ANCOVA) of each truss variable among the three population of *Channa gachua.*

| Truss var. | Descriptive statistic among populations | | | | | | | | | | | | ANCOVA results | |
|---|---|---|---|---|---|---|---|---|---|---|---|---|---|---|
| | CG-BK (n = 31) | | | | CG-NB (n = 31) | | | | CG-KS (n = 36) | | | | *F* | *p* |
| | x̄ | SD | Min. | Max. | x̄ | SD | Min. | Max. | x̄ | SD | Min. | Max. | | |
| SL | 140.85 | 20.45 | 104.54 | 180.88 | 102.58 | 21.80 | 58.53 | 146.00 | 73.97 | 12.62 | 53.77 | 127.17 | 111.3835 | 0.000001* |
| AB | 12.57 | 2.87 | 7.89 | 19.45 | 10.13 | 2.18 | 6.58 | 13.91 | 6.11 | 1.07 | 4.73 | 10.48 | 15.5671 | 0.000001* |
| AL | 23.27 | 8.58 | 13.10 | 42.60 | 12.40 | 2.94 | 7.73 | 16.97 | 7.61 | 1.53 | 5.86 | 13.65 | 12.5158 | 0.000015* |
| BL | 20.26 | 6.47 | 11.60 | 35.42 | 12.47 | 3.17 | 7.52 | 18.37 | 7.62 | 1.57 | 5.47 | 14.45 | 5.1198 | 0.007752* |
| BC | 22.28 | 3.70 | 16.48 | 30.26 | 18.50 | 4.62 | 9.43 | 29.67 | 13.13 | 2.73 | 8.67 | 23.21 | 1.7252 | 0.183733 |
| KL | 15.78 | 3.60 | 9.52 | 23.07 | 15.64 | 4.35 | 8.85 | 25.40 | 11.48 | 1.83 | 8.49 | 17.75 | 23.4432 | 0.000000* |
| BK | 26.59 | 4.35 | 19.36 | 38.54 | 22.40 | 5.52 | 13.51 | 34.62 | 15.45 | 2.77 | 11.40 | 26.62 | 13.0811 | 0.000010* |
| CL | 35.33 | 5.12 | 25.82 | 46.02 | 26.49 | 5.99 | 14.83 | 40.38 | 18.41 | 3.41 | 13.48 | 32.72 | 0.1527 | 0.888571 |
| CK | 21.82 | 4.05 | 15.75 | 29.99 | 17.33 | 4.39 | 10.08 | 27.47 | 11.15 | 2.39 | 7.15 | 20.92 | 16.6315 | 0.000001* |
| CD | 16.33 | 5.40 | 9.66 | 29.97 | 10.84 | 2.83 | 6.43 | 18.44 | 7.20 | 1.68 | 4.24 | 12.90 | 1.7022 | 0.187837 |
| IJ | 28.02 | 4.74 | 20.09 | 40.62 | 20.58 | 7.37 | 10.98 | 42.03 | 15.58 | 2.59 | 11.46 | 24.83 | 19.6603 | 0.000000* |
| JK | 16.63 | 3.20 | 10.63 | 23.07 | 9.82 | 2.56 | 4.56 | 15.56 | 6.83 | 1.79 | 3.52 | 12.96 | 12.3907 | 0.000017* |
| CI | 49.35 | 9.55 | 34.76 | 69.22 | 34.47 | 9.98 | 19.16 | 64.39 | 24.56 | 4.39 | 18.47 | 42.27 | 10.6616 | 0.000067* |
| CJ | 19.25 | 3.79 | 13.33 | 28.63 | 16.28 | 4.99 | 8.99 | 27.41 | 9.81 | 2.31 | 5.49 | 18.33 | 13.3878 | 0.000008* |
| DK | 32.45 | 5.05 | 24.34 | 44.72 | 27.24 | 6.36 | 16.85 | 39.61 | 18.61 | 2.93 | 14.30 | 30.65 | 9.8434 | 0.000131* |
| DJ | 24.77 | 4.10 | 17.82 | 32.37 | 18.94 | 4.70 | 10.84 | 28.44 | 11.95 | 2.76 | 6.92 | 23.62 | 11.4722 | 0.000035* |
| DE | 82.92 | 12.41 | 58.25 | 104.23 | 57.87 | 12.10 | 31.33 | 81.80 | 44.41 | 7.41 | 32.39 | 74.03 | 48.295 | 0.000000* |
| HI | 53.23 | 8.10 | 38.68 | 69.56 | 37.16 | 7.24 | 21.49 | 50.77 | 27.12 | 4.59 | 18.90 | 44.65 | 11.6786 | 0.000030* |
| DH | 82.00 | 12.65 | 56.27 | 103.79 | 57.40 | 12.73 | 31.84 | 84.38 | 42.66 | 7.22 | 30.49 | 70.49 | 37.043 | 0.000000* |
| EI | 59.76 | 8.84 | 44.43 | 78.19 | 42.15 | 7.85 | 23.56 | 55.46 | 31.38 | 5.44 | 22.01 | 53.30 | 14.943 | 0.000002* |
| DI | 36.70 | 6.43 | 23.94 | 51.22 | 26.06 | 7.75 | 13.58 | 48.36 | 18.46 | 3.66 | 12.61 | 32.89 | 12.3275 | 0.000018* |
| EF | 106.32 | 15.48 | 79.75 | 134.86 | 81.73 | 16.96 | 44.48 | 118.20 | 58.32 | 9.80 | 40.79 | 102.38 | 0.474 | 0.623951 |
| GH | 11.08 | 1.77 | 7.84 | 15.50 | 8.80 | 1.85 | 3.97 | 12.14 | 6.03 | 1.35 | 4.21 | 11.11 | 1.7691 | 0.17612 |
| EG | 17.62 | 3.20 | 12.00 | 24.07 | 13.70 | 3.24 | 8.07 | 20.35 | 9.07 | 1.90 | 5.56 | 16.48 | 12.3991 | 0.000017* |
| FH | 19.98 | 3.53 | 13.76 | 26.62 | 14.86 | 3.23 | 8.22 | 22.80 | 10.46 | 2.16 | 6.65 | 18.38 | 1.2362 | 0.295169 |
| EH | 15.42 | 3.00 | 10.56 | 21.63 | 11.90 | 2.86 | 6.89 | 19.25 | 8.33 | 1.64 | 4.79 | 14.54 | 9.9516 | 0.000120* |
| FG | 16.56 | 3.55 | 10.80 | 23.75 | 12.32 | 3.02 | 7.01 | 19.08 | 8.61 | 1.83 | 5.28 | 15.48 | 8.1013 | 0.000568* |

## Results

Correlation analysis of transformed truss variables with SL values indicated that the effect of body size had been successfully removed from truss-network data as none of transformed truss variables showed by the significant correlation with SL ($r < 0.300$, $p > 0.005$, data not shown). The effect of sex on the truss measurement was not examined since *C. gachua* did not exhibit sexual dimorphism on morphometric character, except the difference of coloration between mature male and female (Lim and Ng 1990; Courtenay and Williams 2003; Ward-Campbell and Beamish 2005).

The MANCOVA on transformed truss variables showed highly significant difference of morphometric characters among populations (Pillai's trace = 1.561, F = 10.102, $p < 0.0001$). Univariate analyses revealed that 20 of 26 truss variables associated with morphological characters of head, body and caudal peduncle were differed among populations (Table 2).

In PCA, the first three principal components (PCs) accounted for 49.98% of total variance, which were 21.25% in PC1, 17.09% in PC2, and 11.64% in PC3 (Table 3). The strong factor loadings on the PCs were determined by the value of more than 0.5.

The PC1 composed of four negatively and five positively correlated truss variables which associated with oral cavity and maxillary length (AB, AL and BK), body depth (CI, CJ DH, and DI), and dorsal fin base length (DE). The PC2 composed of nine strongly correlated truss variables which only one variable was positively correlated with PC2. These morphological variations indicated variations in head length (BC, BK and KL), head depth (CK), body depth (DJ and DK), thoracic length (JK), and caudal peduncle depth (EG and EH). The PC3 composed of three negatively and three positively correlated truss variables which associated with predorsal length (CD), abdominal length (IJ), anal fin base length (HI), body depth (CI and EI) and caudal peduncle length (GH).

Scatter plot of each individuals of *C. gachua* on the first three PCs did not show any clear separation among populations (Fig. 3), although the CG-KS population was almost separated from other two populations with positive side of PC1. While CG-BK and CG-NB were separated with positive and negative sides of PC2, respectively.

**Table 3.** Factor loadings of each truss variable on the first three principal components.

| Truss variables | PC1 | PC2 | PC3 |
|---|---|---|---|
| AB | **-0.72280** | 0.06351 | 0.25593 |
| AL | **-0.70718** | 0.50825 | 0.00319 |
| BL | **-0.78228** | 0.40607 | -0.10798 |
| BC | 0.09367 | -0.48400 | 0.24717 |
| KL | 0.43702 | **-0.59960** | 0.03626 |
| BK | 0.23917 | **-0.76273** | 0.04583 |
| CL | **0.53108** | -0.34929 | -0.05214 |
| CK | -0.16361 | **-0.67381** | -0.09897 |
| CD | 0.07912 | 0.32240 | -0.44742 |
| IJ | 0.39834 | 0.01498 | **-0.60651** |
| JK | 0.04924 | **0.53886** | -0.12222 |
| CI | **0.58869** | 0.21011 | **-0.71922** |
| CJ | **-0.57693** | -0.29543 | 0.02372 |
| DK | 0.05240 | **-0.64423** | 0.26995 |
| DJ | -0.30376 | -0.49763 | -0.03059 |
| DE | **0.84926** | 0.32300 | 0.27466 |
| HI | 0.45305 | 0.36902 | **0.67548** |
| DH | **0.84836** | 0.29659 | 0.23209 |
| EI | **0.53117** | 0.34913 | **0.65920** |
| DI | **0.61039** | -0.05212 | -0.49167 |
| EF | -0.13573 | 0.05017 | 0.22073 |
| GH | 0.12903 | -0.04619 | **0.50294** |
| EG | -0.12802 | **-0.53017** | 0.25887 |
| FH | 0.14532 | -0.21887 | -0.02974 |
| EH | 0.08067 | **-0.48838** | -0.25552 |
| FG | 0.05352 | -0.22683 | -0.03934 |
| Variation % | 21.25 | 17.09 | 11.64 |

**Table 4.** Pooled-within groups correlation (r) and standardize coefficients (Z) of each selected truss variables along the first two discriminant functions (DF).

| Truss variables | DF1 | | DF2 | |
|---|---|---|---|---|
| | r | Z | r | Z |
| DE | -0.5166 | -0.6037 | 0.2791 | 0.2918 |
| KL | -0.3258 | -0.3007 | -0.6544 | -0.6603 |
| AL | 0.3807 | 0.4456 | 0.5324 | 0.5292 |
| AB | 0.4091 | 1.0639 | -0.0239 | -0.3785 |
| IJ | -0.2147 | -1.2137 | 0.1458 | 0.6321 |
| BC | 0.0101 | 1.2118 | -0.1469 | -0.4480 |
| CI | -0.2463 | 1.4660 | 0.1365 | -0.4801 |
| CJ | 0.1968 | 0.3733 | -0.2285 | -0.4519 |
| Eigen value | 4.6919 | | 1.7394 | |
| Wilk's lambda | 0.0641 | | 0.3650 | |
| Variation % | 72.95 | | 27.05 | |

**Table 5.** Classification results of *Channa gachua* into their original groups using stepwise discriminant analysis.

| Pre-defined groups | Predicted group memberships | | | Global accuracy |
|---|---|---|---|---|
| | CG-BK | CG-NB | CG-KS | |
| CG-BK | 29 **(93.55%)** | 2 (6.45%) | 0 (0%) | **93.88%** |
| CG-NB | 3 (9.68%) | **28 (90.32%)** | 0 (0%) | |
| CG-KS | 0 (0%) | 1 (2.78%) | **35 (97.22%)** | |

From factor loadings (Table 3) and scatter plots (Fig. 3) of PCA, the results suggested that the three populations had two different patterns of morphological variations. The CG-KS population had different variations compare with others in mouth and jaw sizes, and body length and depth. The difference between CG-BK and CG-NB populations expressed on head depth and length, body depth and caudal peduncle depth. Moreover, all of three populations had the same pattern of variations in predorsal length, abdominal length, and anal fin base length.

Stepwise discriminant analysis was performed within 26 transformed truss variables. Eight out of twenty-six truss variables were selected including the five variables from head and the three variables from body measurements. The results accounted for the first two discriminant functions (DF1 and DF2) with the percentage of shape variation at 71.57 and 28.79, respectively. The most important morphometric characters in the discrimination of each truss variables were dorsal fin base length (DE) and lower head length (KL) for the negative side of DF1, while snout length (AB) and maxillary length (AL) were highly correlated with the positive side of DF1. In contrast, the most influenced variables of the DF2 were lower head length (KL) and maxillary length (AL) for the negative and positive sides, respectively (Table 4).

For population discrimination, ninety of ninety-eight samples (93.88%) of *C. gachua* were correctly classified to actual sampling locations (Wilks' lambda = 0.06413, approx. $F_{(16,176)} = 32.4360$, $p < 0.0001$). The corrected classification rates of each population ranged from 90.32% to 97.22% (Table 5). Interestingly, the classification rates were highly corrected indicating more differences in morphological characteristics among populations.

The examination of the bivariate ordination of each score of all *C. gachua* specimens on the first two discriminant function axes (Fig. 4) revealed a clear separation of the CG-KS population from other populations on negative side of DF1. In addition, CG-BK population was separated from CG-NB populations by DF2, although there was some overlap in spatial distribution between two populations. These results indicated that CG-KS had smaller relative head size especially snout and maxillary lengths. The body shape of CG-KS was more elongated than those of other populations. Moreover, the CG-BK samples had smaller head size than CG-KS specimens, but had larger maxilla length, abdominal length, and dorsal fin base length than CG-NB samples.

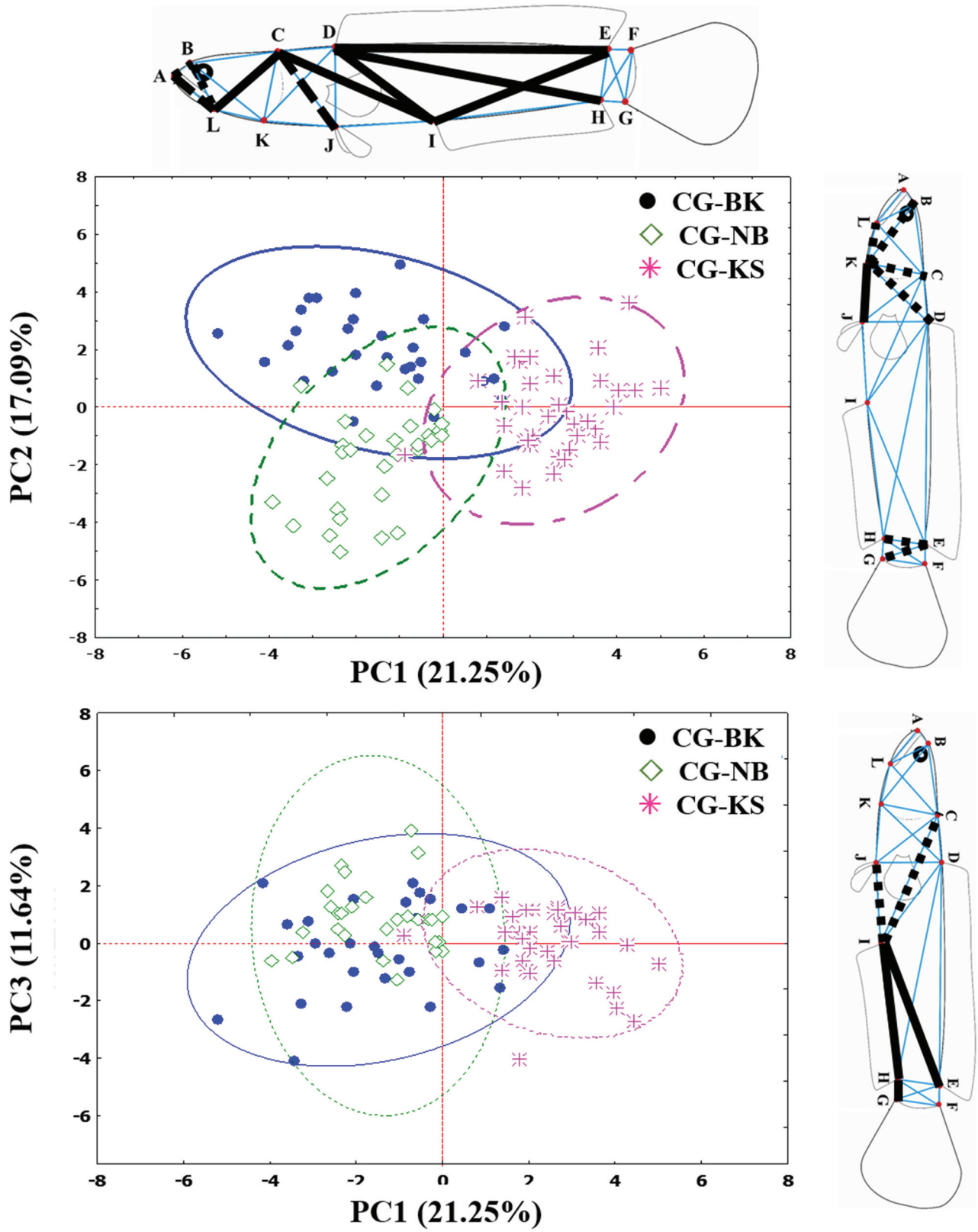


**Figure 3.** Scatter plots of each *Channa gachua* individual from three different localities against the first three principal component axes. Inserting images exhibit locations of measured variables which positively (bold line) and negatively (dash line) with each component.

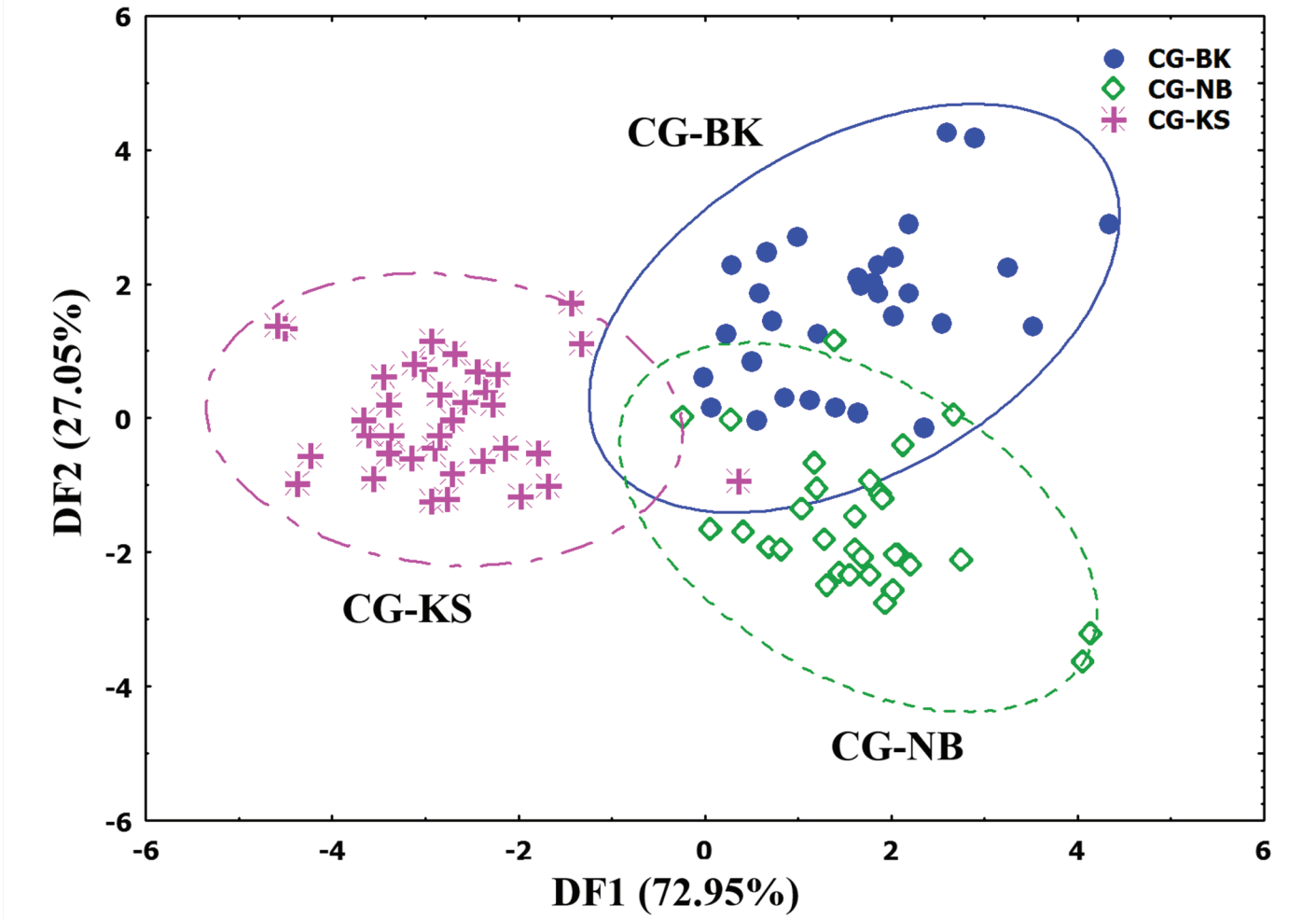


**Figure 4.** Ordination of all *Channa gachua* specimens along the first two discriminant function axes from discriminant function analysis on truss network data.

## Discussion

The non-significant correlation of transformed TNS variable with SL indicated that effect of body size was successfully removed from shape information by using Burnaby's size adjustment on raw measured data (Sajina et al. 2011). The finding suggested that morphometric analyses in the present study only contribute to variations in body shape among the populations of *C. gachua* (AnvariFar et al. 2011; Nie et al. 2013).

The significant differences obtained from multivariate analysis were evidently considered to discriminate the fish into three existence morphological groups according to their localities (Bagherian and Rahmani 2009; Akbarzadeh et al. 2009; Siddik et al. 2016). Theoretically, a high degree of morphological variations both within and between populations prone to be happened in fish more than in other vertebrates (Wimberger 1992; Lostrom et al. 2015; Bernatchez 2016). Those of variations are more liable to the induction of environment rather than the influence of genetics alone or the interaction between genetics and environmental factors (Pinheiro et al. 2005; Drinan et al. 2012). Even though the phenotypic features are built from a genetically determined-scheme during an early ontogeny which is not fixed but also will be influenced by environmental factors, as known as phenotypic plasticity (Poulet 2008).

The results retrieved from PCA obviously showed morphological variations in head and body features among different sampling locations. Such variations could be reflected from a differential habitat use, especially the exploitation of different ecological niche with diet availability (Gatz 1979; Hegrenes 2001; Gerry et al. 2013; Crichigno et al. 2014). The results from DFA also indicated the differentiation of morpho-

metric characters associating with head characters and body length. The variation in head morphology and body length could possibly be related to differences of feeding regimes and habitat conditions such as water depth, current velocity and physico-chemical parameters of the water (Langerhans et al. 2007; Sajina et al. 2011; Drinan et al. 2012; Khan et al. 2013; Lostrom et al. 2015).

The different environmental conditions that have speedy flowing and small waterways on mountain slopes (Brinsmead and Fox 2002; Langerhans et al. 2003) may result in the large head size, shallow body depth, and short dorsal fin in CG-BK and CG-NB populations. The large head size of fish in the CG-BK and CG-NB populations were also explained the involvement of a big prey feeding behaviour (Wainwright and Richard 1995; Magnhagen and Heibo 2001; Mir et al. 2013), which reasonably correlated to the abundance of large-sized preys in fast-flowing water. Additionally, the shallow body depth was recognised to be suitable forms not only for swimming in rapid flow current (Webb 1984; Boily and Magnan 2002), but also adapted for migration to new shallow water for feeding and living appearance (Peres-Neto and Magnan 2004; Seebacher et al. 2017). In contrarily, the CG-KS fish had deep body which are thought to be an adapted form designing for swimming in low-flowing water (Webb 1984; Seebacher et al. 2017).

The morphological variations among three populations of *C. gachua* in the present study could not resolve whether are the results of genetic difference, phenotypic plasticity or interaction of both mechanisms (Cadrin 2000; Khan et al. 2013). Therefore, more details of the environmental factors from each sampling locations should be included in the further analysis of ecomorphological responses (Turan et al. 2005; Xie 2012). In addition, the geographical isolation of *C. gachua* populations are very little chance for exchanges of genetic materials in between different populations. The morphological divergence of C. gachua observed in the present study could possibly be affected by genetic drift and/or differential selection (Samaee and Patzner 2011).

In conclusion, the truss network analysis used in the recent work was successful to exhibit good prospects in the analysis of intraspecific variations of this fish. The analysis also indicated that those three distinctive populations of *C. gahua* analysed here should be considered as the same species with a vast array of morphological variability. The results of the present study suggested that local adaptation responded to environmental conditions can yield morphologically distinct populations. The influence of ecological diversification, especially flow regime, was considerably be involved with the different variations of the whole fish body. To be more accurate, a combination of morphological and molecular approaches will surely bring the light to understand the variations in this fish species, and could reveal relationship between morphological variation and genetic markers.

## Acknowledgements

This work was financially supported by The Incubation Researcher Project, Khon Kaen University, Khon Kaen, Thailand.

## References

Agrawal AA (2001) Phenotypic plasticity in the interactions and evolution of species. Science 294:321-326.

Akbarzadeh A, Farahmand H, Shabani AA, Karami M, Kaboli M, Abbasi K, Rafiee GR (2009) Morphological variation of the pikeperch *Sander lucioperca* (L.) in the southern Caspian Sea, using a truss system. J Appl Ichthyol 25:576-582.

AnvariFar H, Khyabani A, Farahmand H, Vatandoust S, AnvariFar H, Jahageerdar S (2011) Detection of morphometric differentiation between isolated up- and downstream populations of Siah Mahi (*Capoeta capoeta gracilis*) (Pisces: Cyprinidae) in the Tajan River (Iran). Hydrobiologia 673(1):41-52.

Atkins KE, Travis JMJ (2010) Local adaptation and the evolution of species' ranges under climate change. J Theor Biol 266:449-457.

Bagherian A, Rahmani H (2007) Morphological differentiation between two populations of the Shemaya, *Chalcalburnus chalcoides*: a geometrical morphometric approach. Zool Middle East 40:53-62.

Bernatchez L. (2016) On the maintenance of genetic variation and adaptation to environmental change: considerations from population genomics in fishes. J Fish Biol 89:2519-2556.

Bijlsma R, Loeschcke V (2005) Environmental stress, adaptation and evolution: an overview. J Evol Biol 18:744-749.

Bocedi G, Atkins KE, Liao J, Henry RC, Travis JMJ, Hellmann JJ (2013) Effects of local adaptation and interspecific competition on species' responses to climate change. Ann N Y Acad Sci 1297:83-97.

Boily P, Magnan P (2002) Relationship between individual variation in morphological characters and swimming costs in brook charr (*Salvelinus fontinalis*) and yellow perch (*Perca flavescens*). J Exp Biol 205:1031-1036.

Brinsmead J, Fox MG (2002) Morphological variation between lake- and stream-dwelling rock bass and pumpkinseed populations. J Fish Biol 61:1619-1638.

Burnaby TP (1966) Growth-invariant discriminant functions and generalized distances. Biometrics 22:96-110.

Cadrin S (2000) Advances in morphometric identification of fishery stocks. Rev Fish Biol Fisher 10:91-112

Cavalcanti MJ, Monteiro LR, Lopes PRD (1999) Landmark-based morphometric analysis in selected species of serranid fishes (Perciformes: Teleostei). Zool Stud 38:287-294.

Cheng Q-Q, Lu D-D, Ma L (2005) Morphological differences between close populations discernible by multivariate analysis: A case study of genus *Coilia* (Teleostei: Clupeiforms). Aquat Living Resour 18:187-192.

Crichigno SA, Battini MÁ, Cussac VE (2014) Diet induces phenotypic plasticity of *Percichthys trucha* (Valenciennes, 1833) (Perciformes, Percichthyidae) in Patagonia. Zool Anz 253:192-202.

Drinan TJ, McGinnity P, Coughlan JP, Cross TF, Harrison SSC (2012) Morphological variability of Atlantic salmon *Salmo salar* and brown trout *Salmo trutta* in different river environments. Ecol Freshw Fish 21:420-432.

Elliott NG, Haskard K, Koslow JA (1995) Morphometric analysis of orange roughy (*Hoplostethus atlanticus*) off the continental slope of southern Australia. J Fish Biol 46:202-220.

Ferrito V, Mannino MC, Pappalardo AM, Tigano C (2007) Morphological variation among populations of *Aphanius fasciatus* Nardo, 1827 (Teleostei, Cyprinodontidae) from the Mediterranean. J Fish Biol 70:1-20.

Gatz, Jr AJ (1979) Ecological morphology of freshwater stream fishes. Tulane Stud Zool Bot 21:91-124.

Gerry SP, Vogelzang M, Ascher JM, Ellerby DJ (2013) Variation in the diet and feeding morphology of polyphenic *Lepomis macrochirus*. J Fish Biol 82:338-346.

Hammer Ø, Harper DAT, Ryan PD (2001) PAST: Paleontological Statistics Software Package for Education and Data Analysis. Palaeontologia Electronica 4: art. 4.

Hegrenes S (2001). Diet-induced phenotypic plasticity of feeding morphology in the orangespotted sunfish, *Lepomis humilis*. Ecol Freshw Fish 10:35-42.

Khan MA, Miyan K, Khan S (2013) Morphometric variation of snakehead fish, *Channa punctatus*, populations from three Indian rivers. J Appl Ichthyol 29:637-642.

Langerhans RB, Chapman LJ, Dewitt TJ (2007) Complex phenotype-environment associations revealed in an East African cyprinid. J Evol Biol 20:1171-1181.

Langerhans RB, Layman CA, Langerhans AK, Dewitt TJ (2003) Habitat-associated morphological divergence in two Neotropical fish species. Biol J Linn Soc 80:689-698.

Lenormand T (2012) From local adaptation to speciation: specialization and reinforcement. Int J Ecol 2012:508458. DOI: 10.1155/2012/508458.

Lostrom S, Evans JP, Grierson PF, Collin SP, Davies PM, Kelley JL (2015) Linking stream ecology with morphological variability in a native freshwater fish from semi-arid Austral Ecol Evol 5:3272-3287.

Magnhagen C, Heibo E (2001) Gape size allometry in pike reflects variation between lakes in prey availability and relative body depth. Funct Ecol 15:754-762.

McAdam BJ, Grabowski TB, Marteinsdóttir G (2012) Identification of stock components using morphological markers. J Fish Biol 81:1447-1462.

Mir JI, Sarkar UK, Dwivedi AK, Gusain OP, Jena JK (2013) Stock structure analysis of *Labeo rohita* (Hamilton, 1822) across the Ganga basin (India) using a truss network system. J Appl Ichthyol 29:1097-1103.

Nie Z-L, Wei J, Ma Z-H, Zhang L, Song W, Wang W-M, Zhang J (2014) Morphological variations of Schizothoracinae species in the Muzhati River. J Appl Ichthyol 30:359-365.

Peres-Neto PR, Magnan P (2004) The influence of swimming demand on phenotypic plasticity and morphological integration: a comparison of two polymorphic charr species. Oecologia 140:36-45.

Peterson DA, Hilborn R, Hauser L (2014) Local adaptation limits lifetime reproductive success of dispersers in a wild salmon metapopulation. Nat Commun 5:DOI: 10.1038/ncomms4696.

Pinheiro A, Teixeira CM, Rego AL, Marques JF, Cabral HN (2005) Genetic and morphological variation of *Solea lascaris* (Risso, 1810) along the Portuguese coast. Fish Res 73:67-78.

Poulet N (2008) Evidence of morphological discrete units in an endemic fish, the rostrum dace (*Leuciscus burdigalensis* Valenciennes 1844), within a small river basin. Knowl Manag Aquat Ecosyst 388:3. DOI: 10.1051/kmae:2008003.

Poulet N, Berrebi P, Crivelli AJ, Lek S, Argillier C (2004) Genetic and morphometric variations in the pikeperch (*Sander lucioperca* L.) of a fragmented delta. Arch Hydrobiol 159:531-554.

Prado AVR, Goulart E, Pagotto JPA (2016) Ecomorphology and use of food resources: inter-and intraspecific relationships of fish fauna associated with macrophyte stands. Neotrop Ichthyol 14:e150140. DOI: 10.1590/1982-0224-20150140.

Rohlf JF, Marcus LF (1993) A revolution morphometrics. Trends Ecol Evol 8:129-132.

Sajina AM, Chakraborty SK, Jaiswar AK, Pazhayamadam DG, Sudheesan D (2011) Stock structure analysis of *Megalaspis cordyla* (Linnaeus, 1758) along the Indian coast based on truss network analysis. Fish Res 108:100-105.

Samaee SM, Patzner RA (2011) Morphometric differences among populations of Tu'ini, *Capoeta damascina* (Teleostei: Cyprinidae), in the interior basins of Iran: Differences among populations of Tu'ini. J Appl Ichthyol 27:928-933.

Scharnweber K, Watanabe K, Syväranta J, Wanke T, Monaghan MT, Mehner T (2013) Effects of predation pressure and resource use on morphological divergence in omnivorous prey fish. BMC Evol Biol 13:132. DOI:

10.1186/1471-2148-13-132.

Schoenfuss HL, Blob RW (2007) The importance of functional morphology for fishery conservation and management: applications to Hawaiian amphidromous fishes. In Evenhuis NL, Fitzsimons. Eds. Bishop Mus Bull Cult 3:125-141.

Seebacher F, Webster MM, James RS, Tallis J, Ward AJW (2017) Morphological differences between habitats are associated with physiological and behavioural trade-offs in stickleback (*Gasterosteus aculeatus*). R Soc Open Sci 3:160316. DOI: 10.1098/rsos.160316.

Siddik MAB, Hanif MA, Chaklader MR, Nahar A, Fotedar R (2016) A multivariate morphometric investigation to delineate stock structure of gangetic whiting, *Sillaginopsis panijus* (Teleostei: Sillaginidae). SpringerPlus 5:520. DOI: 0.1186/s40064-016-2143-3.

Strauss R, Bookstein F (1982) The truss:body form reconstructions in morphometrics. Syst Zool 31:113-135.

Turan C, Yalcin Ş, Turan F, Okur E, Akyurt İ (2005) Morphometric comparisons of African catfish, *Clarias gariepinus*, populations in Turkey. Folia Zool 54:165-172.

Wainwright PC, Richard BA (1995) Predicting patterns of prey use from morphology of fishes. Env Biol Fish 44:97-113.

Ward-Campbell BMS, Beamish FWH (2005) Ontogenetic changes in morphology and diet in the snakehead, *Channa limbata*, a predatory fish in western Thailand. Environ Biol Fish 72:251-257.

Webb PW (1984) Form and function in fish swimming. Sci Am 251:72-82.

Wimberger PH (1992) Plasticity of fish body shape–the effects of diet, development, family and egg in two species of *Geophagus* (Pisces: Cichlidae). Biol J Linn Soc 45:197-218.

Xie JY (2012) Genetic and morphological variation of three freshwater lake populations of *Coilia ectenes* (Engraulidae). Genetika 48:1200-1206.

**Volume 61(2):129-134, 2017**
**Acta Biologica Szegediensis**
http://www2.sci.u-szeged.hu/ABS

**ARTICLE**

# Temporal dependence between hibernation and post-hibernation period according to biochemical profile of hemolymph in *Helix pomatia* Linnaeus, 1758

Damir Suljević*, Alisa Muhić, Erna Islamagić, Muhamed Fočak

Department of Biology, Faculty of Science, University of Sarajevo, 71 000 Sarajevo, Bosnia and Herzegovina

**ABSTRACT** The first data regarding protein and mineral concentration during hibernation were obtained in the species *Helix pomatia*. Total proteins, albumins, globulins, $Ca^{2+}$ and $K^{+}$ concentrations were measured at the beginning of hibernation, end of hibernation and post-hibernation period (control group). Hemolymph was collected from the pericardial cavity. Total proteins were analyzed using the Biuret method, albumins were analyzed by BCG method, while calcium and potassium concentrations were obtained by CPC method and turbidimetric method, respectively. During hibernation the total protein, globulin and calcium levels were decreased, while the concentration of potassium was evidently increased. Total protein, globulin and calcium levels had the highest values in post-hibernation period. Exceptionally high values were obtained for calcium and globulin concentrations. Significant positive correlation between protein and globulin levels was established. Protein synthesis is the energy-utilizing process during metabolic depression and in our study decreasement of protein concentration in general has been shown during hibernation period. **Acta Biol Szeged 61(2):129-134 (2017)**

**KEY WORDS**

biochemical parameters
calcium ions
hibernation
potassium ions
proteins
snail

## Introduction

In the animal world there are different strategies to survive extreme conditions, especially low temperatures. Survival is maintained at a low metabolic rate in order to reduce body temperature, mobility and other physiological functions at all levels of organization in various organisms due to different reasons (Ansart et al. 2002).

Decreased physiological activity also known as torpor is the main feature of hibernating animals which they use for surviving unfavorable seasonal climate changes and modified climate conditions. The most frequent characteristic of hibernation is lowering of body temperature as a consequence of low environmental temperature, acompained by inactivity, stagnation in growth etc. (Dugbartey et al. 2013). Hibernation is a complex phenological phenomenon during which torpor-physiological activity rhythm is synchronized with the seasonal rhythm and inner signals (Papović et al. 1985). Adjustments of the organism are manifested in both tissues and the system of organs as well as in the genes, proteins, protein complexes of the cell. Within the most important environmental stimulants for initiating hibernation and torpor, except food supply and environmental temperature is the day length which is considered a crucial outdoor signal for ectotherms, specifically snails. Photoperiod is the main cue that triggers supercooling ability in the land snail, *Helix aspersa* (Gastropoda: Helicidae) (Ansart et al. 2002).

During summer months some animals enter in the state of torpor which is called estivation. Gastropods are particularly exposed to estivation, because of the high sensibility to high temperatures (Holtz and Von Brand 1940). This process is very often present in snails because 78-92% of their body substance without the shell is consisted of water, so estivation is a favorable way to survive in conditions of low humidity (Elmslie 1998). To avoid evaporation of their body water (*i.e.* dehydration), they are active during high humidity, otherwise snails retract into the shell or synthesize calcareous epiphragm. In experimental conditions land snails can stay in estivation for many years which means that the decrease of the metabolic rate is not only connected to environmental factors like water availability or temperature regime but also depends on endogenous factors (endogenous circannual clock, antioxidant defence) (Nowakowska 2011). Because of constant possibility of dehydration snails store water or they keep free water in the mantel cavity which is used for moistening feet during the movement (Nowakowska 2011). Change of the amount of water depends on the concentration of $Na^{+}$ and amount of the fraction of proteins as the carriers

Submitted July 27, 2017; Accepted December 9, 2017
*Corresponding author. E-mail: suljevic.damir@gmail.com

of osmotic pressure (Ebanks and Grosell 2008). The increase of osmotic pressure in body liquids occurs in cases of dehydration of the snail and in the presence of water enables fast rehydration (Elmslie 1998).

*Helix pomatia* is a widely spread species so it is exposed to a wide range of ecological factors which affect its distribution. The levels of metabolites in hemolymph highly reflect the physiological condition and the way of living during the year (Nicolai et al. 2011). A significant problem during the cold period of the year for the snail is the maintenance of water levels and ionic balance in the body (Zachariassen and Kristiansen 2000). Freezing is lethal for many organisms because ice formation physically destroys subcellular architectures and results in considerable outflow of water from the cells (Nowakowska et al. 2006). This is avoided by changes in the level and distribution of substances for ice forming, increasement in concentration of low molecular melted substances like polyhydroxyl alcohols (glycerol), sugar and the production of antifreeze proteins (Ansart et al. 2002). Glycerol and sugars are synthesized from large reserves of glycogen which are saved during the summer and autumn through the diet (Ansart et al. 2002).

The aim of research was to analyze biochemical status in the hemolymph of *H. pomatia* in order to understand biochemical and physiological adjustments and surviving during the hibernation. Also, we wanted to determine whether the change in concentrations of biochemical parameters is associated with decreasement in metabolic rate during hibernation and if that significantly contributes to the metabolic depression.

## Materials and Methods

### *Collecting of specimens and experimental design*

For this research we analyzed biochemical parameters in hemolymph of 30 individuals of Roman snail (*Helix pomatia*). Analyzed individuals were collected in Batunac area near Bratunac in Bosnia and Herzegovina (coordinates: 44° 18', 19° 34'). The collecting area was about 1000 $m^2$. Snails were collected during period of hibernation and in period out of hibernation, therefore snails were categorized into following groups: beginning of hibernation (n = 10, group I), end of hibernation (n = 10, group II) and post-hibernation period (n = 10, group III, control group).

At the time of collection, Group I and Group II of snails were in the hibernation period, as it was indicated by the presence of the operculum and that they were buried in the ground. The timing of their sampling in terms of temperature regime and the length of day and night was also adequate for initiation of hibernation. The biochemical analysis of Group I snail hemolymph was conducted in November 2016 and for Group II in March 2017, immediately after awakening from hibernation. During period from November 2016 to March 2017, individuals from Group II were kept and maintained in simulated circumstances similar to outdoor environmental microclimate (in the cage buried in the ground and exposed to certain environmental factors). Group III of snails were collected during May 2017 *in situ*. This group of snails was kept in cages (5 snails in each cage) and reared under controlled conditions at temperature (22 °C) and relative humidity (around 80%) (Group III).

### *Extraction of hemolymph*

For the extraction of the hemolymph the pericardial cavity was used. Before the process, the place of extraction is desinfected by 70% ethanol. Monoscope magnifier (Voyager 10-25 x 42) was used to remove the shell of approximately 10 $mm^2$ and after that 5 mm deep stab was done by needle (0.90 x 38 mm, 20G x 1 ½") through the pericardial cavity and 0.5 ml of hemolymph was collected. For biochemical analysis, hemolypmh was used immediately after collection.

### *Biochemical analysis*

We analyzed biochemical parameters: total proteins, albumins, globulins and minerals ($Ca^{2+}$ and $K^{+}$) by spectrophotometer (Spectronic 20 Genesys, model 4001/4; Thermo Scientific, USA). Total proteins were analyzed using the Biuret method (2095 C; SGM Italy) (Lubran 1978), while albumins were analyzed by bromocresol green method (BCG; Quimica Clinica Aplicada S.A.) (Brackeen et al. 1989). Globulins are obtained by subtracting the total proteins and albumins ($c_{(globulin)} = c_{(proteins)} - c_{(albumins)}$).

The concentration of calcium was obtained by CPC method (o-cresolphtalein complexone with R2 starter, SGM Italy) (Parentoni et al. 2001), while the concentration of potassium is analyzed by the turbidimetric method (SGM Italy) (Karaman et al. 1959).

### *Statistical analysis*

Results of this research are presented as the mean value, standard deviation and range and were analysed using IBM SPSS 17.0. For intergroup differences analysis of variation (ANOVA) was used, while inner group differences were obtained by post hoc analysis. Pearson test was used for analysing the correlation between total protein concentration and concentration of albumins and globulins.

**Table 1.** Concentrations of biochemical parameters, ANOVA analysis and Post hoc test.

| | Mean + stdv | | | Range | | | ANOVA |
|---|---|---|---|---|---|---|---|
| | I | II | III | I | II | III | Sig. |
| Total proteins (g/L) | 16.90 ± 2.86 [b] | 8.97 ± 2.44 [b] | 45.94 ± 4.40 [b] | 11.94-20.81 | 5.33-12.09 | 40.47-54.33 | 0.00* |
| Albumins (g/L) | 3.21 ± 1.32 [b] | 2.59 ± 0.50 [b] | 1.28 ± 0.23 [b] | 1.49-4.50 | 1.98-3.41 | 0.83-1.49 | 0.00* |
| Globulins (g/L) | 14.79 ± 4.76 [a] | 6.38 ± 2.06[a] | 44.67 ± 4.40[b] | 7.43-26.37 | 3.35-9.13 | 39.12-52.87 | 0.00* |
| Calcium (mmol/L) | 4.27 ± 0.21 [b] | 1.82 ± 0.19 [b] | 31.22 ± 1.30 [b] | 3.90-4.65 | 1.54-2.10 | 29.85-33.25 | 0.00* |
| Potassium (mmol/L) | 2.70 ± 0.70 [b] | 9.75 ± 0.33 [b] | 4.75 ± 0.30 [b] | 1.74-3.72 | 9.21-10.20 | 4.32-5.23 | 0.00* |

*p <0.05 (ANOVA)
*a and b – post hoc test (b: the significant value among all test groups, p <0.01; a: value is not statistically significant, p >0,05)
I – beginning of hibernation; II – end of hibernation; III – post-hibernation period

## Results

In general, concentrations of the total proteins, globulins and calcium increase during hibernation in comparison to post-hibernation period (Table 1).

The concentrations of potassium were higher at the end of hibernation. In the pre-hibernation period, the highest values of the total proteins, globulins and calcium were noted, as well as the lowest value of albumins. Significant differences were identified between all three groups. The post hoc analyses show significant differences between group II and III, except in case of globulin concentration.

During hibernation period, the concentrations of total proteins, albumin, globulin and calcium were reduced, while the concentration of potassium was very high at the end of hibernation in comparison to its beginning. In the post-hibernation period, extremely high values of total proteins, globulin and calcium and low values of albumin were detected. Values of potassium concentrations were very different throughout all periods and the highest values were estimated during the awaking period, *i.e.* at the end of hibernation. The post hoc test showed significant differences between three groups regarding analysed biochemical parameters, except for globulin values during hibernation.

There was a positive correlation between total proteins and albumins/globulins (Table 2).

Significant differences were estimated for total proteins and globulin concentrations between all groups, and significant differences regarding albumin concentrations were found when we compared Group I and Group II (beginning and end of hibernation).

## Discussion

Suspended animation known as torpor is an outstanding evolutionary adaptation in animal kingdom, especially in gastropods. For example, snails (Gastropoda) close their shell aperture with a lid and inside the shell they withdraw, the resulting air cushions isolating them further against the cold. Significant changes in biochemical profile of their body fluids are also present during dormancy period. Our study showed changes in content of hemolymph during different period of time due to the exogenic factors (ambient temperature). Great changes of hemolymph content were notable in protein concentration. Accordingly, protein synthesis has been shown to be considerably reduced in types of metabolic depression that involve a physiological stress. Protein synthesis cannot be measured, but reactivation of translation on rehydration has been observed by (Wahba and Woodley 1984). Decreased concentration of total proteins, albumins and globulins were present during process of hibernation. High protein and globulin concentrations were obtained during post-hibernation period, while albumins had low values during same period. Decreased ingestion of food leads to lower amino acid amount in organism for protein synthesis. During hibernation, respiration in snails is suppresed, so hemocyanine as their respiratory pigment is present in low concentrations. According to Markl (2013), Lieb and Todt (2008) molecules of hemocyanin

**Table 2.** Pearson correlation between total proteins and albumins/globulins concentrations.

| Season | Parameters | R | Sig. |
|---|---|---|---|
| Beginning of hibernation | Albumin | 0,463 | 0,178 |
| | Globulins | 0,724 | 0.018* |
| End of hibernation | Albumin | 0,803 | 0.005** |
| | Globulins | 0,99 | 0.000** |
| Post-hibernation period | Albumin | 0,297 | 0,404 |
| | Globulins | 0,999 | 0.000** |

** Correlation is significant at the 0.01 level. Significant differences at the level p <0.01 (99% confidence interval and 1% absolute precision).
* Correlation is significant at the 0.05 level. Significant differences at the level p <0.01 (99% confidence interval and 5% absolute precision).
P values lower than 0.05 (p<0.05) were considered as significant and p-values lower than 0.01 (p<0.01) as highly significant.

are oligomers consisted of protein conglomerations which are made of functional subunits. Hemocyanine subunits are among the biggest polypeptides in nature. Hemocyanin in phylum Arthropoda is an agregate of molecules, while in molluscans hemocyanine consists of 7 to 8 different subunits connected with linker proteins (von Holde and Miller 1995). Accordingly, low protein concentration could be related with decreasement of hemocyanine concentrations during hibernation period due to low respiratory rate. Furthermore, the cupper metallothioneins (family of cysteine-rich, low molecular weight proteins) play an important role in metal homeostasis and hemocyanin synthesis in a cell type called rhogocyte in snails (Dallinger et al. 1997).

Since the shell has to be preserved during hibernation, the protein transport occurrs in the shell to maintain integrity, whereby the amount of protein in the plasma is reduced. Additionally, the decrease of water during hibernation raises the ratio of dissolved particles per volume of water so proteins and hemocyanin are decomposed (Stephenson and Lewis 2011). Since total proteins comprise albumin and globulin, the reduction of total protein concentration correlates with the reduction in albumin and globulin concentrations. Hibernation factors such as RMF, HPF, and YfiA turn off protein synthesis during hibernation process as reported by (Polikanov et al. 2012). The rate of protein synthesis reported by (Pakay et al. 2002), accounts for a significant proportion of the metabolic rate of the tissues in which it is measured. Relatively-low albumin values are the result of reduced protein synthesis during hibernation, while elevated globulins could be related with an increased need of immunoglobulins that are part of globulin protein family. High percentage of pathogens in snails food in post-hibernation period is present and this can be associated with a high concentration of immunoglobulins that play a role in the immune system. Large percentage of protein in hemolymph during post-hibernation period is the result of intense metabolic processes after hibernation. Concentrations of globulines, especially metalloprotein containing copper (hemocyanin) which weights vary from 300 to 9 000 kDa are increased due to high respiratiory rates (Lieb and Todt 2008). High protein concentration in snail meat and hemolymph are reported by Adegoke et al. (2010), Imevbore (1988), Saldanha et al. (2001). Babaloa and Akinsoyinu (2011) found high values of total proteins, low albumin values and low globulin values in *Archachati namarginata*. According to literature data (Babalola and Akinsoyinu 2011; Suljević and Mehinović 2014; Pedrini-Martha et al. 2016) albumin values are more dependent on the type of diet and rate of humidity compared to the globulin concentration. Albumins have many physiological roles in hemolymph as they participate as osmotic pressure carriers (Nowakowska 2011). Albumin also has antioxidant properties. Albumins regulate osmotic pressure, hence the degree of hydration. In this case, the shell has a protective role against dehydration, which causes a low value of albumin. On the other hand, calcium levels vary considerably based on type of diet. Calcium concentrations were increased and they were very high during the pre-hibernation period. Similar results were obtained in research Adegoke et al. (2010). Calcium is the most important element for the gastropod biology in general, including predator protection by creating a solid shell, adult survival, ovulation speed, egg and embryo development (Appleton 1978; Dawies and Erasmus 1984). It is involved in many enzymatic reactions and is required in metabolic processes associated with acid-base equilibrium (Sminia et al. 1977). Many physiological changes may affect the calcium reservoir in the shell and in the hemolymphs of molluscs (Souza et al. 2000). Due to the important role in biochemical processes, such high calcium concentrations are understandable. Low calcium concentration right after hibernation may be the result of additional need for reorganization of the shell and for metabolic needs. After period of hibernation, calcium concentration rapidly grows, as it plays many important roles in enzymatic activity, shell biomineralisation and repairing of cells (Lüss et al. 1998; Ikauniece and Jemeljanovs 2013). Soido et al. (2009) found even over 900 mg of $CaCO_3$/g in shell ash.

In the hibernation period the $Ca^{2+}$ concentration is considerably lower since the epiphragm building requires the investment of these ions (Nowakowska 2011). The presence of calcium ions is also important for phagocytic hemocyte activity (Wilbur 1984), especially due to immunologic role of globulin (Zhang et al. 2004). Potassium has important role in osmoregulation and as a cryoprotectant. Potassium concentration was increased at the beggining of hibernation as a result of its cryoprotective function during winter and decreased during hibernation period. Lower potassium concentration beyond hibernation period were obtained in an invasive aquatic snail *Pomacea canaliculata* as repored by (Cueto et al. 2011). The changes in potassium concentration may be the result of different cell membrane permeability for $Na^+$ and $K^+$ ions during and after hibernating period which is already known (Stöver 1973; Meincke, 1975). Beyond hibernation period, potassium level rises in hemolymph due to its multiple role, especially in muscle contraction and heart rate regulation.

These are the first results regarding concentration of biochemical parameters in *H. pomatia* in context of hibernation as hypometabolic defense. Protein synthesis is the energy-utilizing process during metabolic depression and in our study decreasement of protein concentration in general has been shown during hibernation period. Total protein, globulin and calcium levels were decreased, while the concentration of potassium was evidently increased after hibernation.

Biochemical responses during hibernation period in snail are consequences of adaptations to low environmental temperature which allow tolerance and avoidance of death.

Study of seasonal biochemical patterns in relation to aspects of behavioural ecology in natural snail populations should be useful for understanding functional aspects of biochemistry and behaviour. These results serve us for better understanding of hibernation processes in exotherm animals. Also, studies on the physiological responses of *H. pomatia* to varying environmental conditions should provide information for establishing a biochemical parameters base before, during and after hibernation and for further research which concerns for conservation of this species.

## References


Adegoke AA, Bukola ATC, Comfort IU, Olayinka AA, Amos KO (2010) Snails as meat source: Epidemiological and nutritional perspectives. J Microbiol Antimicrob 2(1):1-5.

Ansart A, Vernon P, Daguzan J (2002) Effects of a freezing event during hibernation on further survival, reproduction and growth in the partially freezing tolerant land snail *Helix aspersa* Müller (Gastropoda: Helicidae). Cryo Letters 23:269-274.

Appleton CC (1978) Review of literature on abiotic factors influencing the distribution and life cycles of bilharziasis intermediate host snails. Malacol Rev 11:1-25.

Babalola OO, Akinsoyinu AO (2011) Proximate, mineral and biochemical evaluation of the haemolymph of growing snails fed fresh lettuce waste, whole lettuce, pawpaw leaves and cabbage waste. Asian J Agric Sci 3(1):1-4.

Brackeen GL, Dover JS, Long CL (1989) Serum albumin. Differences in assay specificity. Nutr Clin Pract 4(6):203-205.

Cueto JA, Giraud-Billoud M, Vega IA, Castro-Vazquez A (2011) Haemolymph plasma constituents of the invasive snail *Pomacea canaliculata* (Caenogastropoda, Architaenioglossa, Ampullariidae). Molluscan Res 31:57-60.

Dallinger R, Berger B, Hunziker P, Kägi JH (1997) Metallothionein in snail Cd and Cu metabolism. Nature 388(6639):237-238.

Dawies TW, Erasmus DA (1984) An ultrastructural study of the effect of parasitism by larval *Schistosoma mansonion* the calcium reserves of host, *Biomphalaria glabata*. Cell Tissue Res 236:643-649.

Dugbartey GJ, Henning RH (2013) PP282-The role of cbs and H2S in the induction of torpor and organ preservation during hibernation. Clin Ther 35(8):106-107.

Ebanks SC, Grosell M (2008) Fluid and osmolyte recovery in the common pond snail *Lymnaea stagnalis* following full-body withdrawal. J Exp Biol 211:327-336.

Elmslie LJ (1998) Humic acid: a growth factor for *Helix aspersa* Müller (Gastropoda: Pulmonata). J Mollus Stud 64:400-401.

Holtz F, von Brand T (1940) Quantitative studies upon some blood constituents of *Helix pomatia*. Bio Stor 79:423-431.

Ikauniece D, Jemeljanovs A (2013) Calcium and phosphorus content in Roman snail (*Helix pomatia*) meat and shell. Annual 19th International Scientific Conference Proceedings, "Research for Rural Development" 1:173-175.

Imevbore A (1988) The nutritive value of African giant land snail *Archachatina marginata*. J Anim Pro Reserv 8(2):76-87.

Karrman KJ, Bladh E, Gedda P (1959) Turbidimetric ultramicro titration of potassium. Microchim Acta 47(5):779-785.

Lieb B, Todt C (2008) Hemocyanin in mollusks-A molecular survey and new data on hemocyanin genes in Solenogastres and Caudofoveata. Mol Phylogenet Evol 49:382-385.

Lubran MM (1978) The measurement of total serum proteins by the Biuret method. Ann Clin Lab Sci 8(2):106-110.

Lüss H, Bokník P, Heusch G, Müller FU, Neumann J, Schmitz W, Schulz R (1998) Expression of calcium regulatory proteins in short-term hibernation and stunning in the in situ porcine heart. Cardiovasc Res 37(3):606-617.

Marin F, Luquet G, Marie B, Medakovic D (2008) Molluscan shell proteins: primary structure, origin, and evolution. Curr Top Dev Biol 80:209-276.

Markl J (2013) Evolution of molluscan hemocyanin structures. BBA-Proteins Proteom 1843(9):1840-1852.

Meincke KF (1975) The chemical ingredients of hemolymph and some selected organs of *Helix pomatia* in constant ambient conditions in the course of the year. Comp Physiol 52(1):135-140.

Nicolai A, Filser J, Lenz R, Bertrand C, Charrier M (2011) Adjustment of metabolite composition in the haemolymph to seasonal variations in the land snail *Helix pomatia*. J Comp Physiol 181:457-466.

Nowakowska A, Caputa M, Rogalska J (2006) Seasonal changes in cryoprotectants concentrations in *Helix pomatia* snails. J Physiol Pharmacol 57(8):93-105.

Nowakowska A (2011) Hypometabolism in land snails: Controlled or passive phenomenon? In Nowakowska A, Caputa M, Eds., Hypometabolism: Strategies of Survival in Vertebrates and Invertebrates. Research Singpost India, pp. 1-17.

Pakay JL, Withers PC, Hobbs AA, Guppy M (2002) In vivo downregulation of protein synthesis in the snail *Helix apersa* during estivation. Am J Physiol 283(1):197-204.

Parentoni LS, Pozzeti RCS, Figueiredo JF, de Faria EC (2001) The determination of total calcium in urine: a comparison between the atomic absorption and the orthocresolphtalein complexone methods. J Bras Patol Med Lab 37(4):235-238.

Popović R, Šapkerev J (1985) Animalna Ekologija. Naučna knjiga, Beograd, Serbia.

Pedrini-Martha V, Niederwanger M, Kopp R, Schnegg R, Dallinger R (2016) Physiological, diurnal and stress-related variability of cadmium-metallothionein gene expression in land snail. PLoS ONE 11(3):e0150442. Doi:10.1371/journal.pone.0150442

Polikanov YS, Blaha GM, Steitz TA (2012) How hibernation factors RMF, HPF, and YfiA turn off protein synthesis. Science 336(6083):915-918.

Roots C (2006) Hibernation. Greenwood Press, London.

Saldanha T, Gaspar A, Santana DN (2001) Composition of meat from the snail (*Achatina fulica*) produced in Iguape, SP. Higiene-Alimentar 15(85):69-74.

Sminia T, de With ND, Bos JL, van Nieuwmegen ME, Witter MP, Wondergem J (1977) Structure and function of the calcium celss of freshwater pulmonate snail *Lymnaea stagnalis.* Neth J Zool 27:195-208.

Soído C, Vasconcellos MC, Diniz AG, Pinheiro J (2009) An improvement of calcium determination technique in the shell of Molluscs. Braz Arch Biol Technol 52(1):93-98.

Souza RM, Gomes EM, Chagas GM, Pinheiro J (2000) The influence of starvation and eurytrema coelomaticum infection on the nitrogenous products of degradation in the hemolymph of *Bradybaena similaris*. Braz Arch Biol Technol 43:365-371.

Stephenson R, Lewis V (2011) Behavioural evidence for a sleep-like quiescent state in a pulmonate mollusc, *Lymnaea stagnalis* (Linnaeus). J Exp Biol 214:747-756.

Stöver H (1973) Cold resistance and freezing in *Arianta arbustorum* L. (Pulmonata). In Wieser W, Ed., Effects of Temperature on Ectothermic Organisms. Springer Verlag, Berlin, Heidelberg.

Suljević D, Mehinović L (2014) Fiziologija homeostaze. Prirodno-matematički fakultet Univerziteta u Sarajevu, Sarajevo.

van Holde KE, Miller KI (1995) Hemocyanins. Adv Protein Chem 47:1-81.

Wahba AJ, Woodley CL (1984) Molecular aspects of development in the brine shrimp *Artemia*. Prog Nucleic Acid Res Mol Biol 31:221-265.

Wilbur KM (1984) The Mollusca. Academic Press, New York.

Zachariassen KE, Kristiansen E (2000) Ice nucleation and antinucleation in nature. Cryobiology 41(4):257-279.

Zhang SM, Adema CM, Kepler TB, Loker ES (2004) Diversification of Ig superfamily genes in an invertebrate. Science 305:251-254.

Volume 61(2):135-140, 2017
Acta Biologica Szegediensis
http://www2.sci.u-szeged.hu/ABS

ARTICLE

# Optimization of mosquitocidal toxins production by *Bacillus thuringiensis* under solid state fermentation using Taguchi orthogonal array

Magda A. El-Bendary[1]*, Mostafa M. Abo Elsoud[2,3], Shimaa R. Hamed[2], Sahar S. Mohamed[2]

[1]Microbial Chemistry Department, National Research Centre, Dokki, Giza, Egypt
[2]Microbial Biotechnology Department, National Research Centre, Dokki, Giza, Egypt
[3]Biotechnology and Genetic Engineering Pilot Plant Unit, National Research Centre, Dokki, Giza, Egypt

**ABSTRACT** Optimization of the culture medium conditions for *Bacillus thuringiensis* var. *israelensis* mosquitocidal toxins production under solid state fermentation using Taguchi experimental design of surface response methodology was studied. The obtained results revealed that the optimum culture medium conditions for the maximum mosquitocidal activity against second instar *Culex pipiens* larvae were 6% substrate concentration, 40% initial moisture content, 2% inoculum size and initial pH 6.5 for 7 days incubation period. The obtained sporulation titer and larval mortality % were 2.2 × $10^{10}$ CFU/g final product and 90%, respectively. $LC_{50}$ of this product was 3.2 ppm.
**Acta Biol Szeged 61(2):135-140 (2017)**

**KEY WORDS**
*Bacillus thuringiensis*
*Culex pipiens*
mosquitocidal toxins, solid state fermentation
surface response methodology

## Introduction

*Bacillus thuringiensis* var. *israelensis* (Bti) has been used in mosquito vector control programs since two decades. Bti forms crystal protein endotoxin during sporulation and it is pathogenic upon ingestion by mosquito larvae (Poopathi and Archana 2012).

Mosquitocidal toxins production by Bti has been reported under both submerged and solid state fermentation (SSF). Advantages of SSF are: (1) low production cost, (2) saving water and energy, (3) low capital investments, (4) low waste effluent, (5) stability of the product, (6) concentrated products, and (7) some microorganisms can form endospores only by growing on a solid substrate (Holker and Lenz 2005).

The conventional growth optimization method namely, one factor at a time, is time-consuming, requires high experimental data sets and is unable to study the interactions between factors. Alternatively, statistical experimental design allows multiple control variables, is faster and cost-effective as compared to traditional univariate approach. It is a collection of mathematical and statistical analysis useful for determining the factors that influence the response or to define their optimum levels (Sunitha et al. 1999). Statistical experimental design has efficiently been applied for optimization of cultural conditions to produce microbial metabolites in many fermentation processes (Li et al. 2002). There are few reports about optimization of toxin production by Bti using statistical experimental design in submerged fermentation (Moreira et al. 2007; Ben Khedher et al. 2011, 2013; Hoa et al. 2014).

This study aimed to optimize the culturing conditions for commercial production of mosquitocidal toxins of Bti under solid state fermentation using Taguchi experimental design of surface response methodology. Substrate concentration, moisture content (%), initial pH, inoculum size and incubation period were evaluated for maximum mosquitocidal activity against second instar larvae of *Culex pipiens*.

Submitted June 5, 2017; Accepted September 18, 2017
*Corresponding author. E-mail: tasnim41@yahoo.com

## Materials and Methods

### *Microorganism and inoculum preparation*

Bti was obtained from Prof. Dr. Fergus G. Priest (Heriot-Watt University, UK). Inoculum was prepared by inoculating nutrient broth medium (5 g/l peptone and 3 g/l beef extract) with the bacterial culture and incubated for 24 h at 30 °C under shaking at 150 rpm.

### *SSF conditions and substrates used*

Previous results of our group have shown that a mixture of

**Table 1.** Taguchi orthogonal array design based on five factors/ five levels.

| Run | By-product concentration (%) | Moisture content (%) | pH | Inoculum size (%) | Incubation period (days) |
|---|---|---|---|---|---|
| 1 | 15 | 40 | 8 | 4 | 5 |
| 2 | 12 | 20 | 8.5 | 4 | 3 |
| 3 | 9 | 20 | 8 | 1 | 7 |
| 4 | 3 | 40 | 8.5 | 10 | 11 |
| 5 | 15 | 25 | 7 | 1 | 11 |
| 6 | 9 | 10 | 7.5 | 10 | 5 |
| 7 | 3 | 30 | 8 | 8 | 9 |
| 8 | 12 | 25 | 6.5 | 8 | 5 |
| 9 | 12 | 40 | 7.5 | 1 | 9 |
| 10 | 12 | 10 | 8 | 2 | 11 |
| 11 | 15 | 10 | 8.5 | 8 | 7 |
| 12 | 6 | 40 | 6.5 | 2 | 7 |
| 13 | 15 | 20 | 6.5 | 10 | 9 |
| 14 | 9 | 30 | 6.5 | 4 | 11 |
| 15 | 9 | 40 | 7 | 8 | 3 |
| 16 | 3 | 25 | 7.5 | 4 | 7 |
| 17 | 9 | 25 | 8.5 | 2 | 9 |
| 18 | 6 | 20 | 7.5 | 8 | 11 |
| 19 | 3 | 20 | 7 | 2 | 5 |
| 20 | 6 | 10 | 7 | 4 | 9 |
| 21 | 6 | 25 | 8 | 10 | 3 |
| 22 | 15 | 30 | 7.5 | 2 | 3 |
| 23 | 3 | 10 | 6.5 | 1 | 3 |
| 24 | 6 | 30 | 8.5 | 1 | 5 |
| 25 | 12 | 30 | 7 | 10 | 7 |

**Table 2.** Summary of Taguchi orthogonal array design.

| Factor code | Name | Units | Factor level | |
|---|---|---|---|---|
| | | | Low | High |
| A | By-product | % | 3 | 15 |
| B | Moisture content | % | 10 | 40 |
| C | Initial pH | - | 6.5 | 8.5 |
| D | Inoculum size | % | 1 | 10 |
| E | Incubation period | days | 3 | 11 |

**Table 3.** Taguchi's actual and predicted results of sporulation and larval mortality (%).

| Run | Sporulation (CFU x $10^8$/g) | | | Mortality (%) at 10 ppm | | |
|---|---|---|---|---|---|---|
| | Mean actual value | Mean predicted value | Residual | Mean actual value | Mean predicted value | Residual |
| 1 | 151.33 | 167.68 | -16.35 | 0.00 | -9.86 | 9.86 |
| 2 | 110.33 | 181.11 | -70.78 | 50.00 | 54.32 | -4.32 |
| 3 | 213.33 | 216.80 | -3.47 | 60.00 | 63.16 | -3.16 |
| 4 | 220.67 | 212.27 | 8.40 | 0.00 | 13.87 | -13.87 |
| 5 | 225.33 | 233.29 | -7.95 | 13.33 | 7.57 | 5.77 |
| 6 | 198.00 | 189.72 | 8.28 | 60.00 | 56.55 | 3.45 |
| 7 | 224.33 | 243.81 | -19.48 | 86.67 | 49.72 | 36.94 |
| 8 | 192.67 | 217.17 | -24.51 | 76.67 | 67.69 | 8.97 |
| 9 | 206.33 | 195.52 | 10.81 | 0.00 | 7.87 | -7.87 |
| 10 | 188.33 | 188.58 | -0.25 | 0.00 | -3.76 | 3.76 |
| 11 | 193.33 | 196.06 | -2.73 | 90.00 | 82.15 | 7.85 |
| 12 | 215.33 | 218.18 | -2.85 | 90.00 | 92.39 | -2.39 |
| 13 | 236.00 | 231.84 | 4.16 | 0.00 | 10.64 | -10.64 |
| 14 | 193.33 | 189.69 | 3.64 | 50.00 | 42.34 | 7.66 |
| 15 | 225.67 | 213.99 | 11.68 | 86.67 | 87.61 | -0.95 |
| 16 | 223.33 | 232.65 | -9.31 | 76.67 | 64.03 | 12.64 |
| 17 | 203.00 | 195.38 | 7.62 | 0.00 | 15.65 | -15.65 |
| 18 | 238.67 | 241.71 | -3.05 | 0.00 | 12.25 | -12.25 |
| 19 | 230.67 | 223.88 | 6.79 | 36.67 | 71.81 | -35.14 |
| 20 | 229.67 | 218.63 | 11.04 | 0.00 | 4.19 | -4.19 |
| 21 | 234.33 | 232.38 | 1.96 | 86.67 | 100.93 | -14.26 |
| 22 | 238.67 | 225.61 | 13.05 | 60.00 | 65.42 | -5.42 |
| 23 | 221.33 | 181.11 | 40.22 | 76.67 | 54.32 | 22.35 |
| 24 | 213.67 | 213.89 | -0.22 | 56.67 | 40.60 | 16.06 |
| 25 | 244.00 | 235.46 | 8.54 | 80.00 | 76.54 | 3.46 |

sugar beet pulp and sesame meal at 1:1 ratio was promising ingredients for Bti toxin production under SSF (El-Bendary et al. 2016a). Fifty grams fine sand (carrier material) and substrates (sugar beet pulp and sesame meal) were taken in 250 ml Erlenmeyer flasks, moistened with tap water (11 ml) and autoclaved. These flasks were inoculated with the tested culture and incubated at 30 °C under static conditions. Each fermentation test was in triplicate.

### *Experimental design*

Taguchi orthogonal array based on five levels for five factors were used for maximum spore and toxins production by Bti under SSF (Tables 1, 2). These factors were substrate concentrations (A), moisture content (B), initial pH (C), inoculum size (D), and incubation period (E). Experimental design was performed using Design-Expert Software Version 7.0.0 (Stat-Ease, Minneapolis, MN, USA). Analysis of variance (ANOVA) was used to estimate the statistical parameters for optimization of culture conditions. All the experiments were done in triplicates.

Two response variables were measured: sporulation of the culture and toxicity against *C. pipiens* larvae. The quality of obtaining model was measured using the correlation coefficient of determination ($R^2$), the significance of each parameter through an F-test (calculated P-value) and the model lack of fit. Coefficients with a P-value<0.05 were considered significant.

### *Spore count*

Endospores were counted by the plate count method. One gram of SSF product was suspended in 100 ml of sterile distilled water and shaken for one hour. Tenfold serial dilu-

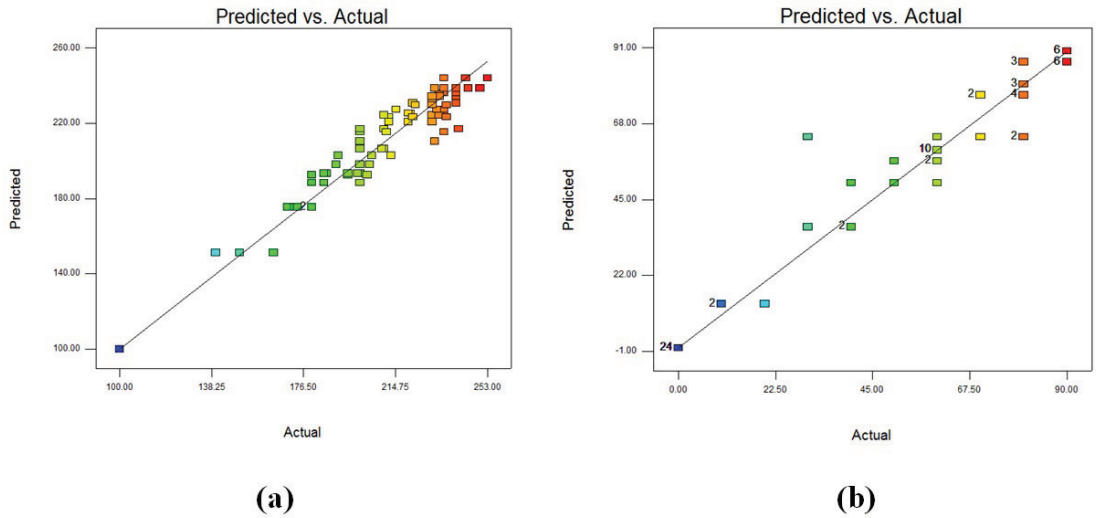


**Figure 1.** Actual versus predicted sporulation (a) and larval mortality % (b) results based on Taguchi's design.

tions of each sample were prepared and heated at 80 °C for 12 min. Dilutions were spread onto nutrient agar plates (three replicates per dilution) and incubated at 30 °C for 48 h.

### *Bioassay*

Bioassay of mosquitocidal activity of fermented culture produced under SSF was adopted from Ampofo (1995) with some modifications. Toxicity was determined using second instar larvae of *C. pipiens*. One gram of fermented culture was mixed with tap water (100 ml) and shaken for one hour. Serial dilutions were prepared and placed into 100 ml beakers in triplicates along with 10 larvae of *C. pipiens* and kept at 26 ± 2 ºC with 10 h light/14 h dark cycle. The mortality percentage was calculated after 48 h.

## Results

In previous study of our group, sugar beet pulp and sesame meal (1:1) at 6% concentration, pH 7-8, moisture content 20-30%, inoculums size 4-10% and 7 days incubation were the best conditions for toxin production by Bti under SSF using the conventional one-factor-at-a-time method (El-Bendary et al. 2016a).

According to Taguchi's design, good correlations among the actual and predicted results (Table 3) can be noticed for both sporulation and mosquitocidal activity due to low residuals. The relations among actual and predicted results were graphed in Figure 1 a, b. The analysis of variance (ANOVA) of the sporulation results (Table 4) obtained from Taguchi's design revealed that the model with F-value of 20.17 is significant and the model terms: E, AB, AC, BC, CD, ABD, ACE, BCD and BCE are significant as well. The F-value of 0.000554 implies that the model lack of fit is not significant relative to the pure error. Regression analysis of the model indicated that correlation coefficient ($R^2$) is 0.900942 and the adjusted $R^2$ of 0.856269 is in reasonable agreement with the predicted $R^2$ of 0.785149. The model coefficient of variation (C.V.) of (4.97) indicated a greater reliability of the experiments performed. The model adequate precision of 24.294, in addition to the previously mentioned parameters, indicates that the model can be used to navigate the design space (Fig. 2).

### *Final equation for sporulation process based on Taguchi's model*

***Sporulation*** (CFU x $10^8$/g) = -9096.649386 + 289.2259698 * A + 202.3358255 * B + 1532.900751 * C - 1312.765921 * D + 1334.384945 * E + 8.071716958 * A * B - 69.37795286 * A * C + 45.43127539 * A * D - 30.55467821 * A * E - 37.4764861 * B * C + 22.17990073 * B * D - 29.85177773 * B * E + 172.4304541 * C * D - 211.3568499 * C * E + 9.754873376 * D * E + 0.32065505 * A * B * D -1.012333282 * A * B * E - 6.120312005 * A * C * D + 7.592903649 * A * C * E - 0.485031566 * A * D * E -3.313657279 * B * C * D + 5.331671129 * B * C * E - 0.198329236 * B * D * E

Where, A: by-product concentration (%), B: initial moisture content (%), C: initial pH, D: inoculum size (%) and E: incubation period (days).

The analysis of variance (ANOVA) of mortality percentage model (Table 5) revealed that its F-value of 79.66 implies the model is significant and the model terms: B, C, D, E, AB, AC, AD, AE, BC, BD, BE, CD, CE, DE, ABC, ABD, ABE,

**Table 4.** ANOVA of sporulation results based on Taguchi's design.

| Source | Sum of squares | Df | Mean square | F-value | P-value Prob>F* |
|---|---|---|---|---|---|
| Model | 50944.28 | 23 | 2214.969 | 20.16749 | <0.0001 |
| A: By-product | 82.83164 | 1 | 82.83164 | 0.75419 | 0.3892 |
| B: Moisture content | 430.4247 | 1 | 430.4247 | 3.919056 | 0.0532 |
| C: Initial pH | 440.5467 | 1 | 440.5467 | 4.011218 | 0.0505 |
| D: Inoculum size | 370.9611 | 1 | 370.9611 | 3.377634 | 0.0719 |
| E: Incubation period | 1289.989 | 1 | 1289.989 | 11.74547 | 0.0012 |
| AB | 785.0195 | 1 | 785.0195 | 7.147674 | 0.0101 |
| AC | 680.381 | 1 | 680.381 | 6.194931 | 0.0161 |
| AD | 414.5053 | 1 | 414.5053 | 3.774108 | 0.0576 |
| AE | 46.11053 | 1 | 46.11053 | 0.419841 | 0.5199 |
| BC | 635.311 | 1 | 635.311 | 5.784564 | 0.0198 |
| BD | 324.4477 | 1 | 324.4477 | 2.954125 | 0.0917 |
| BE | 16.81807 | 1 | 16.81807 | 0.15313 | 0.6972 |
| CD | 824.1224 | 1 | 824.1224 | 7.503709 | 0.0085 |
| CE | 90.50257 | 1 | 90.50257 | 0.824034 | 0.3683 |
| DE | 8.305885 | 1 | 8.305885 | 0.075626 | 0.7844 |
| ABD | 501.5207 | 1 | 501.5207 | 4.566391 | 0.0374 |
| ABE | 425.6583 | 1 | 425.6583 | 3.875657 | 0.0544 |
| ACD | 276.8605 | 1 | 276.8605 | 2.52084 | 0.1185 |
| ACE | 591.507 | 1 | 591.507 | 5.385725 | 0.0243 |
| ADE | 79.13797 | 1 | 79.13797 | 0.720558 | 0.3999 |
| BCD | 495.5149 | 1 | 495.5149 | 4.511709 | 0.0385 |
| BCE | 641.5471 | 1 | 641.5471 | 5.841345 | 0.0193 |
| BDE | 160.5758 | 1 | 160.5758 | 1.462058 | 0.2322 |
| Residual | 5601.262 | 51 | 109.8287 | | |
| Lack of fit | 0.062038 | 1 | 0.062038 | 0.000554 | 0.9813 |
| Pure error | 5601.2 | 50 | 112.024 | | |
| Cor total | 56545.55 | 74 | | | |

*Value of "Prob>F" less than 0.05 indicates model term is significant.

**Table 5.** ANOVA of larval mortality (%) results based on Taguchi's design.

| Source | Sum of squares | Df | Mean square | F-value | P-value Prob>F* |
|---|---|---|---|---|---|
| Model | 93805.33 | 24 | 3908.556 | 79.65806 | <0.0001 |
| A: By-product | 28.62968 | 1 | 28.62968 | 0.583485 | 0.4485 |
| B: Moisture content | 1009.783 | 1 | 1009.783 | 20.57981 | <0.0001 |
| C: Initial pH | 2014.93 | 1 | 2014.93 | 41.06515 | <0.0001 |
| D: Inoculum size | 1060.997 | 1 | 1060.997 | 21.62358 | <0.0001 |
| E: Incubation period | 462.4049 | 1 | 462.4049 | 9.424013 | 0.0035 |
| AB | 2320.415 | 1 | 2320.415 | 47.29106 | <0.0001 |
| AC | 2649.103 | 1 | 2649.103 | 53.98987 | <0.0001 |
| AD | 3070.268 | 1 | 3070.268 | 62.57339 | <0.0001 |
| AE | 2861.235 | 1 | 2861.235 | 58.31322 | <0.0001 |
| BC | 2227.916 | 1 | 2227.916 | 45.40589 | <0.0001 |
| BD | 1173.85 | 1 | 1173.85 | 23.92358 | <0.0001 |
| BE | 3337.242 | 1 | 3337.242 | 68.01444 | <0.0001 |
| CD | 2423.493 | 1 | 2423.493 | 49.39183 | <0.0001 |
| CE | 702.1798 | 1 | 702.1798 | 14.31073 | 0.0004 |
| DE | 3290.32 | 1 | 3290.32 | 67.05815 | <0.0001 |
| ABC | 2653.042 | 1 | 2653.042 | 54.07014 | <0.0001 |
| ABD | 398.7633 | 1 | 398.7633 | 8.12697 | 0.0063 |
| ABE | 419.122 | 1 | 419.122 | 8.541889 | 0.0052 |
| ACD | 636.0368 | 1 | 636.0368 | 12.96271 | 0.0007 |
| ACE | 145.887 | 1 | 145.887 | 2.97324 | 0.0908 |
| ADE | 1081.454 | 1 | 1081.454 | 22.04049 | <0.0001 |
| BCD | 36.99493 | 1 | 36.99493 | 0.753973 | 0.3894 |
| BCE | 35.85313 | 1 | 35.85313 | 0.730702 | 0.3967 |
| BDE | 628.9335 | 1 | 628.9335 | 12.81794 | 0.0008 |
| Pure error | 2453.333 | 50 | 49.06667 | | |
| Cor total | 96258.67 | 74 | | | |

*Value of "Prob>F" less than 0.05 indicates model term is significant.

ACD, ADE, and BDE are significant as well. The results regression analysis indicates that the correlation coefficient ($R^2$) of the model is 0.974513 and the adjusted $R^2$ is 0.962279. The model adequate precision of 22.25409 indicates that the model has an adequate signal. Conclusively, the model can be used to navigate the design space (Fig. 3).

### *Final equation for mortality percentage based on Taguchi's model*

***Larval mortality*** (%) = -3370.208937 - 588.272023 * A + 31.1997336 * B + 771.2283616 * C - 1433.963373 * D + 50.25025007 * E + 31.73485427 * A * B + 34.56531874 * A * C + 89.90219504 * A * D + 51.25275965 * A * E - 16.49680701 * B * C + 4.840581588 * B * D -0.902106539 * B * E + 173.1436901 * C * D - 22.72783355 * C * E + 15.45709935 * D * E - 2.729875158 * A * B * C + 0.291181964 * A * B * D - 1.012706094 * A * B * E - 9.344204356 * A * C * D - 4.049384547 * A * C * E - 1.847729114 * A * D * E - 0.937834283 * B * C * D + 1.26341667 * B * C * E - 0.413341674 * B * D * E

**Table 6.** Optimum conditions and validation of the model.

| By-product concentration (%) | Moisture content (%) | pH | Inoculum size (%) | Incubation period (days) | Sporulation (CFU x $10^8$/g) | | Mortality (%) at 10 ppm | |
|---|---|---|---|---|---|---|---|---|
| | | | | | Predicted | Actual | Predicted | Actual |
| 6 | 40 | 6.5 | 2 | 7 | 218 | 215 | 92 | 90 ± 0 |

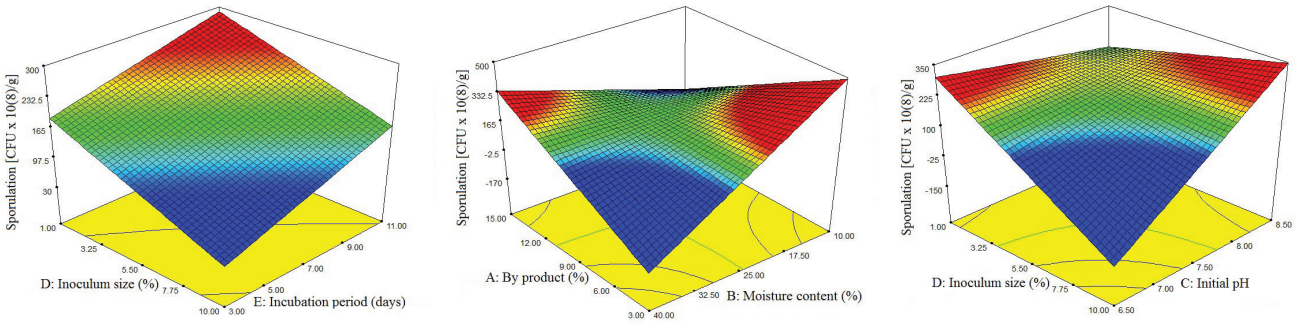


**Figure 2.** 3D response surface plots of the effect of various factors on sporulation.

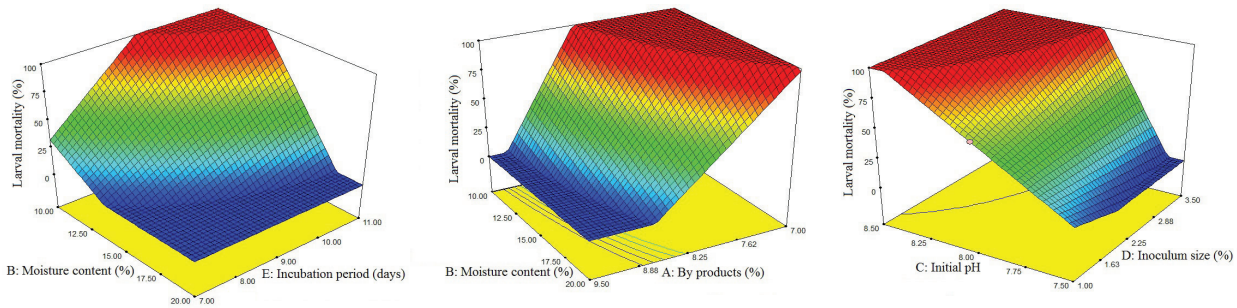


**Figure 3.** 3D response surface plots of the effect of various factors on larval mortality (%).

Where, A: by-product concentration (%), B: initial moisture content (%), C: initial pH, D: inoculum size (%) and E: incubation period (days).

### *Optimization and validation of the model*

The optimum conditions for maximum mosquitocidal activity against second instar *C. pipiens* larvae were theoretically predicted from the model and then practically applied in triplicates and reported as (mean ± standard deviation) as shown in Table 6. Data shows that the model is 100% valid and the conditions can be used for production of *Bacillus thuringiensis* var. *israelensis*.

## Discussion

In previous study using conventional one-at-a-time factorial design experiments, the optimum conditions for the maximum toxicity of Bti were 9% of sugar beet pulp-sesame meal (1:1) at pH 7-8, 20-30% moisture, 4-10% inoculum and 7 days incubation (El-Bendary et al. 2016a). In this study, Taguchi experimental design of surface response methodology was studied and the optimum conditions for the maximum mosquitocidal activity was 6% sugar beet pulp-sesame meal (1:1) at pH 6.5, 40% moisture, 2% inoculum size and 7 days incubation period. The difference between these two methods is statistical analysis shows the interactive effects among the variables tested, needs low experimental data sets and reduces time and cost.

Some reports about efficient application of the statistical experimental design for optimization of the cultural conditions for production of endotoxins of *Bacillus thuringiensis* under submerged fermentation were published by Moreira et al. (2007), Ben Khedher et al. (2011, 2013), and Hoa et al. (2014). It was reported that mosquitocidal toxins of *Lysinibacillus sphaericus* was successfully produced under SSF through applying response surface methodology design (El-Bendary et al. 2016b).

## Conclusions

Optimization of the microbial cultivation medium and conditions are critical since they affect overall process economics. In this study, statistical experimental design (Taguchi

orthogonal array) was applied in order, to optimize the mosquitocidal toxins production by Bti under SSF. Five factors, namely substrate concentration, moisture content, initial pH, inoculums size, and incubation periods were optimized for this commercially important bacterium. The predicted results of this design were confirmed by practical experiments. According to these results, the optimum conditions were 6% substrate concentration, 40% moisture content, initial pH 6.5, inoculum size 2% and 7 days incubation period to obtain high sporulation titer ($2.2 \times 10^{10}$ CFU/g) and the maximum mosquitocidal activity of about 90%.

## Acknowledgement

The authors would like to thank the National Research Centre of Egypt for its professional and financial support provided for this study.

## References

Ampofo JA (1995) Use of local raw materials for the production of *Bacillus sphaericus* insecticides in Ghana. Biocont Sci Technol 5:417-423.

Ben Khedher S, Kamoun A, Jaoua S, Zouari N (2011) Improvement of *Bacillus thuringiensis* bioinsecticide production by sporeless and sporulating strains using response surface methodology. New Biotechnol 28:705-712.

Ben Khedher S, Jaoua S, Zouari N (2013) Application of statistical experimental design for optimisation of bioinsecticides production by sporeless *Bacillus thuringiensis* strain on cheap medium. Braz J Microbiol 44:927-933.

Box GEP, Wilson KB (1951) On the experimental attainment of optimum conditions (with discussion). J Royal Stat Soc Ser B13:1-45.

El-Bendary MA, Moharam ME, Mohamed SS, Hamed SR (2016a) Pilot scale production of mosquitocidal toxins by *Bacillus thuringiensis* and *Lysinibacillus sphaericus* under solid state fermentation. Biocon Sci Technol 26:980-994.

El-Bendary MA, Abo Elsoud MM, Mohamed SS, Hamed SR (2016b). Optimization of Mosquitocidal toxins production by *Lysinibacillus sphaericus* under solid state fermentation using statistical experimental design. Acta Biol Szeged 60:57-63.

Han D, San NO, Angun P, Onarman Umu OC, Demirci A, Tekinay T (2014) Response surface optimization of the cultivation conditions and medium composition a novel probiotic strain *Bacillus pumilus* STF26. Int Food Res J 21:1355-1361.

Hoa NT, Chinh TT, Anh DTM, Binh ND, Thanh LTM (2014) Optimization of fermentation medium compositions from dewatered wastewater sludge of beer manufactory for *Bacillus thuringiensis* delta endotoxin production. Am Agric Forest 2:219-225.

Holker U, Lenz J (2005) Solid state fermentation-are there any biotechnological advantage? Curr Opinion Microbiol 8:301-306.

Li C, Bai J, Cai Z, Ouyang F (2002) Optimization of a cultural medium for bacteriocin production by *Lactococcus lactis* using response surface methodology. J Biotechnol 93:27-34.

Moreira GA, Michelouf GA, Beccaria AJ, Goicoechea HC (2007) Optimization of the *Bacillus thuringiensis* var. *kurstaki* HD-1δ-endotoxins production by using experimental mixture design and artificial neural networks. Biochem Eng J 35:48-55.

Poopathi S, Archana B (2012) A novel cost-effective medium for the production of *Bacillus thuringiensis* subsp. *israelensis* for mosquito control. Trop Biomed 29:81-91.

Sunitha K, Lee Jung-Kee TK (1999) Optimization of medium components for phytase production by *E. coli* using response surface methodology. Bioprocess Biosyst Eng 21:477-481.

**Volume 61(2):141-147, 2017**
**Acta Biologica Szegediensis**
http://www2.sci.u-szeged.hu/ABS

**ARTICLE**

# Extraction and partial purification of *Aspergillus flavus* cell wall associated saponin hydrolase

Hala A. Amin[1]*, Faten M. Ahmed[1], Hanem M. Awad[2], Sayeda S. Mohamed[1], Abeer Shokeer[3]

[1]Department of Chemistry of Natural and Microbial Products, National Research Centre, Dokki, Cairo, Egypt
[2]Department of Tanning Materials and Leather Technology, National Research Centre, Dokki, Cairo, Egypt
[3]Department of Molecular Biology, National Research Centre, Dokki, Cairo, Egypt

**ABSTRACT** In spite of the importance of saponin hydrolase (SH) enzyme, in the production of biologically active compounds from natural saponins, it is surprising that many aspects of its nature are unknown. The results of the present work revealed that *Aspergillus flavus* was capable of expressing three SH forms; extracellular, intracellular and cell wall-bound forms. SH cell bound enzyme constituted to more than 75% of the total enzymatic activity in the production medium. The sequential extraction process of SH cell bound enzyme revealed that 47.5% of SH was cytosolic and the rest (52.5%) was associated with the cell wall. The highest SH extraction yield was achieved when 0.25 M Tris-HCl lysis buffer supplemented with 1% Triton X-100 for 24 h at 4-25 °C and pH 8 were applied. Under these optimized conditions, *A. flavus* SH yield increased from 23.6 to 85.83%. The partial purification was achieved by applying successively acetone precipitation, lyophilization, dialysis, and anion exchange chromatography on Fractogel EMD DEAE-650S to the extract. The specific activity of the enzyme extract was 0.27 U/mg after 75% acetone fractionation, while that after anion exchange chromatography was 0.65 U/mg protein. The final enzyme preparation was 7.3-fold purer than the crude extract.
**Acta Biol Szeged 61(2):141-147 (2017)**

**KEY WORDS**

*Aspergillus flavus*
optimization
saponin hydrolase
sequential extraction

## Introduction

Soybean saponins (SS) are oleanane triterpenoid glycosides found in soy and other legumes (Ruiz et al. 1996). These saponins have been divided into group A, B and E saponins according to their aglycone structures; soyasapogenol A, B and E, respectively (Berhow et al. 2002). They have a common structure of glucuronic acid linked to the C-3 site of soyasapogenol A or B as aglycones. Soyasapogenols A and B are generally being more biologically active compared to their glycosides (Gurfinkel and Rao 2003). Soyasapogenol B (SB) is known to have hepatoprotective, antiviral, anti-inflammatory, antimutagenic and growth suppressing effects on cells derived from human ovarian cancer, colon cancer, breast cancer and Hep-G2 cells (Kuzuhara et al. 2006; Watanabe et al. 2006; Zhang and Popovich 2008; Kamo et al. 2014). SB can be obtained from group B SS by hydrolyzing β-D-glucuronic acid residues from SS using the enzyme (β-D-glucuronidase, EC 3.2.1.31) called soybean saponin hydrolase (SH), produced by microorganisms belonging to genera *Neocosmospora, Eupenicillium* and *Aspergillus* (Kudou et al. 1991; Watanabe et al. 2005, 2006). The bioconversion of soyasaponin I (SS I) to SB by SH is shown in Figure 1.

The presence of synthetic as well as hydrolytic enzymes in fungal cell wall was postulated some time ago (Burnett 1979). Extraction procedures were developed including the utilization of diverse salts and hydrophilic and lipophilic solvents to better understand the association of enzymes with the cell wall (Lee and Lin 1995; McDougall and Morrison 1995). Additionally, sequential extraction protocols were elaborated for a more straightforward classification of the enzymes associated with the cell wall. The obtained extracts were sequentially washed with different solutions and/or solvents, resulting in different fractions or degrees of enzymatic association with the cell wall (Sassoon and Mooibroek 2001; Rast et al. 2003; Pérez-de-Mora et al. 2013). Fungal SH is usually known to be present in mycelium as well as in medium (Kudou et al. 1991). Although, many studies were carried out on extracellular SH, little is known about the location and the role of intracellular SH. Nevertheless, the status of SH association with fungal cell wall has remained eventless and not thoroughly characterized.

In a previous research (Amin et al. 2016), it was reported that SH was a cell wall associated glucuronidase, because

Submitted August 8, 2017; Accepted October 3, 2017
*Corresponding author. E-mail: halaamin2007@yahoo.com

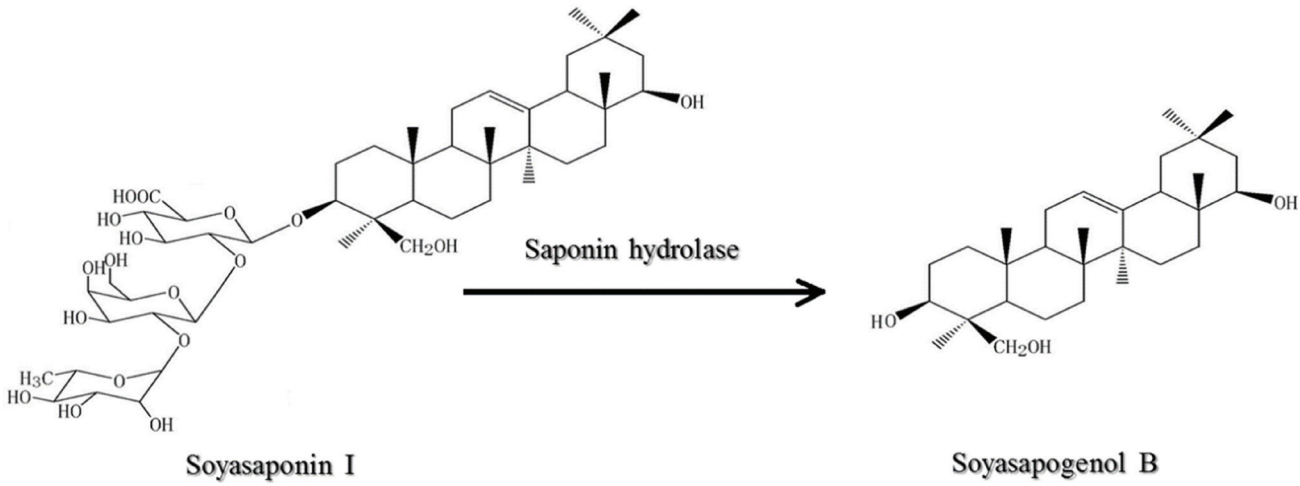


**Figure 1.** Bioconversion of SS I to SB by SH.

the majority of enzyme activity was detected in the whole cells compared to the extracellular and intracellular enzyme preparations. Here, we studied the activity and association of SH with the cell wall of *Aspergillus flavus* by means of a sequential extraction procedure. Followed by optimization of the extraction procedure in a trial to obtain a complete extraction of cell wall associated SH.

## Materials and Methods

### *Microorganism and cultivation*

*A. flavus*, a fungus isolated from popcorn seeds, was maintained on potato dextrose agar (PDA-Difco). SH production was carried out in production medium, containing (g/l) 20 SS, 40 malt extract, 20 yeast extract, 2 $KH_2PO_4$, 2 $(NH_4)_2SO_4$, 0.3 $MgSO_4 \cdot 7H_2O$, and 0.3 $CaCl_2 \cdot 2H_2O$ with a pH adjusted to 9 (Amin et al. 2016). Erlenmeyer flasks (250 ml) containing 100 ml of production medium were inoculated separately with 1 ml spore suspension ($10^8$ spores/flask) of 6 days old *A. flavus* slant culture and incubated for 48 h at 30 °C on a rotary shaker at 150 rpm.

### *Localization of A. flavus SH enzyme*

*A. flavus* was grown in the previously described production medium for 48 h at 30 °C. The enzyme activity was assayed in cultural filtrate, whole cells and cell extract. For preparation of cell extract, cells were washed twice with saline (0.9%) and grinded with approximately twice its weight of washed cold sand in a cold mortar and extracted by acetate buffer (200 mM acetate, pH 5).

### *Sequential extraction procedure*

The sequential extraction procedure was carried out using a method described previously (Pérez-de-Mora et al. 2013) with the following modifications. Lyophilized fungal cells were grinded with a cooled mortar and pestle under liquid nitrogen and stored at -80 °C until further usages. Three aliquots of cell (50 mg each) were thawed on ice and 2 ml lysis buffer I (250 mM Tris-HCl buffer, pH 8) was added to each tube, then cells were sonicated 5 times at 50% duty cycle for 1 min with Hielscher ultrasonic processor UP200S (Teltow, Germany). Completeness of cell disruption was examined microscopically. The resulting homogenate represents the total cell extract. The sample was clarified by centrifugation at 12000 x g for 10 min at 4 °C. The recovered supernatant was sampled, marked as cytosol (Tris extract). In all subsequent extractions, sonication and centrifugation were performed as per the previously described process. The insoluble pellets were resuspended in 50 mM phosphate buffer, pH 7 (P-buffer). The supernatant was sampled, stored and labeled as P extract. The same procedure was duplicated. The pellet was resuspended using Triton X-100 buffer (P-buffer + 0.5% Triton X-100), the suspension was incubated for 2 h at 4 °C under gentle overhead shaking, after which the suspension was centrifuged and the supernatant sampled (Trit extract). A second extraction using Triton X-100 buffer (P-buffer + 0.5% Triton X-100) was conducted. In a similar fashion, two extractions using 1 M NaCl solution followed (NaCl extract). Enzyme assays were conducted in all extracts in addition to the insoluble pellet after separation of the last extract, which was marked as rest. Enzyme extraction yield (%) was calculated using the following equation (Eq. 1).

Extraction yield (%) = Extraction yield (%) = Cell extract SH activity/Total SH activity x 100 (Eq. 1.)

### *Optimization of the extraction procedure*

The effect of different operational parameters on enzyme extraction was studied including; sonication time and intensity, the use of different detergents (ionic and nonionic ones), varying concentrations of the best detergent, extraction time and extraction temperature. All experiments were conducted using lyophilized grinded *A. flavus* cells suspended in 250 mM Tris-HCl buffer, pH 8 in the presence of a protease inhibitor cocktail (Sigma, St. Louis, Mo), 1 mM EDTA, 2 mM β-mercaptoethanol and 150 mM NaCl and centrifuged at 12000 x g for 10 min at 4 °C.

### *Partial purification of A. flavus SH enzyme*

The crude SH enzyme extracted from *A. flavus* cells under the optimized extraction conditions was centrifuged at 10.000 rpm at 4 °C for 10 min. The supernatant was precipitated using 75% acetone then the precipitate was lyophilized. The lyophilized material was dissolved in minimum volume of 20 mM phosphate buffer, pH 7.5 and dialyzed against the same buffer. Dialyzed enzyme was centrifuged and the supernatant was applied on Fractogel EMD DEAE-650 (1.5 x 20 cm) equilibrated by 10 mM phosphate buffer, pH 7.5. The column was eluted with a 0 to 200 mM NaCl linear gradient in 10 mM phosphate buffer, pH 7.5 (4 h, flow rate 1 ml/min). The active fractions were pooled then dialyzed in cold against water, and after that lyophilized.

### *Measurement of SH activity*

SH activity was measured in cultural filtrate or cell extract as follows: to 1 ml of 2% SS suspended in MUB (modified universal buffer, Skujins 1962), 1 ml of enzyme solution was added, and the mixture was allowed to react at 40 °C for 1 h. The MUB pH was adjusted to achieve a final pH of 6 during the incubations. Reaction products were extracted with 2 ml of ethyl acetate. In case of using whole cells in the reaction mixture, 1 g wet cells was added to 5 ml of 1% SS suspended in 200 mM acetate (pH 5) and the mixture was allowed to react at 40 °C for 1 h. Reaction products were extracted with 5 ml of ethyl acetate. The quantity of SB in the sample was analyzed by high-pressure liquid chromatography (HPLC). One unit of enzyme activity is defined as the amount of enzyme that produces 1 µmol of aglycone (SB)/h from the substrate. Cell based specific activity (whole cells or cell extract) can be defined as µmol of aglycone/h/g dry weight cells.

### *SB analytical methods*

Thin layer chromatography (TLC) was carried out on precoated silica gel plates (Merck, silica gel 60F-254). The plates were chromatographed for SB with a solvent system of benzene:ethylacetate:acetic acid (12:4:0.5, v/v/v). SB having an Rf value of 0.35 was detected on TLC plates by acid charring (10% $H_2SO_4$, 120 °C, 10 min).

HPLC was performed with Waters Alliance E2695 HPLC System (XE Separations Module, Austria) under the following conditions; column: SunFire Prep C18 (5µm, 10 x 150 mm), column temperature: 40 °C; mobile phase: acetonitrile-methanol-water (50:15:35), flow rate: 1 ml/min, and UV detector operating 200 nm. From ethyl acetate 100 µl of containing reaction products was diluted with 900 µl of the mobile phase. From this dilution 10 µl was analyzed by HPLC and the quantity of SB in the sample was determined by comparison with authentic SB (Watanabe et al. 2004). The SB yield (%) in the reaction mixture was calculated using Eq. 2.

$$\text{SB yield (\%)} = \frac{[\text{SB weight} / \text{SBMW}]\times 100}{[\text{SS I weight} / \text{SS I MW}]} \quad \text{(Eq. 2.)}$$

Where, MW is the molecular weight; SS I (soyasaponin I) represents soybean saponins.

### *Statistical analysis*

All the experiments were performed in triplicate, and the values obtained represent the means of duplicate measurements of three independent samples. When ANOVA indicated a significant F-value, least significant difference values at $P<0.05$ were used to separate treatment means.

## Results and Discussion

### *Localization of A. flavus SH enzyme*

Hydrolytic enzymes can be classified as (a) intracellular, (b) membrane- or cell wall-associated, and (c) extracellular depending on their location (Alvarez et al. 2004). Data presented in Table 1 revealed that among three different enzyme fraction preparations, the whole cells fraction produced the highest total enzyme activity. Total enzyme activity of this fraction was 3.1 and 4.2 times more active than that of extracellular (cultural filtrate) and intracellular (cell extract) enzyme fractions, respectively (Table 1). In addition, SB yield of the whole cells under mentioned assay conditions was about 6

**Table 1.** Effect of different SH preparations on SH activity and SB yield.

| SH preparations | SH total activity (U/g) | SB yield (%) |
|---|---|---|
| Cultural filtrate | 22.91 ± 1.14 | 2.26 ± 0.15 |
| Cell extract | 16.73 ± 0.66 | 4.13 ± 0.23 |
| Whole cells | 71.05 ± 3.20 | 17.55 ± 0.78 |

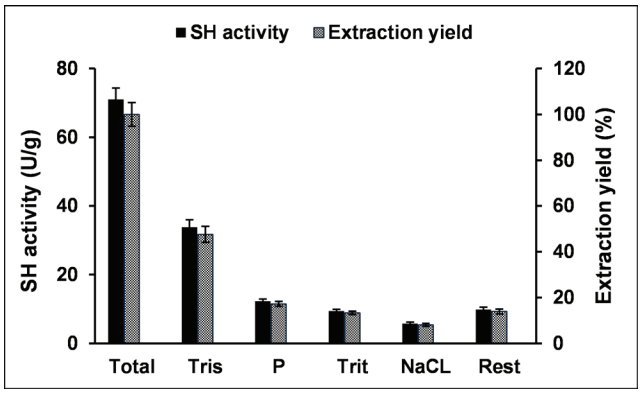


**Figure 2.** SH activities and percentage of activities in the various fractions of *A. flavus.* Extraction yield (SH %) of each fraction was calculated according to the activity of total cell extract. The experiments were performed in triplicate and the standard deviations were lower than ± 8.1%.

and 4 times that of extracellular and intracellular enzyme preparations, respectively. These results indicated that SH was distributed in three forms, which are extra-, intracellular and cell wall-associated forms. Moreover, cell wall-associated SH contributed to more than 75% of the total enzymatic activity in the production medium.

### *Sequential extraction procedure*

The target enzyme is mainly cell wall-associated one as observed in the results above. The sequential extraction procedure was applied to specify SH associations to the cell wall. Consequently, a suitable protocol could be applied to release it from fungal cells. According to Pérez-de-Mora et al. (2013), this procedure divides enzymes into the following categories: 1) cytosolic (Tris extract), 2) loosely bound (P extract), 3) hydrophobically bound (Trit extract), 4) ionically bound (NaCl) extract, and 5) covalently bound (Rest). Figure 2 shows SH enzymatic compartmentalization among the cytosol (Tris extract) and the cell wall fractions (P extract, Trit extract, NaCl extract, and Rest). The highest proportion of SH activities (47.5% of total activity) was found in Tris fraction (33.77 U/g) and it represented about twice the activity observed in the previous experiment (16.7 U/g) using acetate buffer at pH 5. It was concluded that increasing buffer pH to pH 8 enhanced SH extraction. Schindler et al. (2006) reported that high salt or high pH solutions can separate membrane proteins from membranes. On the other hand, sum of activity in cell wall fractions formed about 52.5% of total activity. This means that 47.5% of SH enzyme is cytosolic and the rest (52.5%) is associated with the cell wall.

### *Optimization of extraction procedure*

According to the above results, more than 50% of SH is associated with the cell wall or membrane protein. Integral membrane proteins need to be solubilized from the lipid bilayer to produce individual proteins before purification. Detergents with amphipathic properties are commonly used to solubilize integral membrane proteins from membranes (Lin and Guidotti 2009). Consequently, the effect of different operational parameters on enzyme extraction was studied including; sonication time and intensity, the use of different detergents (ionic and nonionic ones), application of different concentrations of the best detergent, extraction time and extraction temperature.

Data presented in Table 2 show that not only the extraction yield was affected by the sonication time and intensity, but also the total SH activity. At 25% amplitude, both the total SH activity and the extraction yield increased by time. On the other hand, SH total activity was increased when increasing both the sonication time and intensity up to 3 min at 35% amplitude, whereas the extraction yield was increased up to 5 min at 45% amplitude.

**Table 2.** Effect of sonication time and intensity on SH total activity and extraction yield.

| Sonication condition | Total (U/g) | Cell extract (U/g) | Extraction yield (%) |
|---|---|---|---|
| Amp. 25(%) | | | |
| 1 min | 65.18 ± 4.28 | 14.81 ± 0.52 | 22.73 ± 1.37 |
| 3 min | 77.04 ± 5.23 | 23.28 ± 1.40 | 30.21 ± 1.70 |
| 5 min | 79.16 ± 2.02 | 29.75 ± 1.88 | 37.58 ± 2.17 |
| Amp. 35(%) | | | |
| 1 min | 75.72 ± 2.88 | 20.49 ± 1.31 | 27.05 ± 1.61 |
| 3 min | 82.71 ± 3.85 | 27.93 ± 1.79 | 33.78 ± 2.04 |
| 5 min | 71.05 ± 3.17 | 32.82 ± 2.06 | 46.20 ± 1.76 |
| Amp. 45(%) | | | |
| 1 min | 82.69 ± 2.22 | 26.07 ± 0.51 | 31.53 ± 0.76 |
| 3 min | 76.41 ± 3.05 | 31.66 ± 1.35 | 41.43 ± 2.86 |
| 5 min | 70.99 ± 4.16 | 40.05 ± 2.94 | 56.42 ± 2.36 |

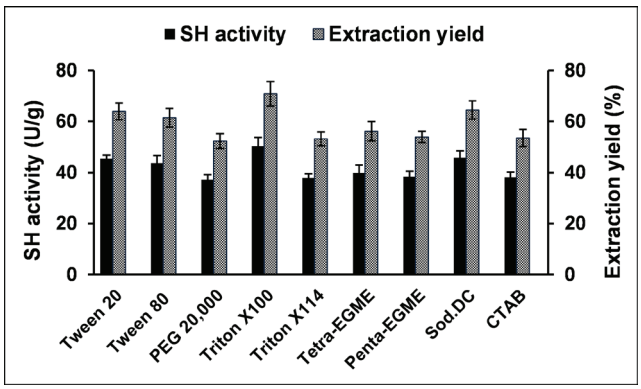


**Figure 3.** Screening of different detergents for SH activity and extraction from *A. flavus* cells. Extraction yield (SH %) of each fraction was calculated according to the activity of the total cell extract. The experiments were performed in triplicate and the standard deviations were lower than ± 6.8%. PEG: polyethylene glycol 20 000; Tetra-EGME: tetra-ethylene glycol mono *n*-dodecyl ether; Penta-EGME: penta-ethylene glycol mono *n*-dodecyl ether; Sod DC: sodium deoxycholate; CTAB: Cetyltrimethylammonium bromide.

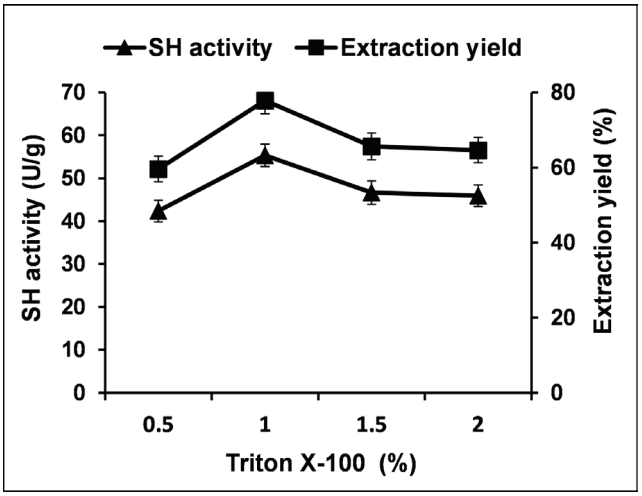


**Figure 4.** Effect of different Triton X-100 concentrations on SH activity and extraction from *A. flavus* cells. The experiments were performed in triplicate and the standard deviations were lower than ± 4.5%.

Detergent molecules consist of two parts: a hydrophobic hydrocarbon moiety, and a polar or charged head group. Detergents are classified into four types based on their head-groups; namely nonionic, anionic, cationic or zwitter ionic detergents (Lin and Guidotti 2009). Detergent screening must be carried out for each membrane protein as not only one detergent works for all membrane proteins. Figure 3 shows the effect of different detergent types; nonionic (Tween 20, Tween 80, polyethylene glycol 20000, Triton X-100, Triton X-114, tetra-ethylene glycol mono *n*-dodecyl ether, and penta-ethylene glycol mono *n*-dodecyl ether), anionic (sodium deoxycholate), and cationic (Cetyltrimethylammonium bromide, CTAB) on SH extraction from *A. flavus* when evaluated experimentally. Among all detergents, Triton X-100 proved to be the best one followed by sodium deoxycholate showing extraction results of 77.87 and 70.86% of total SH activity, respectively. Consequently, different concentrations of Triton X-100 (0.5-2%) were used in lysis Tris buffer, pH 8 in an attempt to improve the extraction process of the enzyme part associated to the cell wall. Results in Figure 4 revealed that 1% Triton X-100 is the most favorable concentration for enzyme extraction, as it resulted in about 77.87% of enzyme activity of the total extract. Ahmad and Goswami (2013) used the same concentration of Triton X-100 (1%) for extraction of cell-bound cholesterol oxidase from *Rhodococcus* sp. (NCIM 2891).

Regarding the effect of extraction time, the extraction ability of the lysis buffer increased gradually by time to reach a maximum (85.83%) after 24 h incubation (Fig. 5). Thereafter, there was no significant changes in SH extraction yields with further incubation. Additionally, data in Table 3 show

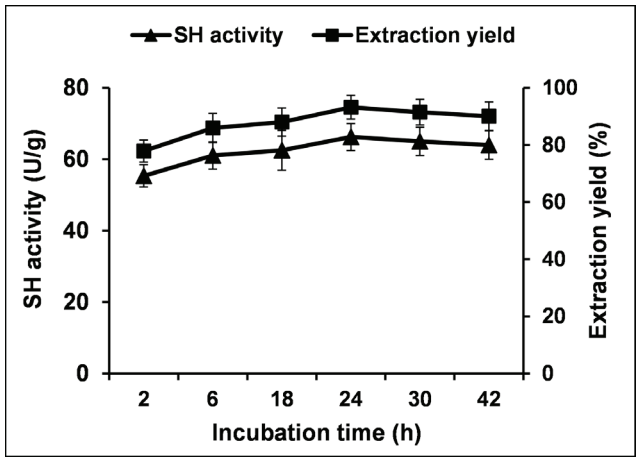


**Figure 5.** Effect of incubation time with 1% Triton X-100 on SH activity and extraction from *A. flavus* cells. The experiments were performed in triplicate and the standard deviations were lower than ± 6%.

**Table 3.** Effect of incubation temperature with 1% Triton X-100 on SH activity and extraction from *A. flavus* cells.

| Temperature (°C) | SH activity (U/g) | Extraction yield (%) |
|---|---|---|
| 4 | 66.20 ± 3.5 | 93.18 ± 5.2 |
| 25 | 67.01 ± 3.2 | 94.31 ± 4.8 |
| 40 | 49.43 ± 2.8 | 69.57 ± 3.1 |

the effect of the incubation temperature on SH activity and extraction from *A. flavus*. There was almost stability in SH activity and the extraction yield in a temperature range from

**Table 4.** Partial purification of SH extracted from *A. flavus.*

| Purification step | Total activity (U) | Total protein (mg/ml) | Specific activity (U/mg protein) | Yield (%) | Purification fold |
|---|---|---|---|---|---|
| Cell extract | 1166 | 12993 | 0.09 | 100 | 1 |
| Precipitation with acetone | 420 | 1576 | 0.27 | 36.0 | 2.97 |
| After lyophilisation | 416 | 1468 | 0.28 | 35.6 | 3.15 |
| After dialysis | 370 | 1381 | 0.27 | 31.7 | 2.98 |
| After DEAE column | 142 | 218 | 0.65 | 12.2 | 7.27 |

4 to 25 °C. However, increasing the temperature to 40 °C resulted in decreased SH activity and extraction yield probably due to the denaturation effect of temperature on SH.

### *Partial purification of SH*

The SH enzyme extracted from *A. flavus* cells, under the optimized extraction conditions was precipitated by 75% acetone followed by lyophilisation, dialysis and DEAE column purification. These purification steps enhanced the overall enzyme activity as shown in Table 4. It is noticed that, the SH specific activity of 0.27 U/mg protein was obtained using 75% acetone precipitation, which represents about 3-fold purification. In addition, the obtained yield after precipitation with acetone was 36% of the initial crude enzyme activity. There are no significant changes in the specific activity after both lyophilisation and dialysis steps. However, the yield was decreases to 12.2% after DEAE column. Interestingly, the purification of *A. flavus* SH that has been done by DEAE Fractogel column, led to increase the purification fold to 7.27 with a specific activity of 0.65 U/mg protein compared to the crude extract. Further purification and characterization are being carried out and will be separately published elsewhere.

## Acknowledgements

This work was supported by the International Centre for Genetic Engineering and Biotechnology (ICGEB), Italy [grant numbers CRP/EGY14-04].

## References

Ahmad S, Goswami P (2013) Enhanced production of cell-bound cholesterol oxidase from *Rhodococcus* sp. NCIM 2891 by the statistical method. Ann Microbiol 63:199-205.

Alvarez M, Godoy R, Heyser W, Härtel S (2004) Surface-bound phosphatase activity in living hyphae of ectomycorrhizal fungi in Nothofagusobliqua. Mycologia 96:479-487.

Amin HA, Abo Elsoud MM, Sahab AF (2016) Whole cell biocatalyst for soyasapogenol B production from soybean saponin. Open Conf Proceed J 7:134-143.

Berhow MA, Cantrell CL, Duval SM, Dobbins TA, Maynes J, Vaughn SF (2002) Analysis and quantitative determination of group B saponins in processed soybean product. Phytochem Anal 13:343-348.

Burnett JH (1979) Aspects of the structure and growth of hyphal walls. In Burnett JH, Trinci APJ Eds., Fungal walls and hyphal growth. Cambridge University Press, Cambridge. pp. 1-25.

Gurfinkel LDM, Rao AV (2003) Soyasaponins: The relationship between chemical structure and colon anticarcinogenic activity. Nutr Cancer 47:24-33.

Kamo S, Suzuki S, Sato T (2014) Comparison of bioavailability (I) between soyasaponins and soyasapogenols, and (II) between group A and B soyasaponins. Nutr 30:596-601.

Kudou S, Tsuizaki I, Shimoyamada M, Uchida T, Okubo K (1990) Screening for microorganisms producing soybean saponin hydrolase. Agric Biol Chem 54:3035-3037.

Kuzuhara H, Nishiyama S, Minowa N, Sasaki K (2006) Effects of triterpene compounds on cytotoxicity, apoptosis, and immune response in cultured cells. J Nat Med 60:113-120.

Lee TM, Lin YH (1995) Changes in soluble and cell wall-bound peroxidase activities with growth in anoxia-treated rice (*Oryza sativa* L.) coleoptiles and roots. Plant Sci 106:1-7.

Lin SH, Guidotti G (2009) Purification of membrane proteins. Methods Enzymol 463:619-629.

McDougall GJ, Morrison IM (1995) Ionically-bound and covalently bound wall peroxidases differ in their substrate specificity. Biochem Soc Trans 23:150S.

Pérez-de-Mora A, Reuter B, Lucio M, Ahne A, Schloter M, Pritsch K (2013). Activity of native hydrolytic enzymes and their association with the cell wall of three ectomycorrhizal fungi. Mycorrhiza 23:185-197.

Rast DM, Baumgartner D, Mayer C, Hollenstein GO (2003) Cell wall associated enzymes in fungi. Phytochem 64:339-366.

Ruiz RG, Price KR, Arthur AE, Rose ME, Rhodes MJC, Fenwick RG (1996) Effect of soaking and cooking on

the saponin content and composition of chickpeas (*Cicer-arietinum*) and lentils *(Lens culinaris*). J Agric Food Chem 44:1526-1530.

Sassoon J, Mooibroek H (2001). A system of categorizing enzyme-cell wall associations in *Agaricus bisporus* using operational criteria. Appl Microbiol Biotechnol 56:613-622.

Schindler J, Jung S, Niedner-Schatteburg G, Friauf E, Nothwang HG (2006) Enrichment of integral membrane proteins from small amount of brain tissue. J Neural Transm 113:995-1013.

Skujins JJ, Braal L, Mc Laren AD (1962) Characterization of phosphatase in a terrestrial soil sterilized with an electron beam. Enzymologia 25:125-133.

Watanabe M, Mido N, Tamura T, Sumida N, Yaguchi T (2006) Saponin digesting enzymes, genes thereof and soyasapogenol B mass production system. US Patent 7-022-508 B2.

Watanabe M, Sumida N, Yanai K, Murakami T (2004) A novel saponin hydrolase from *Neocosmospora vasinfecta* var. *vasinfecta*. Appl Environ Microbiol 70:865-872.

Watanabe M, Sumida N, Yanai K, Murakami T (2005) Cloning and characterization of saponin hydrolases from *Aspergillus oryzae* and *Eupenicillium brefeldianum*. Biosci Biotechnol Biochem 69:2178-2185.

Zhang W, Popovich DG (2008) Effect of soyasapogenol A and soyasapogenol B concentrated extracts on hep-G2 cell proliferation and apoptosis. J Agric Food Chem 56:2603-2608.

**Volume 61(2):149-156, 2017**
**Acta Biologica Szegediensis**
http://www2.sci.u-szeged.hu/ABS

**ARTICLE**

# Purification and characterization of a 1-deoxy-D-xylulose 5-phosphate synthase from *Cymbopogon flexuosus*

Ashish Kumar Gupta[1], Deepak Ganjewala[2]*

[1]Drug Discovery and Development Division, Patanjali Research Institute, Haridwar, U.P., India
[2]Amity Institute of Biotechnology, Amity University Uttar Pradesh, Noida, U.P., India

**ABSTRACT** Here we report purification and characterization of the enzyme 1-deoxy-D-xylulose 5-phosphate synthase (DXS) of the 2-C-methyl-D-erythritol 4-phosphate (MEP) pathway from lemongrass (*Cymbopogon flexuosus*) leaves. The DXS catalyzes the condensation of pyruvate and glyceraldehyde 3-phosphate (G3P) to produce 1-deoxy-D-xylulose 5-phosphate (DOXP), which is the first and rate-limiting step of the MEP pathway. It is the main flux-controlling step and an attractive target to manipulate the formation of the MEP-derived products. The DXS was extracted from immature (15 days old) leaves of lemongrass cv. Suvarna and purified to homogenity using ion exchange DEAE column and gel filtration (Sephadex G-150) chromatography. The purified DXS was referred as *Cf*DXS. The *Cf*DXS had specific activity 8.56 U/mg. The $K_m$ values for the two substrates, pyruvate and G3P were 4.4 and 8.8 µM, respectively and for the cofactor TPP 62 µM. The $V_{max}$ of the *Cf*DXS was 20 µmol/min. The optimum pH and temperature of the *Cf*DXS were 7.5 and 40 °C, respectively. The *Cf*DXS activity enhanced significantly in the presence of $Mg^{2+}$ (1 mM), whereas affected moderately by $Mn^{2+}$ and $Zn^{2+}$ (1 mM each). The enzyme was purified upto 11.64 fold with an yield of 32.34%. Its molecular weight was 130 kDa. The DXS was quite stable and retaining more than 80% of the initial activity upon storage at 4 °C in 100 mM Tris-HCl buffer (pH 8) for one month. **Acta Biol Szeged 61(2):149-156 (2017)**

**KEY WORDS**

2-C-methyl-D-erythriotol 4-phosphate
*Cymbopogon flexuous*
glyceraldehyde-3-phosphate
lemongrass
monoterpene
pyruvate

## Introduction

*Cymbopogon flexuosus* (Nees ex Steud.) popularly known as East Indian lemongrass provides the lemon scented essential oil, which is referred as lemongrass oil (LO). Lemongrass oil is a complex mixture of several monoterpenes, of which citral, an acyclic monoterpene aldehyde is the dominating constituent (Ganjewala and Luthra 2010; Gupta and Ganjewala 2015a). The percentage of the citral in the LO range from 70-80% and it imparts unique lemon like aroma to the LO. Lemongrass oil owing to its lemon like aroma has wide applications in flavors, fragrances, perfumery, cosmetics, food and pharmaceuticals (Ganjewala and Gupta 2013). A number of reports have documented many useful bioactive properties from simple antimicrobial to anticancer and anti-HIV of the lemongrass oil and citral (Shah et al. 2011; Mirghani et al. 2012; Ganjewala et al. 2012; Ganjewala and Gupta 2013; Olorunnisola et al. 2014; Gupta and Ganjewala 2015a).

In lemongrass, citral is biosynthesized *via* recently elucidated 2-C-methyl-D-erythritol 4-phosphate (MEP) pathway (Ganjewala et al. 2009; Gupta and Ganjewala 2015b). The first indication of the presence of the MEP pathway in lemongrass was came from earlier study conducted using mevinolin (a potent inhibitor of the hydroxymethyl-glutaryl-CoA reductase (HMGR) of the acetate-MVA pathway) (Ganjewala and Luthra 2007). At present, the MEP pathway has been elucidated from a number of plants, where it is utilized exclusively for the biosynthesis of monoterpenes (Eisenreich et al. 1998; Lichtenthaler 1999; Dudareva et al. 2005; Seemann et al. 2006; Ganjewala et al. 2009; Ganjewala and Luthra 2010). The MEP pathway was originally discovered from the *Escherichia coli* by Rohmer et al. (1993).

The first step of the MEP pathway involves the thiamine diphosphate (TPP) dependent condensation of the glyceraldehyde 3-phosphate (G3P) and pyruvate to produce 1-deoxy-D-xylulose 5-phosphate (DXP), which is catalyzed by the enzyme 1-Deoxy-D-xylulose 5-phosphate synthase (DXS) (Fig. 1). This is also a regulatory or committed step of the MEP pathway, thus control and regulate the overall supply of the IPP derived products by the flux distribution between pyruvate and G3P (Farmer and Liao 2001; Lee et al. 2007). The DXS requires TPP as a cofactor and divalent metal ions $Mg^{2+}$ or $Mn^{2+}$ for the activity (Wang et al. 2014). The optimum pH and temperature of the DXS from *E. coli* has been reported

Submitted February 25, 2017; Accepted July 27, 2017
*Corresponding author. E-mail: deepakganjawala73@yahoo.com

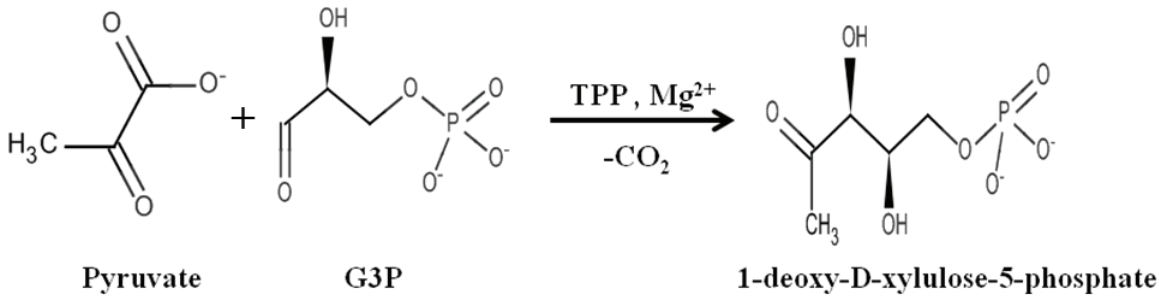


**Figure 1.** Reaction catalyzed by DXS.

to be 8.0 and 40 °C, respectively (Sprenger et al. 1997). The DXS has been cloned from several higher plants (Bouvier et al. 1998; Estevez et al. 2001) and bacteria *viz., Escherichia coli* (Sprenger et al. 1997) and *Agrobacterium tumefaciens* (Lee et al. 2007). Several studies have shown that the DXS significantly influences the rate of the biosynthesis of the IPP derived through the MEP pathway. The DXS could also be a promising target for the metabolic engineering in order to manipulate the monoterpene content and composition in plants. Currently, we have very limited knowledge of the enzymic regulation of MEP pathway in lemongrass, except our previous report highlighting the role of the DXR in the biosynthesis of the essential oil (Gupta and Ganjewala 2015c). In view of the important roles of the DXS, here we performed purification and characterization of this enzyme from lemongrass cv. Suvarna immature (15 days old) leaves to gain more deeper insight in to the regulation of the MEP pathway.

## Materials and Methods

### *Chemicals*

Glyceraldehyde 3-phosphate, sodium pyruvate, thiamine pyrophosphate (TPP), $MgCl_2$, $ZnCl_2$, Tris-base, EDTA-$Na_2$, 2-mercaptoethanol, ascorbic acid, sucrose, Sephadex G-150, DEAE cellulose, polyvinyl pyrophosphate (PVPP) were purchased from Sigma-Aldrich (Germany). Other chemicals and reagents used were of highest purity grade.

### *Plants*

*Cymbopogon flexuosus* (Steud) Wats cv. Suvarna plants were grown in the Organic Farm House of the Amity University, Noida, Uttar Pradesh, India following the standard agronomic practices. Fully-grown lemongrass plants were harvested from 10 cm above the ground level. A fully-grown lemongrass plant has six enfolded leaves in the form a whorl. The leaves from inside to outside of the whorl are numbered from 1 to 6, which represent gradient increase in the leaf age. The innermost leaf represents the youngest leaf stage, while the outermost fully matured leaf stage. In the present study, second leaf (immature) was used for the extraction of the DXS enzyme.

### *Extraction of DXS*

The DXS enzyme was extracted according to Wright and Phillips (2014). Leaf tissues (1 g) was homogenized in 50 mM Tris-HCl buffer (pH 8.0) consisting of 1 mM TPP, 50 mM sodium metabisulfite, 10 mM 2-mercaptoethanol, 10 mM ascorbic acid, 0.15 M sucrose, 1 mM EDTA, 10% glycerol and 1 mM NaF, polyvinyl pyrophosphate (PVPP) (50% of the tissue weight) was added prior to homogenization. The homogenate was filtered through four layers of muslin cloth and centrifuged at 13000 × g for 30 min at 4 ºC. The supernatant was collected in the screw capped graduated tubes and used as crude enzyme extract.

### *Protein estimation*

Protein content of the crude enzyme extract was estimated by Bradford method (Bradford 1976).

### *DXS assay*

A coupled spectrophotometric assay was used for rapid screening of the DXS activity. The DXS activity was determined using a reaction mixture (3 ml) containing 50 mM Tris-HCl, 1 mM $MgCl_2$, 1 mM TPP, 0.1 M NADPH, 0.1 M sodium pyruvate, 0.05 M DL-glyceraldehyde 3-phosphate (G3P), 1 mM NaF and 0.2 mg/ml DXR at pH 8.0. The reaction was initiated by adding the enzyme extract to the assay mixture.

In this assay, DXP generate by DXS is further converted to MEP in a NADPH-dependent reaction by an excess of the DXR. The change in absorption at 340 nm due to conversion

of NADPH in to NADP was monitored. One unit of the DXS activity (U) was defined as the amount of the enzyme required to produce 1 µM of DXP second$^{-1}$ under the conditions described above (Altincicek et al. 2000). Enzyme activities were expressed as nkatal/ml. The molar extinction coefficient value for NADPH 6220 $M^{-1}cm^{-1}$ at 340 nm was used for the calculation. A control with the boiled enzyme was also run simultaneously.

### *Purification of DXS enzyme*

The DXS was purified in three steps. All purification procedures were carried out at 4 ºC. In the first step, the crude enzyme extract (25 ml) prepared from immature leaves was fractionated by ammonium sulfate ($(NH4)_2SO_4$) precipitation as 0-40 and 40-80% saturation. Proteins precipitating at all the $(NH4)_2SO_4$ saturation steps were collected by centrifugation at 13000 x g for 15 min, suspended in extraction buffer (50mM Tris-HCl buffer, pH 8.0) and proceeded to the dialysis.

The desalting was done using dialysis bags (Himedia; AV width-42.44 nm, AV diameter-25.4 mm, capacity-5.07 ml/cm) as per molecular weight cut off size of the membrane (25 kDa) against three changes of the buffer, which was used for extraction of the DXS. The dialyzed sample was applied to the pre-equilibrated (Tris-HCl 10 mM, pH 8.0) DEAE cellulose matrix packed in a column (Borosil, 200 x 10 mm column). The fractions (2 ml each) were collected by washing the matrix with Tris-HCl buffer (10 mM, pH 8.0).

Thereafter, the column was eluted by salt step gradient method, using increasing concentration of NaCl (50 mM, 100 mM, 200 mM, 300 mM, 400 mM in 10 mM Tris-HCl buffer, pH 8.0). Total 120 fractions (2 ml each) were collected. Peaks were obtained during the elution process, and the fractions corresponding to the peaks were pooled and specific activity was determined. Pools with maximum values were further dialyzed and processed to the gel filtration chromatographic separation using the Sephadex-G150 packed in a column (Borosil, 200 x 10 mm column). The column was washed with equilibration buffer (0.01 M Tris-HCl buffer pH 8.0). The pool obtained from the previous chromatographic procedure was loaded on to the pre-swelled and pre-equilibrated Sephadex G-150 matrix and eluted by using Tris-HCl 0.01 M, pH 8.0) 36 fractions (2 ml each) were collected and assayed for the DXS activity.

### *Determination of molecular mass*

Appropriate molecular mass of the DXS was determined by the SDS-PAGE technique according to Laemmli (1971) using 10% polyacrylamide gel of 1 mm thickness. The purified protein was loaded into the wells in the gel along with a standard protein molecular weight marker (Merck Millipore, Germany). Separation was carried out in electrophoresis device (Double-sided Vertical Gel Electrophoresis System, Genetix-SCZ) at current of 15 mA for approximately 4 h. Protein bands were visualized by staining with Coomassie Brilliant Blue G-250 according to a previously published report. The molecular mass of the protein bands was determined by the comparison with the standard molecular marker set.

### *Effects of substrate concentration*

The optimum concentration of substrates (G3P and sodium pyruvate) required for the maximum activity of the DXS was determined in terms of $V_{max}$ and $K_m$. The rate ($V_0$) of the DXS catalyzed reaction was measured using different concentrations of G3P (10-50 µM), sodium pyruvate (20-100 µM) and cofactor TPP (200 µM-1 M). The $V_{max}$ and $K_m$ values were determined from the double reciprocal (Lineweaver-Burk) plot.

### *Effects of temperature and pH*

Temperature and pH optima were determined by performing the enzymatic reaction at different temperature 0-100°C and pH 6.0-9.0.

### *Effect of metal ions*

Effect of the various metal ions such as $MgCl_2$, $CoCl_2$, $MnCl_2$, $CuCl_2$, $CaCl_2$ and $ZnCl_2$ on activity of the DXS enzyme was evaluated. The enzymatic reaction was performed in the presence of 1 mM concentration of each metal ion. Effective metal ion, $MgCl_2$ as a cofactor was checked for optimum DXS enzyme activity.

## Results

### *Purification of the DXS*

The DXS was purified in three steps. Results of the purification procedure are summarized in Table 1. In the first step, the crude enzyme extract was purified by ammonium sulfate fractionation and dialysis. Results revealed that approximately 60% of the DXS activity was precipitated between 0-40% $(NH_4)_2SO_4$ saturation with specific activity recorded 2.44 U/mg protein$^{-1}$. The purification fold was increased three times compared to the crude enzyme extract. Dialysis of the 0-40% fraction against Tris-HCl buffer (50 mM, pH 8.0) resulted in a significant increase in the specific activity of the DXS from 2.44-3.37 U/mg protein$^{-1}$ with a yield of ~ 58%. The dialyzed fraction was subjected to the ion exchange chromatography using DEAE column and eluted with increasing concentration

**Table 1.** Purification of DXS from *C. flexuosus* cv. Suvarna leaves.

| Step | Total protein (mg) | Total activity (U/min) | Specific activity (U/mg protein) | Yield (%) | Purification (fold) |
|---|---|---|---|---|---|
| Crude enzyme extract | 120.0 | 87.60 | 0.73 | 100 | 1.0 |
| Ammonium sulfate 0-40% | 71.07 | 173.41 | 2.44 | 59.23 | 3.31 |
| Ammonium sulfate 40-80% | 42.82 | 76.65 | 1.79 | 35.69 | 2.29 |
| Dialysis of 0-40% fraction | 69.94 | 235.70 | 3.37 | 58.29 | 4.59 |
| DEAE-cellulose (pool 5) | 55.66 | 291.66 | 5.24 | 46.39 | 7.14 |
| DEAE-cellulose (pool 5) dialyzed | 54.97 | 328.17 | 5.97 | 45.81 | 8.13 |
| Sephadex G-150 (pool 3) | 38.80 | 332.13 | 8.56 | 32.34 | 11.64 |

of NaCl. The elution profile (Fig. 2A, B) depicts prominent peaks of the DXS protein and DXS activity with increasing concentrations of the NaCl.

It showed that the pool number 5 comprising of fractions 67-72 (100 mM NaCl-200 mM NaCl) (Fig. 2B) had most of the DXS activity. By the end of ion exchange chromatography, specific activity of the DXS significantly increased from 3.37 to 5.97 U/mg protein$^{-1}$ with 7 times increase in the purification fold.

Finally, concentrated sample was dissolved in 10 mM Tris-HCl buffer for further purification by gel filtration chromatography using the Sephadex G-150 column (100 x 10 mm). Elution profiles (Fig. 3A, B) indicated the highest concentration of the DXS protein and its activity in the pool 3 comprising of fractions number 21-26. At the end, specific activity of the DXS increased markedly from 5.97 to 8.56 U/mg protein$^{-1}$ with almost 12% rise in the purification fold. Homogenity of the DXS containing fraction was evaluated by SDS-PAGE. A single band corresponding to the 130 kDa was detected in the gel electrophoretogram, which was identified as the DXS and named as *Cf*DXS (Fig. 4).

### *Characterization of DXS, substrate concentration*

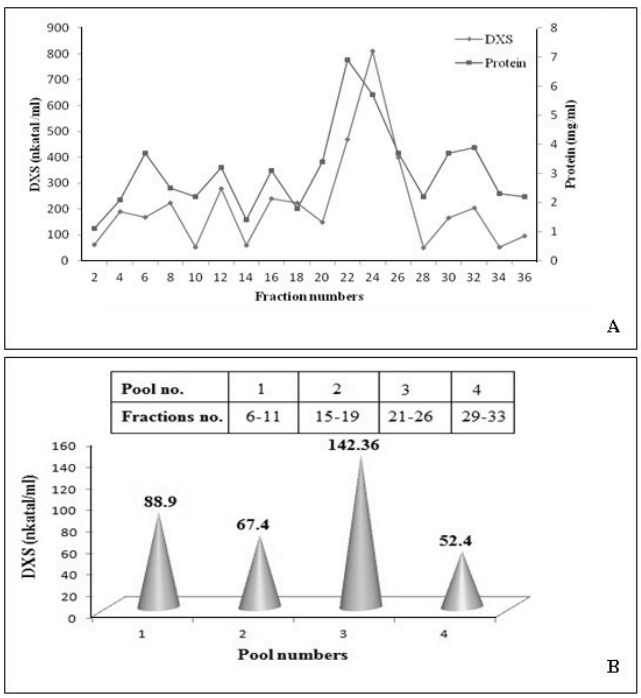


**Figure 2. (A)** DEAE-cellulose anion-exchange chromatogram (200×10 mm) showing elution profile of the dialyzed ammonium sulfate fraction (0-40%) from *C. flexuosus*; eluted by step ascending gradient method, using NaCl (50-400 mM) in Tris-HCl buffer (10 mM, pH 8.0); **(B)** DXS activities in ion exchange chromatography purified fractions.

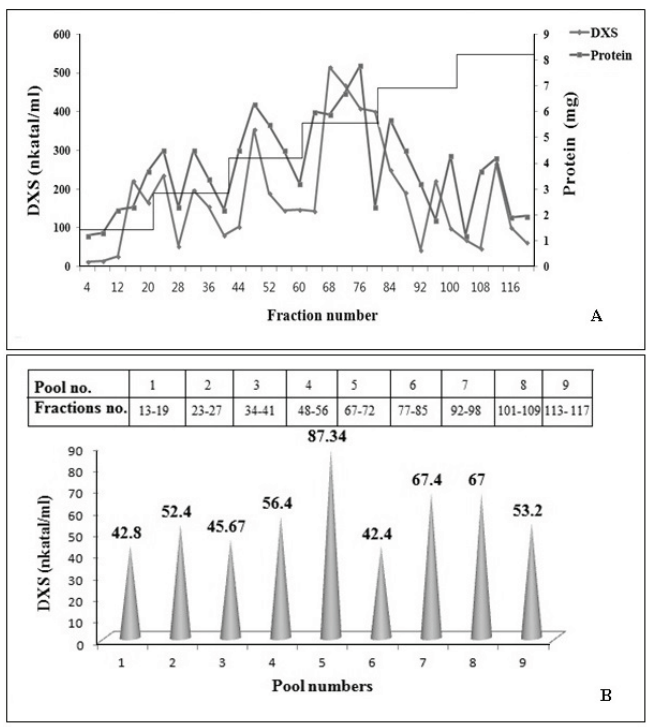


**Figure 3. (A)** Elution profile of the DXS enzyme on Sephadex G-150 (200 ×10 mm) by gel filtration chromatography. Column was eluted by using Tris-HCl 10 mM, pH 8.0. **(B)** DXS activities in gel chromatography fractions.

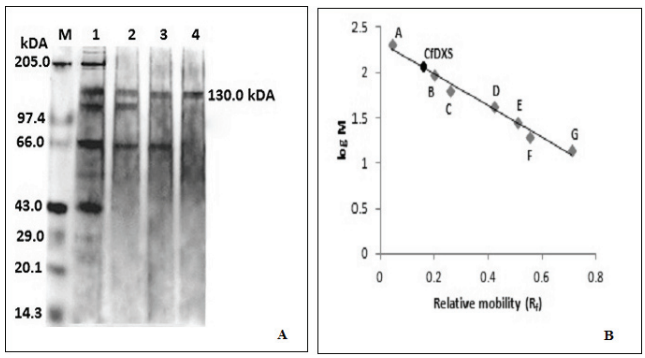


**Figure 4.** SDS-PAGE analysis of the *Cf*DXS enzyme **(A)** Lane M, protein marker with the indicated molecular masses; lane 1, crude enzyme extract; lane 2, ammonium sulfate precipitated sample; lane 3, DEAE-Cellulose; lane 4, Sephadex G-150 purified *Cf*DXS. **(B)** Calibration curve for the determination of the *Cf*DXS molecular weight by SDS-PAGE (10%). Marker proteins used for calibration: A : Myosin, rabbit muscle (205.0 KDa); B: phosphorylase b (97.4 KDa); C: bovine serum albumin (66.0 KDa); D: ovalbumin (4E: carbonic anhydrase (29.0 KDa); F: soyabean trypsin inhibitor (20.1 KDa); F: lysozyme (14.3 KDa); *Cf*DXS (130.0 KDa).

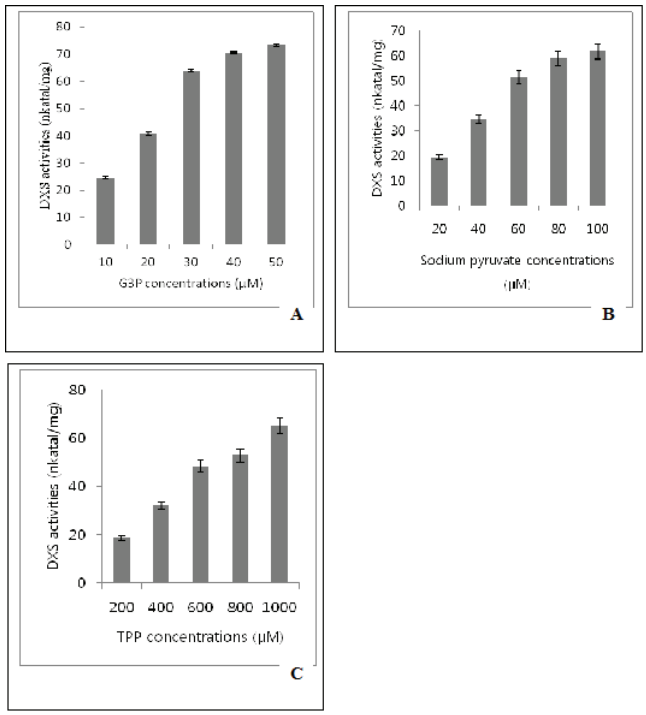


**Figure 5.** Effects of substrates (A) G3P (B) sodium pyruvate and (C) cofactor TPP on *Cf*DXS activity.

The optimum concentration of substrates G3P and sodium pyruvate measured were 50 and 100 µM, respectively, while that of cofactor TPP 1 mM (Fig. 5). Concentrations > 50 µM (for G3P) and 100 µM (for sodium pyruvate) were also tested, however, it did not result in any increment in the DXS activities (data not shown). After the optimum substrate concentration point, no increment in the enzyme activity was seen, which suggested the highest activity of any enzyme is observed only at the optimum substrate concentration. However, other factors like pH, temperature and cofactors also influence activity of any enzyme.

### *Temperature and pH*

The pH and temperature optima determined for the *Cf*DXS were 8.0 and 40 °C, respectively (Fig. 6). The pH stability of the *Cf*DXS was found to be 6.0 to 9.0 in 50 mM Tris-HCl buffer, whereas the temperature stability 20 to 60 °C. The *Cf*DXS was quite stable (up to one month) when kept in 50 mM Tris-HCl buffer (pH 8.0) at 4 °C in the refrigerator retaining about 70% of the activity.

### *Effect of metal ions*

Effects of metal ions such as $Co^{2+}$, $Mn^{2+}$, $Mg^{2+}$, $Cu^{2+}$, $Fe^{2+}$, $Ca^{2+}$ and $Zn^{2+}$ were evaluated on the *Cf*DXS activity. The results revealed that the *Cf*DXS activity enhanced significantly (~15 fold) in the presence of 1 mM $Mg^{2+}$ (Fig. 7). Two metal ions namely, $Zn^{2+}$ and $Mn^{2+}$ moderately increase the *Cf*DXS

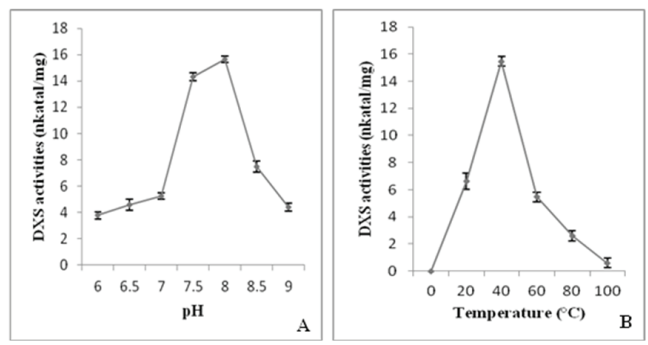


**Figure 6.** Effects of (A) pH and (B) temperature on *Cf*DXS activity.

activity, while the remaining metal ions $Ca^{2+}$, $Co^{2+}$ $Cu^{2+}$ and $Fe^{2+}$ did not show any effect on the *Cf*DXS activity. The different concentrations (0.1 to 1 mM) of $Mg^{2+}$ were used. The most effective concentration was found to be 1 mM.

The $K_m$ for substrate pyruvate and G3P determined were 4.4 and 8.8 µM, respectively. The $K_m$ for the cofactor TPP was measured 62 µM. The $V_{max}$ of the *Cf*DXS measured were 20, 17 and 200 $\mu M^{-1} min^{-1}$, respectively of the pyruvate, G3P, pyruvate and TPP.

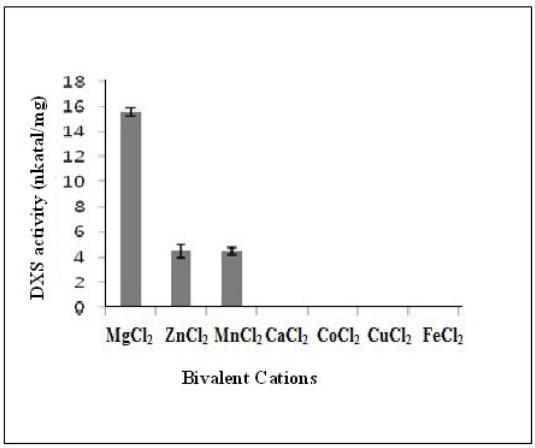


**Figure 7.** Effects of various metal ions (1mM) on *Cf*DXS activity.

## Discussion

Very recently, the MEP pathway has been elucidated from the lemongrass (Gupta and Ganjewala 2015), which is utilized for the biosynthesis of the citral, a major monoterpene constituent of the lemongrass oil. The first step, which is also a regulatory step of the MEP pathway is catalyzed by the DXS enzyme, which is believed to control and regulate the over all rate of the biosynthesis of the citral. In view of the regulatory roles of the DXS in the MEP pathway, here we carried out its purification and characterization from the lemongrass cv. Suvarna immature leaves. Earlier, we carried out purification and characterization of the DXR enzyme, which catalyzes the second regulatory step of the MEP pathway (Gupta and Ganjewala 2015c).

The purification and characterization of both these regulatory enzymes have provided deeper knowledge of their kinetic parameters and catalytic principles, which has been very useful for understanding their roles in control and regulation of the substrates/precursor supply *via* the MEP pathway in lemongrass and other plants. Here, we used the similar three step procedures for purification of the *Cf*DXS, which was used earlier for the C*f*DXR with minor modifications. Due to the rate limiting nature of the DXS, we extracted it from the second leaf of a fully-grown tiller of lemongrass. The second leaf represents rapidly growing stage of the leaf development and biogenetically most active in the synthesis and accumulation of the essential oil. Hence, a very high CfDXS activity was expected in the second leaf.

Despite, the DXS being a key enzyme of the MEP pathway is present at very low concentration in cellular systems, therefore highly sensitive methods are required to detect the DXP production. The quantification of the DXP in living cells is performed by using recombinant technique (Lois et al. 1998), spectrofluorometer (Querol et al. 2001) and spectrophotometric assay (Altincicek et al. 2001). The yield of purified *Cf*DXS was 32.34% with specific activity of 8.56 U/mg protein$^{-1}$. At the end of the purification procedure, purification fold was increased 12 times compared to crude enzyme extract.

The *Cf*DXS was characterized by studying different parameters *viz.,* effect of substrate concentrations, pH, temperature and metal ions on the *Cf*DXS activity. These studies have revealed that the *Cf*DXS is similar to other DXSs reported from plants, *Mentha piperita* (Bouvier et al. 1998; Lange et al. 1998), *Arabidopsis thaliana* (Estévez et al. 2001; Flores-Perez 2008), *Zea mays* (Cordoba et al. 2011), *Oryza sativa* (Kim et al. 2005) and bacteria like *Escherichia coli* (Sprenger et al. 1997) and *Agrobacterium tumefaciens* (Lee et al. 2007). Like other DXSs, the *Cf*DXS is also a TPP-dependent enzyme with high catalytic efficiency (Lee et al. 2007). Studies of kinetic parameters of the *Cf*DXS showed relatedness with a class of TPP-dependent enzymes and displayed the properties of pyruvate decarboxylases and transketolases (Hahn et al. 2001). Reaction catalyzed by the DXS proceeds in two steps. In the first step, TPP-dependent decarboxylation of pyruvate occurs, which is analogous to decarboxylation catalyzed by the pyruvate decarboxylase. In the second step, enzyme-bound thiamine-stabilized acetyl anion is then transferred to the aldehyde moiety, which is analogous to trans-ketolase reaction (Hahn et al. 2001).

The present study revealed that the *Cf*DXS was dependent on $Mg^{2+}$ ions for its activity. The $Zn^{2+}$ and $Mn^{2+}$ ions too moderately affected the *Cf*DXS activity, but $Ca^{2+}$, $Cu^{2+}$, and $Fe^{2+}$ ions showed no effect on the *Cf*DXS activity. The order (descending) of the effectiveness of metal ions was $Mg^{2+} > Zn^{2+} > Mn^{2+}$. These characters of the *Cf*DXS have been consistent with several previously reported DXSs from *A. tumefaciens* (Lee et al. 2007), *R. capsulatus* (Hahn et al. 2001), *M. tuberculosis* (Bailey et al. 2002) and *A. thaliana* (Flores-Perez et al. 2008), which required $Mg^{2+}$ as a cofactor for the activity. It is reported that the $Mg^{2+}$ helps the DXS to maintain its activity in native form, and its removal does lead to the permanent loss of the DXS activity (Bailey et al. 2002). The TPP helps in the decarboxylation of pyruvate (Hahn et al. 2001). Here, the optimum concentration (1 mM) of the TPP determined matched with the earlier published reports (Hahn et al. 2001; Lee et al. 2007; Wright and Phillips 2014). The pH optima for *Cf*DXS was 8.0 and small deviation in it caused significant decline (60 to 80%) in the *Cf*DXS. These results are in complete agreement with several previous studies, which reported the similar pH optima 7.5-8.0 for the DXS (Sprenger et al. 1997; Bouvier et al. 1998; Hahn et al. 2001; Lee et al. 2007; Wang et al. 2014; Wright and Phillips 2014).

The optimum temperature for the *Cf*DXS was 37-40 ºC. The $K_m$ for G3P (20 µM) and sodium pyruvate (4.4 µM) were found to be the same as reported previously (Lee et al.

2007; Wang et al. 2014). Relative molecular mass *Mr* of the DXS from plants such as tomato (Paetzold et al. 2010) and bacteria *viz., Haemophilus influenza* (Matsue et al. 2010), *Streptomyces* sp. strain CL190 reported was ranged from 65-70 kDa. The *Mr* of the C*f*DXS as determined by SDS-PAGE was 130 suggesting that it is most likely a dimeric enzyme. Similar dimeric DXSs with *Mr* 130 kDa have been reported previously from *Haemophilus influenzae* (Matsue et al. 1997), *Plasmodium vivax* (Handa et al. 2013) and *Streptomyces* sp. strain CL190 (Kuzuyama et al. 2000). To the best of our knowledge, this is for the first time the DXS enzyme has been purified and characterized from a member of the *Cymbopogon* genus.

## Acknowledgements

I duly acknowledge financial support (Grant No. 1235/EMR-II/2010) received from Council of Scientific and Industrial Research (CSIR), New Delhi to carry out the research work. Also, I extend my sincerest thanks to Dr. Ashok K Chauhan, founder president and Mr. Atul Chauhan, Chancellor Amity University Uttar Pradesh, Noida, India for providing necessary support and facilities.

## References

Altincicek B, Hintz M, Sanderbrand S, Wiesner J, Beck E, Jomaa H (2000). Tools for discovery of inhibitors of the 1-deoxy-D-xylulose 5-phosphate (DXP) synthase and DXP reductoisomerase: an approach with enzymes from the pathogenic bacterium *Pseudomonas aeruginosa*. FEMS Microbiol Lett 190:329-333.

Bailey AM, Mahapatra S, Brennan PJ, Crick DC (2002) Identification, cloning, purification, and enzymatic characterization of *Mycobacterium tuberculosis* 1-deoxy-D-xylulose 5-phosphate synthase. Glycobiol 12:813-820.

Bouvier F, d'Harlingue A, Suire C, Backhaus RA, Camara B (1998) Dedicated roles of plastid transketolases during the early onset of isoprenoid biogenesis in pepper fruits. Plant Physiol 117:1423-1431.

Bradford MM (1976) A rapid and sensitive method for the quantitative determination of microgram quantities of protein utilizing the principle of protein-dye binding. Anal Biochem 72:248-254.

Cordoba E, Porta H, Arroyo A, San RC, Medina L, Rodríguez-Concepción M, León P (2011) Functional characterization of the three genes encoding 1-deoxy-D-xylulose 5-phosphate synthase in maize. J Exp Bot 62:2023-2038.

Dudareva N, Andersson S, Orlova I, Gatto N, Reichelt M, Rhodes D, Boland W, Gershenzon J (2005) The non-mevalonate pathway supports both monoterpene and sesquiterpene formation in snapdragon flowers. Proc Nat Acad Sci (USA) 102:933-938.

Eisenreich W, Schwarz M, Cartayrade A, Arigoni D, Zenk MH, Bacher A (1998) The deoxyxylulose phosphate pathway of terpenoid biosynthesis in plants and microorganisms. Chem Bio 5:221-233.

Estévez JM, Cantero A, Reindl A, Reichler S, León P (2001) 1-Deoxy-D-xylulose 5-phosphate synthase, a limiting enzyme for plastidic isoprenoid biosynthesis in plants. J Biol Chem 76:22901-22909.

Farmer WR, Liao JC (2001). Precursor balancing for metabolic engineering of lycopene production in *Escherichia coli*. Biotechnol Prog 17:57-61.

Flores-Pérez Ú, Sauret-Güeto S, Gas E, Jarvis P, Rodríguez-Concepción M (2008) A mutant impaired in the production of plastome-encoded proteins uncovers a mechanism for the homeostasis of isoprenoid biosynthetic enzymes in *Arabidopsis* plastids. Plant Cell 20:1303-1315.

Ganjewala D, Gupta AK (2013) Lemongrass (*Cymbopogon flexuosus* Steud.) Wats essential oil:overview and biological activities. In Govil JN, Bhattacharya S, ed., Recent Progress in Medicinal Plants Vol 37: Essential oils II, Studium Press LLC, 235-271.

Ganjewala D, Gupta AK, Muhury R (2012) An update on bioactive potential of a monoterpene aldehyde citral. J Biol Active Prod Nat 2:186-199.

Ganjewala D, Kumar S, Luthra, R (2009) An account of cloned genes of methyl-erythritol 4-phosphate pathway of isoprenoids biosynthesis in plants. Curr Issues Mol Biol S1:35-45.

Ganjewala D, Luthra R (2007) Inhibitors of essential oil biosynthesis in *Cymbopogon flexuosus* Nees ex. Steud. mutant cv. GRL-1 leaves. Am J Plant Physiol 2:227-232.

Ganjewala D, Luthra R (2010) Essential oil biosynthesis and regulation in genus *Cymbopogon*. Nat Prod Commun 5:163-172.

Gupta AK, Ganjewala D (2015a) A study on developmental changes in essential oil content and composition in *Cymbopogon flexuosus* cultivar Suvarna. Acta Biol Szeged 59:119-125.

Gupta AK, Ganjewala D (2015b) A study on biosynthesis of "citral" in lemongrass (*C. flexuosus)* cv. Suvarna. Acta Physiol Plant 37:1-8.

Gupta AK, Ganjewala D (2015c) Purification and characterization of the 1-Deoxy-D-xylulose-5-phosphate reductoisomerase from *Cymbopogon flexuosus* leaves. Res J Pharm Technol 8:320-327.

Hahn F, Eubanks M, Testa LM, Blagg CA, Baker JA, Poulter CD (2001) 1-Deoxy-d-xylulose 5-phosphate synthase, the gene product of open reading frame (ORF) 2816 and ORF 2895 in *Rhodobacter capsulatus*. J Bacteriol 183:1-11.

Handa S, Ramamoorthy D, Spradling TJ, Guida WC, Adams JH, Bendinskas KG, Merkler DJ (2013) Production of recombinant 1-deoxy-D-xylulose 5-phosphate synthase from *Plasmodium vivax* in *Escherichia coli*. FEBS Open Bio 3:124-129.

Kim BR, Kim SU, Chang YJ (2005) Differential expression of three 1-deoxy-D-xylulose-5-phosphate synthase genes in rice. Biotechnol Lett 27:997-1001.

Kuzuyama T, Seto H, Kamiya Y, Leon P (2000) Analysis of the expression of *CLA1*, a gene that encodes the 1-deoxy-D-xylulose-5-phosphate synthase of the 2-C-methyl-D-erythritol-4-phosphate pathway in *Arabidopsis*. Plant Physiol 124:95-103.

Laemmli UK (1970) Cleavage of structural protein during the assembly of the head of bacteriophage T4. Nature 227:680-685.

Lange BM, Wildung MR, McCaskill D, Croteau R (1998) A family of transketolase that directs isoprenoid biosynthesis via a mevalonate independent pathway. Proc Nat Acad Sci USA 95:2100-2104.

Lee JK, Oh DK, Kim SY (2007) Cloning and characterization of the DXS gene, encoding 1-deoxy-D-xylulose 5-phosphate synthase from *Agrobacterium tumefaciens*, and its overexpression in *Agrobacterium tumefaciens*. J Biotech 128:555-566.

Lichtenthaler HK (1999) The plants 1-deoxy-D-xylulose 5-phosphate pathway for biosynthesis of isoprenoid. Lipid 100:128-138.

Lois LM, Campos N, Putra SR, Danielsen K, Rohmer M, Boronat A (1998) Cloning and characterization of a gene from *Escherichia coli* encoding a transketolase-like enzyme that catalyzes the synthesis of 1-deoxy-D-xylulose 5-phosphate, a common precursor for isoprenoid, thiamin, and pyridoxol biosynthesis. Proc Nat Acad Sci USA 95:2105-2110.

Matsue Y, Mizuno H, Tomita T, Asami T, Nishiyama M, Kuzuyama T (2010) The herbicide ketoclomazone inhibits 1-deoxy-D-xylulose 5-phosphate synthase in the 2-C-methyl-D-erythritol 4-phosphate pathway and shows antibacterial activity against *Haemophilus influenzae*. J Antibiot 63:583-588.

Mirghani MES, Liyana Y, Parveen J (2012) Bioactivity analysis of lemongrass (*Cymbopogan citratus*) essential oil. Int Food Res J 19:569-575.

Olorunnisola SK, Hammed AM, Simsek S (2014) Biological properties of lemongrass: an overview. Int Food Res J 21:455-462.

Paetzold H, Garms S, Bartram S, Wieczorek J, Urós-Gracia EM, Rodríguez-Concepción M, Boland W, Strack D, Hause B, Walter MH (2010) The isogene 1-deoxy-D-xylulose 5-phosphate synthase 2 controls isoprenoid profiles, precursor pathway allocation, and density of tomato trichomes. Mol Plant 3:904-916.

Querol J, Besumbes O, Lois LM, Boronat A, Imperial S (2001) A fluorometric assay for the determination of 1-deoxy-D-xylulose 5-phosphate synthase activity. Anal Biochem 296:101-105.

Rohmer M, Knani M, Simonin P, Sutter B, Sahm H (1993) Isoprenoid biosynthesis in bacteria: A novel pathway for early steps leading to isopentenyl diphosphate. Biochem J 295:517-524.

Seemann M, Tse Sum Bui B, Wolff M, Miginiac-Maslow M, Rohmer M (2006) Isoprenoid biosynthesis in plant chloroplasts via the MEP pathway: Direct thylakoid/ferredoxin-dependent photoreduction of GcpE/IspG. FEBS Letters 580:1547-1552.

Shah G, Shri R, Panchal V, Sharma N, Singh B, Mann AS (2011) Scientific basis for the therapeutic use of *Cymbopogon citratus*, stapf (Lemongrass). J Adv Pharm Tech Res 2:3-8.

Sprenger GA, Scharken U, Weigert T, Grolle S, de Graaf AA (1997) Identification of thiamine dependent synthase in *Escherichia coli* required for the formation of 1-deoxy-D-xylulose 5-phosphate precursor to isoprenoids, thiamine and pyridoxal. Proc Nat Acad Sci USA 94:12857-12862.

Wang J, Shen Y-M, Li B, Zhou X-z, Liu C-c, Zhang J-y (2014) Characterization of a functionally active recombinant 1-deoxy-D-xylulose 5-phosphate synthase from *Babesia bovis*. J Vet Med Sci 76:1021-1027.

Wright LP, Phillips MA (2014) Measuring the activity of 1-deoxy-D-xylulose 5-phosphate synthase, the first enzyme in the MEP pathway, in plant extracts. Methods Mol Biol 1153:9-20.

**Volume 61(2):157-162, 2017**
**Acta Biologica Szegediensis**
http://www2.sci.u-szeged.hu/ABS

**ARTICLE**

# Pollen morphology of *Senecio* L. and *Iranecio* B. Nord. (Asteraceae: Senecioneae) in Iran

Rosa Eftekharian[1]*, Masoud Sheidai[1], Farideh Attar[2], Zahra Noormohammadi[3]

[1]Faculty of Life Sciences & Biotechnology, Shahid Beheshti University, Tehran, Iran
[2]Faculty of Biological Sciences, University of Tehran, Tehran, Iran
[3]Department of Biology, Science and Research Branch, Islamic Azad University, Tehran, Iran

**ABSTRACT** The genus *Senecio* L. is one of the largest genera in the family Asteraceae. The number of taxa included in this genus is 1250. Pollen morphology has proved useful in the systematics of Asteraceae as well as in that of some of its genera and species. The pollen morphology of 16 taxa of the genus *Senecio* and *Iranecio* was investigated in detail by scanning electron microscopy (SEM). Examination showed pollen grains to be isopolar and radiosymmetric, prolate spheroidal. The close relationships are observed between the species of the section *Quadridentati* and the genus *Iranecio*. The species of the section *Jacobaea* showed a palynological overlap with the section *Senecio*. The results indicate that the palynological characters of the genus *Senecio* are valuable for taxonomic applications and are useful for classification.
**Acta Biol Szeged 61(2):157-162 (2017)**

**KEY WORDS**
*Iranecio*
palynological characters
pollen
scanning electron microscopy
*Senecio*

## Introduction

The Asteraceae is the most numerous family of the Angiosperms, with approximately 23.600 species (Montes and Murray 2015). Senecioneae is one of the largest tribe in the family with more than 3000 species in 150 genera (Pelser et al. 2007), classified into three subtribes; Blennospermatinae, Senecioninae, and Tussilagininae. Approximately one-third of Senecioneae species are placed in the genus *Senecio*, making it one of the largest genera of flowering plants (Willis 1918).

Nordenstam (1989) transferred some species of *Senecio* into the genus *Iranecio* B. Nord. and introduced 4 sections and 17 taxa of this genus in Iran. The genus *Senecio* after Nordenstam (1989) draft of Flora Iranica has been subject of several studies; partly circumscription of the genus has been changed. Jeffrey (1992) based on anatomical characteristics of what transferred species that belonged to *Senecio* sect. *Quadridentati* Boiss. to the genus *Iranecio*. Also, Pelser et al. (2006) and Nordenstam (2006) based on molecular systematic studies regarded the section *Jacobaea* (Mill.) Dumort. as a distinct genus.

Pollen morphology has been proved to be useful in the systematics of the Asteraceae family as well as that of some of its genera and species (Moore et al. 1991). Osman (2011) defined the *Senecio* pollen type for the tribe Senecioneae as tricolporate. Montes and Murray (2015) showed the presence of the mesoaperture in the *Senecio bergii* Hieron pollen contributes to the general knowledge of the *Senecio* pollen type. Moreover, it will be of importance in the taxonomic delimitation of species in this genus.

The present study aims to study general pollen morphological characters and to assess their taxonomical value in separation of taxa in different level.

## Materials and Methods

We employed SEM in order, to conduct palynological studies of 14 species of the genus *Senecio* belonging to four sections (Nordenstam 1989):

a) *Crociseris* – *S. pseudo-orientalis* Schischk., *S. doriiformis* subsp. *orientalis* (Fenzl) V. A. Matthews., *S. paulsenii* subsp. *khorasanicus* (Rech.f. & Aellen) B.Nord.

b) *Quadridentati* – *S. taraxacifolius* (M. B.) DC., *S. davisii* Matthews., *S. lipskyi* Lomak.

c) *Jacobaea* – *S. mollis* Willd, *S. erucifolius* subsp. *grandidentatus* (Ledeb.) V.E.A vet.

d) *Senecio* – *S. glaucus* L., *S. vulgaris* L., *S. breviflorus* (Kadereit) Greuter, *S. leucanthemifolius* subsp. *vernalis* (Waldst. & Kit.) Greuter, *S. iranicus* B. Nord., *S. kotschyanus* Boiss.

Submitted June 17, 2017; Accepted October 3, 2017
*Corresponding author. E-mail: rozaeftekharian@yahoo.com

**Table 1.** List of studied taxa of *Senecio* and *Iranecio* (Asteraceae) with localities and voucher numbers.

| Section/Species | Locality | N | E | Alt (m) | Voucher number |
|---|---|---|---|---|---|
| *Senecio* | | | | | |
| *S. breviflorus* | Karaj, Azimieh | 51.00 | 35.50 | 1469 | HSBU-4369 |
| *S. kotschyanus* | Kerman, Gughar village | 57.14 | 29.26 | 3059 | TUH-23455 |
| *S. iranicus* | Mazandaran, Polur | 52.02 | 35.51 | 4300 | IRAN-53397 |
| *S. vulgaris* | Tehran,Velenjak | 51.23 | 35.48 | 1758 | HSBU-4372 |
| *S. glaucus* | Kashan, Abyaneh | 51.35 | 33.35 | 2216 | HSBU-4373 |
| *S. leucanthemifolius subsp. vernalis* | Mazandaran, Alasht | 52.50 | 36.04 | 1684 | HSBU-4375 |
| *Crociseris* | | | | | |
| *S. paulsenii subsp. khorasanicus* | Mazandaran, Balade to Noor | 51.55 | 36.24 | 919 | TUH- 38605 |
| *S. pseudo-orientalis* | West Azarbaijan, Shahindej | 46.41 | 36.32 | 1799 | TARI-69861 |
| *S. doriiformis subsp. orientalis* | Kordestan, Paveh | 46.21 | 35.03 | 2600 | TUH-7980 |
| *Quadridentati* | | | | | |
| *S. taraxacifolius* | East Azarbaijan, Bostanabad | 46.41 | 37.54 | 3700 | TARI-48593 |
| *S. lipskyi* | East Azarbaijan, Mishodagh | 45.47 | 38.13 | 1911 | TUH-11951 |
| *S. davisii* | West Azarbaijan, Silvana | 73.57 | 40.48 | 35 | TARI-69903 |
| *Jacobaea* | | | | | |
| *S. erucifolius subsp. grandidentatus* | Golestan, Gorgan | 55.39 | 37.21 | 531 | IRAN-35506 |
| *S. mollis* | Kordestan, Sanandaj | 47.05 | 35.39 | 2056 | TUH-40393 |
| *Iranecio* | | | | | |
| *I. elbursensis* | Tehran, Chlus road, Gachsar, Dizin | 52.12 | 39.39 | 1856 | TUH-6981 |
| *I. oligolepis* | Mazandaran, Rineh, kuh-e Damavand | 49.41 | 36.02 | 1700 | IRAN-10430 |

**Table 2.** Palynological characters of studied taxa. P: polar axis; E: equatorial diameter; P/E: ratio of polar axis to equatorial diameter; SL: spine length; SW: spine width; SN: spine number; PN: perforation number; ISD: interspine distance; IPD: interperforation distance; PP/SL: perforated part/spine length. Units for quantitative characters.

| Taxa | P | E | P/E | SL | SW | SN | PN | ISD | IPD | PP/SL |
|---|---|---|---|---|---|---|---|---|---|---|
| *S. breviflorus* | 26.26 ± 1.70 | 23.21 ± 1.25 | 1.13 ± 0.74 | 2.14 ± 0.04 | 2.30 ± 0.08 | 8 | 20 | 1.06 ± 2.34 | 0.28 ± 1.12 | 1 |
| *S. kotschyanus* | 24.91 ± 1.23 | 22.40 ± 1.19 | 1.11 ± 0.54 | 2.85 ± 0.54 | 3.00 ± 0.05 | 8 | 30 | 0.85 ± 2.11 | 0.28 ± 1.47 | 1 |
| *S. iranicus* | 22.35 ± 1.55 | 20.29 ± 1.28 | 1.11 ± 0.56 | 3.00 ± 0.11 | 2.65 ± 0.09 | 8 | 25 | 1.05 ± 2.24 | 0.26 ± 1.24 | 1 |
| *S. vulgaris* | 25.33 ± 1.27 | 22.42 ± 1.30 | 1.12 ± 0.67 | 3.72 ± 0.03 | 3.30 ± 0.10 | 8 | 20 | 1.17 ± 2.19 | 0.30 ± 1.30 | 1 |
| *S. glaucus* | 22.80 ± 1.34 | 21.00 ± 1.09 | 1.08 ± 0.49 | 3.08 ± 0.10 | 2.51 ± 0.08 | 8 | 35 | 1.05 ± 2.43 | 0.28 ± 1.62 | 1 |
| *S. leucanthemifolius* | 19.95 ± 1.43 | 18.03 ± 1.21 | 1.10 ± 0.33 | 2.65 ± 0.13 | 1.80 ± 0.11 | 8 | 20 | 1.18 ± 2.27 | 0.28 ± 1.52 | 1 |
| *S. paulsenii* | 30.81 ± 1.63 | 28.52 ± 1.12 | 1.08 ± 0.52 | 3.03 ± 0.16 | 2.55 ± 0.17 | 6 | 5 | 1.17 ± 2.49 | 0.50 ± 1.39 | 2 |
| *S. pseudo-orientalis* | 30.34 ± 1.82 | 27.60 ± 1.22 | 1.09 ± 0.67 | 3.42 ± 0.11 | 2.47 ± 0.21 | 6 | 15 | 1.47 ± 2.31 | 0.34 ± 1.45 | 2 |
| *S. doriiformis* | 27.63 ± 1.72 | 25.20 ± 1.39 | 1.09 ± 0.82 | 3.43 ± 0.06 | 3.10 ± 0.16 | 6 | 15 | 1.37 ± 2.10 | 0.37 ± 1.19 | 2 |
| *S. taraxacifolius* | 32.50 ± 1.18 | 30.10 ± 1.09 | 1.07 ± 0.71 | 3.00 ± 0.16 | 3.14 ± 0.05 | 4 | 5 | 2.4 ± 2.92 | 0.32 ± 1.13 | 2 |
| *S. lipskyi* | 33.61 ± 1.39 | 29.30 ± 1.73 | 1.14 ± 0.84 | 2.85 ± 0.19 | 2.93 ± 0.25 | 4 | 12 | 2.27 ± 3.20 | 0.30 ± 1.37 | 2 |
| *S. davisii* | 36.82 ± 1.90 | 33.12 ± 2.04 | 1.11 ± 0.77 | 3.20 ± 0.23 | 3.30 ± 0.09 | 4 | 5 | 2.43 ± 2.89 | 0.36 ± 1.41 | 2 |
| *S. erucifolius* | 24.00 ± 1.13 | 22.30 ± 1.95 | 1.07 ± 0.12 | 2.36 ± 0.17 | 2.00 ± 0.10 | 7 | 30 | 1.11 ± 2.68 | 0.30 ± 2.01 | 1 |
| *S. mollis* | 25.20 ± 1.22 | 23.71 ± 1.87 | 1.06 ± 0.10 | 2.42 ± 0.11 | 2.30 ± 0.22 | 7 | 30 | 1.16 ± 3.42 | 0.33 ± 1.87 | 1 |
| *I. elbursensis* | 35.00 ± 2.66 | 32.10 ± 2.97 | 1.09 ± 0.37 | 2.90 ± 0.21 | 3.00 ± 0.29 | 4 | 10 | 2.45 ± 2.21 | 0.35 ± 2.31 | 2 |
| *I. oligolepis* | 31.50 ± 3.01 | 28.91 ± 2.55 | 1.08 ± 0.09 | 3.00 ± 0.07 | 3.10 ± 0.32 | 4 | 5 | 2.40 ± 2.75 | 0.40 ± 1.97 | 2 |

In this study four species of the genus *Senecio* (*S. kotschyanus*, *S. iranicus*, and *S. vulcanicus*) are endemic to Iran.

We also studied two species of the genus *Iranecio*: *I. elbursensis* and *I. oligolepis* are endemic to Iran. Voucher specimens are listed in Table 1 and deposited in the Central Herbarium of Tehran University (TUH), Herbarium of the Iranian Research Institute of Plant Protection (IRAN), the Herbarium of Shahid Beheshti University (HSBU) and Research Institute of Forests and Rangelands Tehran (TARI).

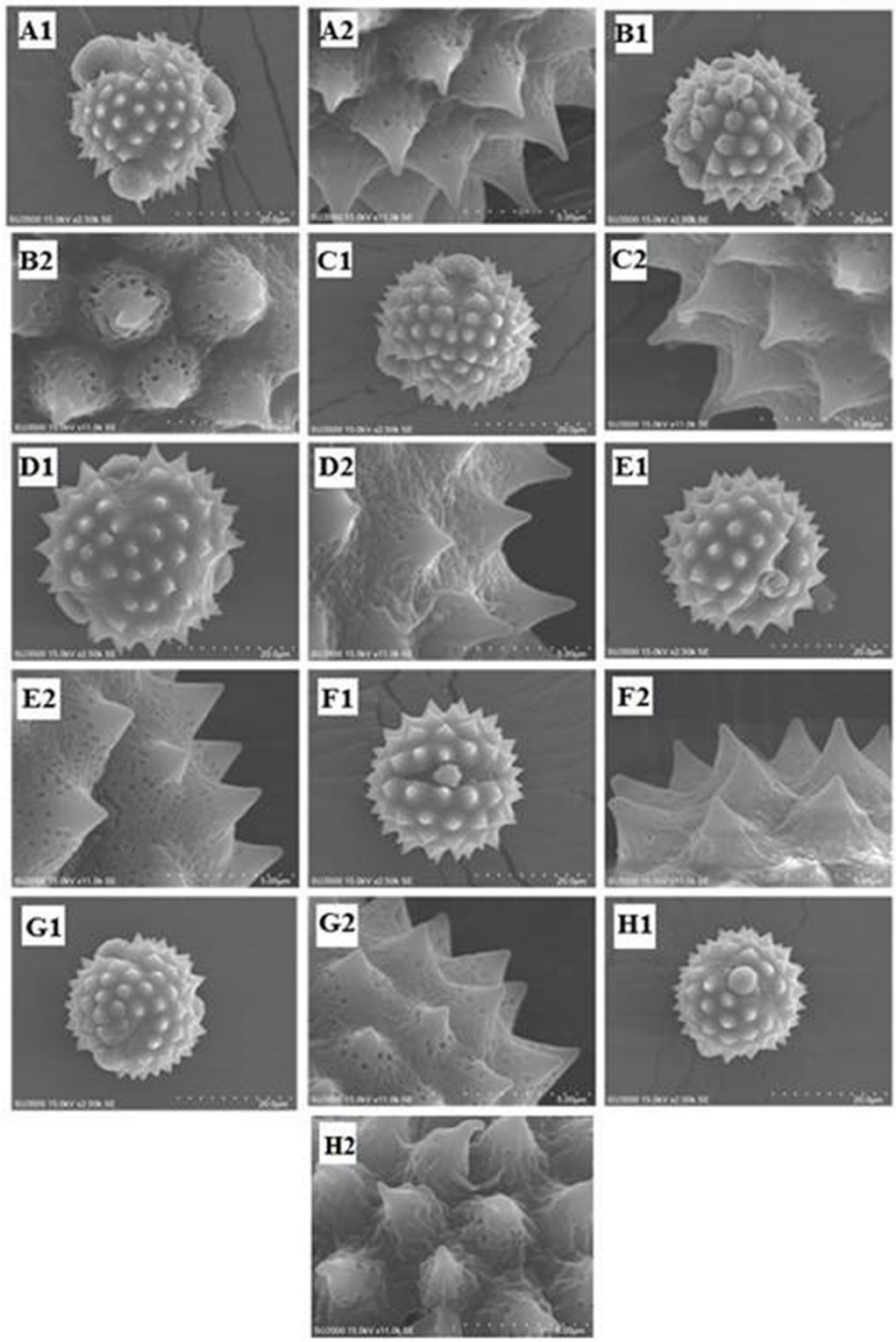


**Figure 1.** SEM photographs show pollen grain morphology of the studied species of genus *Senecio* L. (Asteraceae). A1-A2: *S. pseudo-orientalis*; B1-B2: *S. doriiformis* subsp. *orientalis*; C1-C2: *S. paulsenii* subsp. *khorasanicus*; D1-D2: *S. davisii*; E1-E2: *S. lipskyi*; F1-F2: *S. taraxacifolius*; G1-G2: *S. mollis*; H1-H2: *S. erucifolius subsp. grandidentatus*. The first photographs represent general view of the pollen grains and the second ones show the details of the surface ornamentation.

The study using scanning electron microscopy (SEM) was performed on 16 taxa representing 14 species of the genus *Senecio* and 2 species of the genus *Iranecio* (Table 1). Palynological characters were randomly measured by using minimum 50 pollen grains of 15 individuals belong to 3 populations and the means were used in analyses. We studied a total of 10 quantitative and qualitative pollen characters (Table 2). The specimens were examined and photographed

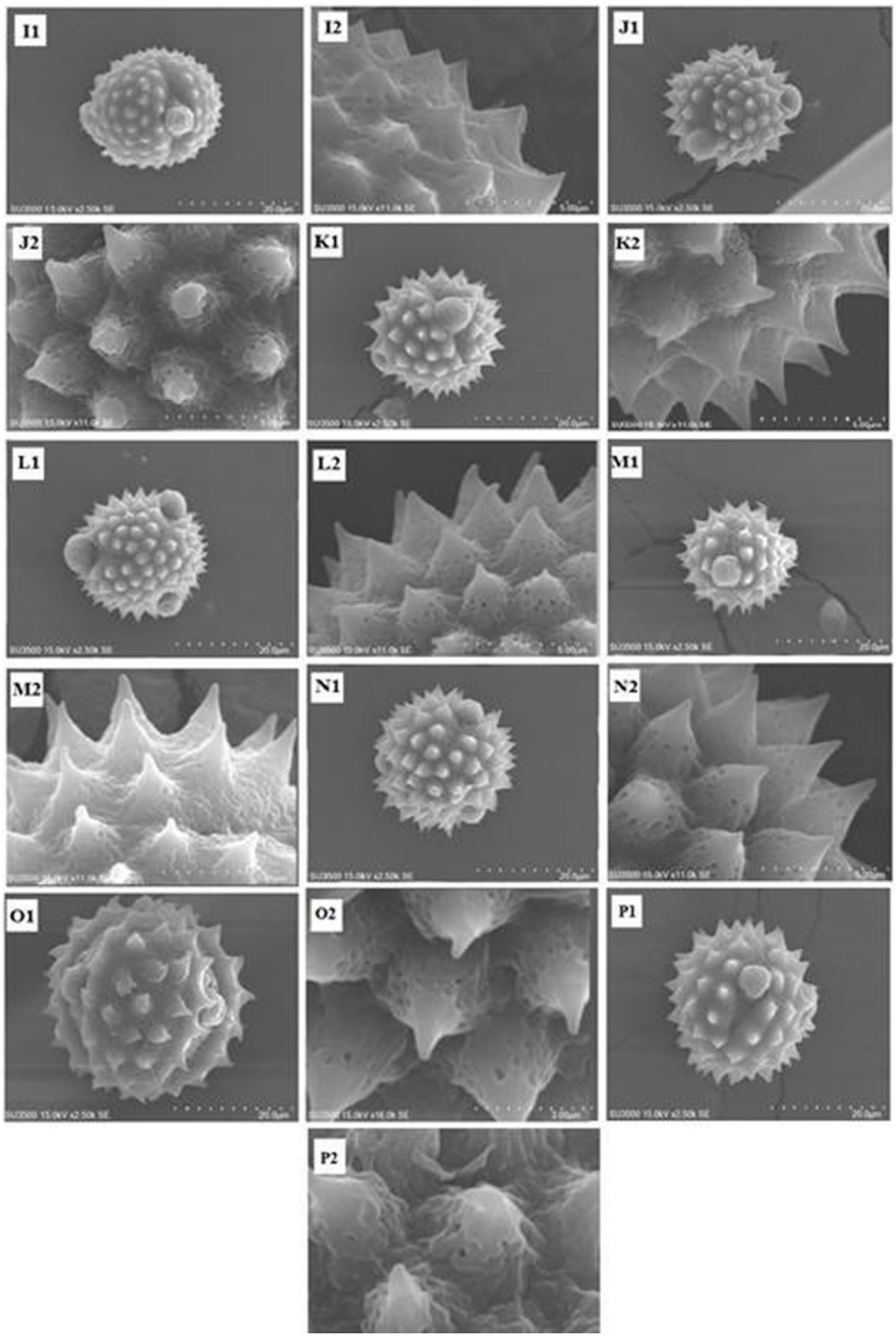


**Figure 2.** SEM photographs show pollen grain morphology of the studied species of genus *Senecio* L. and *Iranecio* L. (Asteraceae). I1-I2: *S. breviflorus*; J1-J2: *S. glaucus*; K1-K2: *S. iranicus*; L1-L2: *S. kotschyanus*; M1-M2: *S. leucanthemifolius* subsp. *vernalis*; N1-N2: *S. vulgaris*; O1-O2: *I. elbursensis*; P1-P2: *I. oligolepis*. The first photographs represent general view of the pollen grains and the second ones show the details of the surface ornamentation.

with a scanning electron microscope (SU3500; HITACHI, Japan) at an accelerating voltage of 20 kV. The terminology follows mainly Erdtman (1952).

Statistical analyses including PCA were performed using PAST ver. 2.17 software for plotting variation among populations and species (Hammer et al. 2009).

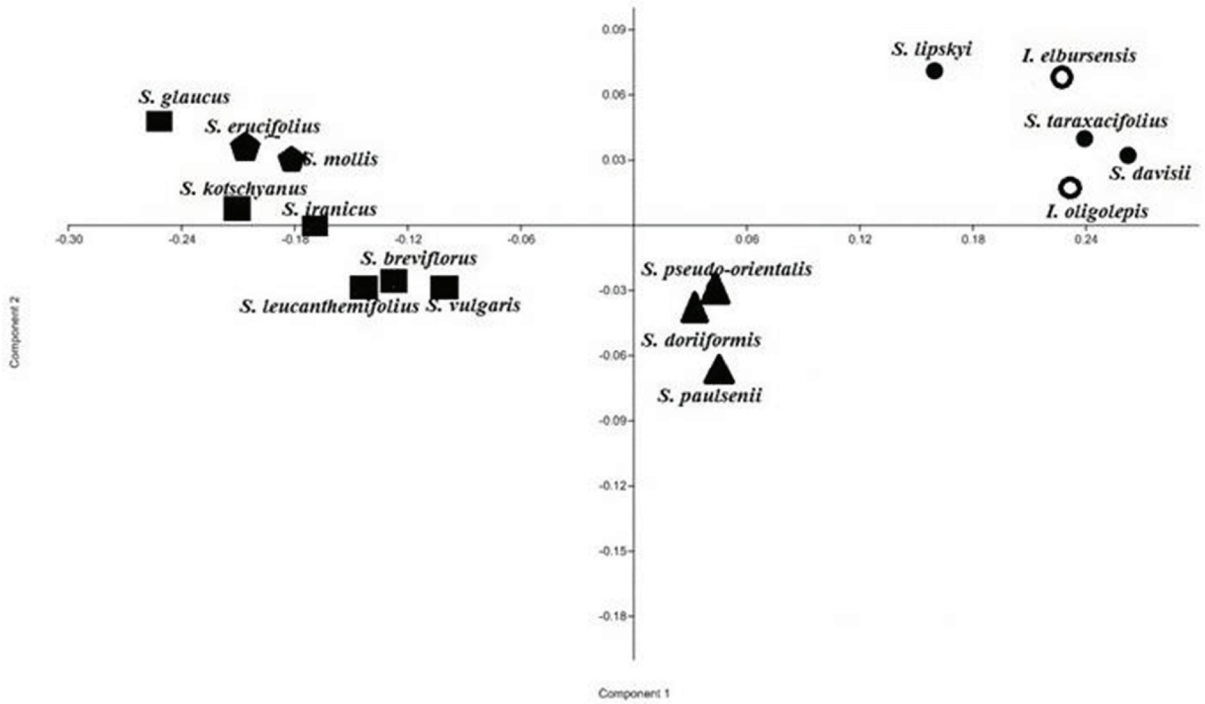


**Figure 3.** PCA plot of palynological characters.

## Results

In the present study, the pollen grains of 14 species from 4 sections belong to the genus *Senecio* and 2 species belong to the genus *Iranecio* were investigated and SEM micrographs of all species were taken (Figs. 1, 2).

Pollen grains are isopolar and radiosymmetric, prolate-spheroidal. Their apertures are tricolporate. Polar diameters of the pollen grains ranged from 19.95 µm (*S. leucanthemifolius* sect. *Senecio*) to 36.82 µm (*S. davisii* sect. *Quadridentati*) and the equatorial diameters ranged from 1.06 µm (*S. leucanthemifolius* sect. *Senecio*) to 33.12 µm (*S. davisii* sect. *Quadridentati*) (Table 2).

According to the 16 analyzed species, the P/E ratio varied from 1.06 (*S. mollis* sect. *Jacobaea*) to 1.14 (*S. lipskyi* sect. *Quadridentati*). Spine length varied from 2.14 (*S. breviflorus*) to 3.72 µm (*S. vulgaris*). The largest number of spines was found in the species of sect. *Senecio*, (8) while species of the section *Quadridentati* and the genus *Iranecio* had the lowest numbers of spine (4). The widest distances between spines were determined in *S. davisii* sect. *Quadridentati* and *I. elbursensis* (2.45 µm) and the shortest in *S. kotschyanus* sect. *Senecio* (0.85 µm).

PCA analysis revealed that the first three components comprised about 88% of the total morphological variability. Palynological characters like spine number, perforation number and length of perforated part/spine length ratio showed the highest positive correlation (>0.80) with the first PCA component, while interspine distance and interperforation distance showed the highest positive correlation (>0.50) with the second PCA component. These characters may be use in the taxonomy of the genus and the delimitation of *Senecio* species.

The PCA plot (Fig. 3) separated the studied species into three groups. The species of the section *Quadridentati* were placed close to the species of the genus *Iranecio* (showing palynological similarities) and formed first group. Also, the species of the section *Senecio* and *Jacobaea* were grouped together (second group) and the species of the section *Crociseris* were placed close to each other and formed third group.

## Discussion

Species delimitation in the genus *Senecio* is considered to be a taxonomic and phylogenetic importance that can be

achieved through molecular studies (Pelser et al. 2007). In our study, palynological characters could delimit the studied *Senecio* species.

In this study, the results of PCA plot based on palynological characters showed seperation of the species of the section *Quadridentati* from the other species of *Senecio*. The species of the section *Quadridentati* were placed close to the species of the genus *Iranecio.* Jeffrey (1992) based on anatomy characters transferred the species of the sect. *Quadridentati* to the genus *Iranecio*. Therefore, the present study supports this transfer and shows close affinity between the species of the section *Quadridentati* and the species of the genus *Iranecio* based on palynological characters.

Molecular studies using nuclear and plastid DNA have been used to resolve phylogenetic relationships within the genus *Senecio* (Greuter 2008; Nordenstam et al. 2009; Hamzaoglu et al. 2011). In some of these studies, molecular results have conflicted with morphological classification. For example, the section *Jacobaea* has been considered to be a distinct genus (Pelser et al. 2006) accompanied by a morphological overlap shared with several species of *Senecio*. In the present study, the species of the section *Senecio* and the section *Jacobaea* were grouped together showing palynological overlap. The species of the section *Crociseris* were placed close to each other. The palynological characters used could also delimit the species of the section *Crociseris*.

Species delimitation is the first step toward understanding the evolution of plants and mechanisms of their divergence. However, it is a very difficult task in plant species with recent speciation events and the complex species that faced hybridization and reticulate evolution in their history (Medrano et al. 2014). In our study, palynological characters could delimit the studied *Senecio* and *Iranecio* species. Also, palynological data could approve the transfer of the section *Quadridentati* to the genus *Iranecio*. In the present study, pollen characters (perforated part/spine length, spine number and spine length) proved to be useful characters for classification. Therefore morphological, anatomical, palynological and molecular studies could help resolve problems related to the taxonomy of *Senecio*.

## Acknowledgements

The authors are grateful to Mr. Amini and Ms. Sajedi of Iranian Research Institute of Plant Protection.

## References

Erdtman G (1952) Pollen Morphology and Plant Taxonomy. Stockholm. Almqvist & Wiksell.

Greuter W (2008) *Senecio* L. In Greuter W, Raab-Straube E, von eds., Med-Checklist, Dicotyledones (Compositae). Vol 2. Conservatoire et Jardin botaniques de la Ville de Genève, Switzerland. pp.711-720.

Hammer Ø, Harper DAT, Ryan PD (2009) PAST-PAlaeontological STatistics, ver.1.89. University of Oslo, Oslo, 1-31.

Hamzaoğlu E, Budak U, Aksoy A (2011) A new genus, Turanecio, of the Asteraceae (tribe Senecioneae). Turk J Bot 35:479-508.

Jeffrey C (1992) Notes on Compositae, VI: The tribe Senecioneae (Compositae) in the Mascarene Islands with an annotated world check-list of the genera of the tribe. Kew Bull 47:49-109.

Medrano M, López-Perea E, Herrera CM (2014) Population genetics methods applied to a species delimitation problem: Endemic trumpet daffodils (*Narcissus* section *Pseudonarcissi*) from the Southern Iberian Peninsula. Int J Plant Sci 175:501-517.

Montes B, Murray MG (2015) Pollen morphology of *Senecio bergii* (Asteraceae) with special attention to the mesoaperture. Phyton 84:201-208.

Moore PD, Webb JA, Collinson ME (1991) Pollen Analysis. 2nd ed., Blackwell Scientific, Oxford.

Nordenstam B (1989) Tribus Senecioneae. In Rechinger KH eds, Flora Iranica, Akademische Druck- und Verlagsanstalt, Graz.

Nordenstam B (2006) Additions to the genus *Jacobaea* Mill. (Compositae-Senecioneae). Compos Newsl 44:12-13.

Nordenstam B, Pelser PB, Kadereit JW, Watson LE (2009) Senecioneae. In Funk VA, Susanna A, Stuessy T, Bayer R, eds., Systematics, Evolution & Biogeography of the Compositae. Vienna, Austria. pp. 503-525.

Osman AK (2011) Numerical taxonomic study of some tribes of Compositae (subfamily Asteroideae) from Egypt. Pak J Bot 43:171-180.

Pelser PB, Nordenstam B, Kadereit JW, Watson LE (2007) An ITS phylogeny of tribe Senecioneae (Asteraceae) and a new delimitation of *Senecio* L. Taxon 56:1077-1104.

Pelser PB, Veldkamp JF, van der Meijden R (2006) New combinations in *Jacobaea* Mill. (Asteraceae: Senecioneae). Compos Newsl 44:1-11.

Willis JC (1918) The age and area hypothesis. Science 47:626.

**Volume 61(2):163-171, 2017**
**Acta Biologica Szegediensis**
http://www2.sci.u-szeged.hu/ABS

**ARTICLE**

# Modulation of nickel toxicity by glycinebetaine and aspirin in *Pennisetum typhoideum*

Roseline Xalxo, Bhumika Yadu, Piu Chakraborty, Vibhuti Chandrakar, Sahu Keshavkant*

School of Studies in Biotechnology, Pt. Ravishankar Shukla University, Raipur 492 010, India

**ABSTRACT** Germinated *Pennisetum typhoideum* seeds were grown under phytotoxic amount of nickel (Ni) and its combinations with aspirin (Asp) and/or glycinebetaine (GB). The results revealed that exposure to Ni caused reduced growth and membrane stability index of *P. typhoideum*, which were correlated with the accumulated Ni and reactive oxygen species. Oxidative stress markers; malondialdehyde, 4-hydroxy-2-nonenal and lipoxygenase were also elevated by Ni, while were diminished significantly by exogenously applied Asp and/or GB. However, considerable loss in protein and DNA contents were discernible in Ni subjected tissues, but were stimulated largely in the Asp and/or GB applied radicles. Additionally, alteration in the activities and native-PAGE profiles of antioxidant enzymes (superoxide dismutase, catalase, guaiacol peroxidase and ascorbate peroxidase) were discernible in response to Ni, which are reputed to counterbalance the oxidative condition. However, exogenous addition of Asp and/or GB activated the defense system and uplifted proline accumulation in stressed *P. typhoideum*. The results approved that combined addition of Asp and GB performed far better in Ni-stress mitigation than their alone application. Conducted study indicated that combined application of Asp and GB served as complementary tool to confer tolerance by up-regulating the antioxidant enzymes and thus can be implicated in the mitigation of Ni-toxicity.
**Acta Biol Szeged 61(2):163-171 (2017)**

**KEY WORDS**

antioxidant enzymes
aspirin
glycinebetaine
nickel toxicity
oxidative stress

## Introduction

Nickel (Ni) is necessarily required by the plants for their normal growth/development and completion of life cycle, but is equally toxic in excess leading to altered growth and metabolism (Negi et al. 2014). It is essentially required by the enzyme urease that metabolizes the nitrogenous compounds like urea, inside the plant (Hussain et al. 2013). Therefore, its deficiency not only lowers down the nitrogen assimilation rate, but also results superoxide ($O_2^{\cdot -}$) accumulation (Negi et al. 2014). In normal course, Ni is required by the plants within 0.05 to 10 μg $g^{-1}$ dry mass (DM) for their optimum growth and development, synthesis of anthocyanin, and to resist diseases (Stanisavljevic et al. 2012). However, over accumulation of it alters metabolic status and uptake of both water and nutrients (Gajewska et al. 2012). Nickel also causes hindrance in the activities of key enzymes like amylase, protease and ribonuclease, thereby inhibited seed germination and growth responses. The most obvious symptoms of Ni-toxicity includes decreased root and shoot growth, chlorosis, necrosis, wilting, altered mineral nutrition and water relations, photosynthesis, respiration, nitrogen and carbohydrate metabolism in plants (Kazemi et al. 2010; Hussain et al. 2013).

Although, Ni is not a redox-active metal, even though studies indicate that toxicity of it is associated with production of reactive oxygen species (ROS) like; $O_2^{\cdot -}$, hydrogen peroxide ($H_2O_2$) and hydroxyl radical (·OH) consequently oxidative stress in plants. Regardless of this fact, studies on antioxidant system in Ni-stressed plants confirmed that it interferes with the defense responses (Hussain et al. 2013). Therefore, over accumulation of ROS prompts degenerative modifications in nucleic acids, proteins and lipids (Chandrakar et al. 2016a, 2017). Poly unsaturated fatty acids (PUFAs) of membrane lipid are prone to ROS assault and lipoxygenase (LOX: EC 1.13.11.12), which releases aldehydic cytotoxic products after like malondialdehyde (MDA) and 4-hydroxy-2-nonenal (4-HNE) (Chandrakar et al. 2016a). To adjust with oxidative condition plants developed an integrated network of defense system comprising both enzymatic and non-enzymatic candidates, former includes superoxide dismutase (SOD: EC 1.15.1.1), catalase (CATEC: in between CAT and EC. 1.11.1.6), ascorbate peroxidase (APX: EC 1.11.1.11) and guaiacol peroxidase (POD: EC 1.11.1.7), while later consists of α-tocopherol, ascorbic acid, glycinebetaine (GB), and pro-

Submitted May 8, 2017; Accepted July 27, 2017
*Corresponding author. E-mail: skeshavkant@gmail.com

line, which possesses free radical scavenging ability (Jafari et al. 2015; Chandrakar et al. 2016b; Yadu et al. 2017).

In the past, efforts have been made to restore normal growth and development in plants exposed to abiotic stresses including Ni (Kazemi et al. 2010; Siddiqui et al. 2013). Even though, roles of GB and/or aspirin (Asp) in the Ni-stress mitigation in plants are still to be established completely. Glycinebetaine, a compatible solute, largely accumulates in stressed tissues (Lou et al. 2015). Moreover, its exogenous application awards stress tolerance to the affected plants by protecting the photosynthetic machinery, stabilizing proteins and scavenging ROS (Nusrat et al. 2014). Till now, involvement of GB in salinity and few of the metal stress mitigation in plants has only been shown (Kaya et al. 2013; Nusrat et al. 2014; Ali et al. 2015), however its role in Ni-stress amelioration is still to be resolved fully. Correspondingly, Asp provides stress tolerance to the plants by controlling the ROS and up-regulating antioxidants (Zhen et al. 2010). Till this date, it has been exploited to modulate adverse effects of both salinity and drought (Senaratna et al. 2000; Daneshmand et al. 2009), but its mitigation efficiency against metal stress, particularly Ni, remains to be obscure. Considering the protective functions of GB and Asp, in the present study an effort has been made to investigate the protective roles of these two compounds on growth of Ni subjected *P. typhoideum*. Application of GB and/or Asp may improve the growth performance of tested radicles by lowering the Ni uptake, ROS generation and lipid peroxidation, while improving vital metabolic activities such as viability, membrane stability index (MSI), antioxidant enzymes and contents of protein, proline and DNA.

## Materials and Methods

### Seed germination, treatments and growth analysis

Seeds of *Pennisetum typhoideum* were disinfected with sodium hypochlorite solution (0.1%, v/v) for 3 min, and washed thoroughly (5 times) with MilliQ water (MW) (Millipore, Gradient A-10, USA). Sterilized seeds were placed over two layers of filter paper pre-soaked with MW, in germination boxes of 26 x 16 x 6 cm size (Chandrakar et al. 2016a). These boxes were kept in the dark at room temperature (RT, 26-28 $^{o}$C) until the emergence of 1 mm sized radicles in seeds.

The 1 mm radicle bearing seeds were now supplemented with prefixed treatments: MW (control), 135 ppm Ni ($NiCl_2$, as source), 100 µM each of GB and Asp separately, GB + Asp, Ni + GB, Ni + Asp and Ni + GB + Asp. On 5$^{th}$ day of growth, radicles were carefully harvested for the assessment of different parameters. Initially, change in the radicle length (of 10 radicles) was noted, and then to monitor DM, five sets of randomly selected 10 radicles each, were oven dried at 103 °C for 48 h and weighed electronically. Left over excised radicles were ground in liquid nitrogen ($LN_2$) and stored at -80 °C in sterile vials for further usage. All the evaluations were done in five replicates and repeated twice.

### Membrane stability index

To monitor MSI, 1 g of radicles was taken in a test tube, containing 10 mL of MW and then divided into two sets. Out of these, one set was heated at 40 °C for 30 min, and second was at 100 °C for 10 min in water baths, and electrical conductivity of the solutions were recorded as $T_1$ and $T_2$ respectively, using EC-TDS analyzer (CM-183, Elico, India) (Chandrakar et al. 2017). Membrane stability index was calculated using the formula: MSI (%) = $[1-T_1/T_2)] \times 100$.

### Determination of viability

For tissue viability, 0.2 g of radicles were overnight soaked in 2 mL 0.5% (w/v) 2,3,5-triphenyltetrazolium chloride (TTC) solution in the dark at RT (Lakon 1949). Thereafter, tissues were extracted with ethanol (2 mL) and centrifuged (5000 rpm, 10 min). Absorbance of the supernatants were read at 520 nm using an UV-spectrophotometer (Lambda-25, Perkin Elmer, USA), and values were expressed as $A_{520}$ $g^{-1}$ FM (fresh mass).

### Estimation of Ni

Oven dried (65 °C for 24 h) tissues were digested with a mixture of $HNO_3$:$H_2SO_4$:$H_2O_2$ (4:1:1) at 80 °C for 3 h. Digested samples were filtered through Whatman paper (42), and their volumes were adjusted by MW (Zheljazkov and Nielson 1996). For quality assurance, standard reference (NIST, USA) was included. Concentration of Ni was determined using an atomic absorption spectrophotometer (AA 8000, Labindia, India), and values were presented as µg $g^{-1}$ DM.

### Determination of ROS

The $LN_2$ crushed samples (0.2 g) were homogenized in 2 mL chilled sodium phosphate buffer (0.2 M, pH 7.2) consisting 0.001 M diethyldithiocarbamate and centrifuged (12000 rpm, 15 min, 4 $^{o}$C). To the supernatant (200 µL), 2.4 mL sodium phosphate buffer (0.2 M, pH 7.2) and 100 µL nitroblue tetrazolium (NBT, 2.5 x $10^{-4}$ M) were added and absorbance was recorded at 540 nm (Sangeetha et al. 1990). The $O_2^{\cdot -}$ content was expressed as µmol $min^{-1}$ $g^{-1}$ FM. For determination of H2O2, the samples (0.2 g) were homogenized with 0.1% (w/v) trichloroacetic acid (TCA, 2 mL), and then centrifuged (10000 rpm, 15 min). The 0.5 mL of sodium phosphate buffer (10 mM, pH 7.0) and 1 mL of potassium iodide (1 M)

were added to the supernatant (0.5 mL), and absorbance was recorded at 390 nm (Velikova et al. 2000). Content of $H_2O_2$ was expressed as µmol $g^{-1}$ FM. For ·OH, 0.2 g sample was homogenized in 2 mL sodium phosphate buffer (10 mM, pH 7.4) comprising 15 mM 2-deoxy-ribose and centrifuged (11000 rpm, 15 min). Supernatant was incubated at 37 °C for 2 h. To this (0.7 mL), added 3 mL of thiobarbituric acid {TBA, 0.5% (w/v) in 5 mM NaOH}, and 1 mL of glacial acetic acid, incubated at 100 °C for 30 min and then cooled at 4 °C. Absorbance was read at 532 nm and corrected for non-specific absorbance at 600 nm (Chandrakar et al. 2016a). Content of ·OH was expressed as nmol $g^{-1}$ FM.

### *Monitoring of MDA and 4-HNE*

The $LN_2$ crushed radicles (0.2 g) were homogenized with 2 mL of 0.5% (w/v) TBA {prepared in 20% (w/v) TCA} (Velikova et al. 2000). The homogenate was incubated at 95 °C for 30 min, then quickly cooled in an ice bath (10 min), and centrifuged (10000 rpm, 10 min). The absorbance of the supernatant was recorded at 532 nm and non-specific absorbance was read at 600 nm. Amount of MDA was expressed as mmol $g^{-1}$ FM. For 4-HNE estimation, 0.2 g samples were extracted with 2 mL cold borate buffer (0.2 M, pH 7.4), and 1.5 mL 10% (w/v) TCA, then centrifuged (11000 rpm for 15 min). Supernatant (1 mL) was mixed with 1 mL of 2,4-dinitrophenyl hydrazine (1 mg $mL^{-1}$, in 0.5 M HCl) and allowed to stand for 2 h at RT. Now, the sample was extracted with hexane and dried under $LN_2$. After cooling, added 2 mL of methanol and absorbance was read at 350 nm against methanol as blank (Ray et al. 2007). The level of 4-HNE was expressed as mmol $g^{-1}$ FM.

### *Estimation of LOX*

Lipoxygenase was extracted by homogenizing 0.2 g samples in 2 mL cold borate buffer (0.2 M, pH 7.4) followed by centrifugation (11000 rpm, 15 min at 4 °C). Substrate was prepared by adding 10 µL of linoleic acid in 25 mL of 0.1% (w/v) sodium tetraborate containing 0.1% (v/v) Tween-20. The 0.1 mL of substrate was suspended in 2.9 mL of sodium phosphate buffer (0.1 M, pH 4.5), and shaken vigorously. To initiate reaction, 0.1 mL extracted enzyme was added and absorbance at 234 nm was recorded (Chandrakar et al. 2016a). Activity of LOX was expressed in terms of µmol $min^{-1}$ $g^{-1}$ FM.

### *DNA: extraction and estimation*

Genomic DNA was isolated following the CTAB method (Doyle and Doyle 1987). DNA content was expressed as mg $g^{-1}$ FM.

### *Extraction of protein and enzymes*

Radicles (0.5 g) were extracted with 10 mL of cold potassium phosphate buffer (10 mM, pH 7.2) containing 1 mM EDTA, 2 mM DTT and 0.2% (v/v) Triton X-100, and centrifuged (11000 rpm, 20 min, 4 °C). The supernatant was used as source of both protein and enzymes.

### *Estimation of protein and proline*

Protein was assayed following Bradford (1976). Bovine serum albumin was used as standard and content of protein was expressed as µg $g^{-1}$ FM. Proline was quantified following the method of Bates et al. (1973). The L-proline was used as standard and content of proline was expressed as mg $g^{-1}$ FM.

### *Determination of antioxidant enzymes*

Following Marklund and Marklund (1974), the activity of SOD was monitored by measuring percent inhibition of pyrogallol auto-oxidation by the enzyme at 420 nm. Enzyme activity was expressed as units of SOD $min^{-1}$ $g^{-1}$ FM. CAT was assayed spectrophotometrically at 240 nm by the procedure of Chance and Maehly (1955) and its activity was expressed as nmol $min^{-1}$ $g^{-1}$ FM. Activity of POD was measured after Chance and Maehly (1955) by estimating oxidation of guaiacol in presence of $H_2O_2$ at 470 nm. Activity of it was expressed as µmol $min^{-1}$ $g^{-1}$ FM. APX was assayed following the method of Nakano and Asada (1981) by monitoring the rate of ascorbate oxidation at 290 nm. Enzyme activity was expressed as mmol $min^{-1}$ $g^{-1}$ FM.

### *Isozyme analysis*

Electrophoretic performance of SOD, CAT, POD and APX were analyzed over Native-PAGE gels (10%) using Tris-Glycine buffer (5 mM, pH 8.3) (in case of APX, running buffer consisted of 4 mM ascorbate), at 4 °C for 2 h with a constant current of 20 mA, using Mini-Protean tetra cell (BioRad, USA). After running, gels were imaged and analyzed using Gel-Doc (BioRad, USA). To determine the SOD activity, gels were incubated in dark for 20 min in NBT (2.45 mM) solution, and then immersed in 36 mM dipotassium hydrogen phosphate (pH 7.8), containing 28 µM riboflavin and 28 mM TEMED, until the gel turns blue, except the region(s) showing SOD activity (Chandrakar et al. 2016a). Gel for CAT activity was stained following the method of Woodbury et al. (1971). Initially, the gels were incubated in 0.03% (v/v) $H_2O_2$ solution for 10 min. Thereafter, they were rinsed quickly in MW and stained with 1% (w/v) each of potassium ferricyanide and ferric chloride, sequentially. As soon as a green color began to appear, generally within 5-10 min, gels were washed with MW. For APX detection, gels were equilibrated with 50 mM

**Table 1.** Effects of different combinations of nickel (Ni), aspirin (Asp) and glycinebetaine (GB) on growth, viability, membrane stability index (MSI) and Ni content of *P. typhoideum* radicles. Data represents mean (± SD) of five replicates. Each value followed by small alphabets indicates significant differences at 0.05% level.

| Treatments | Radicle length (mm) | Dry mass (mg) | Viability ($A_{520}$ $g^{-1}$ FM) | MSI (%) | Ni content (µg $g^{-1}$ DM) |
|---|---|---|---|---|---|
| Control | $41^{c} \pm 3$ | $13.13^{d} \pm 0.25$ | $6.75^{d} \pm 0.5$ | $20.9^{c} \pm 0.6$ | ND |
| Ni | $19^{g} \pm 4$ | $7.13^{h} \pm 0.75$ | $1.7^{h} \pm 0.2$ | $5.60^{f} \pm 1.7$ | $5.60^{a} \pm 0.23$ |
| GB | $48^{b} \pm 1$ | $18.20^{b} \pm 0.26$ | $9.932^{b} \pm 0.06$ | $29.13^{b} \pm 2.2$ | ND |
| Asp | $41^{c} \pm 1$ | $15.03^{c} \pm 0.58$ | $7.82^{c} \pm 0.22$ | $22.7^{c} \pm 0.6$ | ND |
| GB + Asp | $53^{a} \pm 3$ | $21.30^{a} \pm 0.36$ | $12.75^{a} \pm 0.5$ | $32.01^{a} \pm 2.75$ | ND |
| Ni + GB | $36^{e} \pm 2$ | $10.16^{f} \pm 0.32$ | $3.73^{f} \pm 0.15$ | $12.45^{d} \pm 0.2$ | $4.02^{c} \pm 0.14$ |
| Ni + Asp | $33^{f} \pm 1$ | $8.73^{g} \pm 0.35$ | $2.62^{g} \pm 0.05$ | $8.50^{e} \pm 0.7$ | $4.75^{b} \pm 0.09$ |
| Ni+ GB + Asp | $37^{d} \pm 1$ | $11.46^{e} \pm 0.58$ | $4.67^{e} \pm 0.05$ | $13.57^{d} \pm 0.1$ | $2.19^{d} \pm 0.30$ |

ND = Not determined

sodium phosphate buffer (pH 7) containing 4 mM ascorbate for 20 min (Mittler and Zilinskas 1993). Afterwards, the gels were incubated with 50 mM sodium phosphate buffer (pH 7) containing 4 mM ascorbate and 4 mM $H_2O_2$ for 20 min. Finally, gels were washed twice with sodium phosphate buffer (50 mM, pH 7) and stained in 50 mM sodium phosphate buffer (pH 7.8) containing 28 mM TEMED and 2.45 mM NBT for 10-15 min. Isozymes of POD were revealed following Srivastava and Huystee (1977). Initially, the gels were equilibrated with 100 mM sodium phosphate buffer (pH 6.5) for 15 min and then stained for 10 min with 12.5 mM guaiacol solution consisting benzidine (1.7 mM) and $H_2O_2$ (12 mM). After gentle shaking, brown colored bands appeared against a clear background.

### *Statistical analysis*

Data were analyzed applying one-way ANOVA to unravel interaction of Ni with GB and/or Asp. Means were compared using Duncan's multiple range tests using SPSS (Ver. 16.0) and expressed as mean ± SD of five replicates. Significance difference was tested at $P < 0.05$.

## Results

### *Growth traits*

Physiological traits of *P. typhoideum* radicles were affected adversely, compared to the control when was subjected to Ni, but addition of Asp and/or GB in combination, revealed enhancement in these parameters (Table 1). Data witnessed that Ni remarkably reduced length (53%), biomass (36%), tissue viability (74%) and MSI (73%) of seedlings, compared to the controls. However, addition of Asp or GB into Ni significantly (35-88%) alleviated these effects. Moreover, joint application of Asp and GB enhanced growth and vitality of stressed radicles far better (up to 93%) than their alone addition (Table 1).

### *Nickel content*

Considerable amount (5.6 µg $g^{-1}$ DM) of Ni was measured in the *P. typhoideum* radicles exposed to 135 ppm Ni. However, exogenous Asp and/or GB allowed limited (15-60% lesser) accumulation of it in the Ni-stressed samples (Table 1).

### *Oxidative stress markers*

Treatment of Ni aggravated the production of all the three ROS in *P. typhoideum* radicles, compared to control (Table 2). Enhancement of around 206%, 112% and 160% in the $O_2^{\cdot-}$,·OH and $H_2O_2$ generation respectively, were observed in response to Ni. On the other hand, blending of Ni with Asp or GB resulted in limited accrual (42-124%) of ROS. Moreover, joint addition of Asp and GB permitted least accumulation of ROS in Ni-stressed seedlings (Table 2).

In Ni exposed radicles, levels of MDA, 4-HNE and LOX raised considerably (109%, 98% and 58% respectively) than their respective controls. Exogenous Asp or GB permitted low abundance of MDA, 4-HNE and LOX activity in Ni-stressed *P. typhoideum*. Moreover, combined addition of Asp and GB revealed least levels of MDA, 4-HNE and LOX (Table 2).

Exposure to Ni caused lowering of both protein (37%) and DNA (38%) in *P. typhoideum* radicles, compared to their respective controls (Table 3). However, these reductions were significantly (75-91%) alleviated by exogenous Asp or GB. Additionally, joint application of Asp and GB uplifted both protein and DNA (88-95%) turnover in Ni subjected radicles.

**Table 2.** Changes in superoxide radical ($O_2^{\cdot-}$), hydroxyl radical (·OH), hydrogen peroxide ($H_2O_2$), malondialdehyde (MDA), 4-hydroxy-2 -nonenal (4-HNE) and lipoxygenase (LOX) in *P. typhoideum* radicles subjected to nickel (Ni), aspirin (Asp) and/or glycinebetaine (GB). Each data represents the mean (± SD) of five observations. Mean followed by different letters indicate significant differences at the 0.05% level compared with the control.

| Treatments | $O_2^{\cdot-}$ (μmol $min^{-1}$ $g^{-1}$ FM) | ·OH (nmol $g^{-1}$ FM) | $H_2O_2$ (μmol $g^{-1}$ FM) | MDA (mmol $g^{-1}$ FM) | 4-HNE (mmol $g^{-1}$ FM) | LOX (μmol $min^{-1}g^{-1}$ FM) |
|---|---|---|---|---|---|---|
| Control | $92.5^{d}$ ± 2.16 | $0.25^{de}$ ± 0.02 | $2.00^{de}$ ± 0.22 | $48.60^{d}$ ± 3.0 | $2.28^{d}$ ± 0.17 | $8.42^{cd}$ ± 2.0 |
| Ni | $283.75^{a}$ ± 10.11 | $0.53^{a}$ ± 0.01 | $5.21^{a}$ ± 0.20 | $101.62^{a}$ ± 4.1 | $4.53^{a}$ ± 0.1 | $13.34^{a}$ ± 2.0 |
| GB | $77.5^{f}$ ± 1.94 | $0.24^{d}$ ± 0.01 | $1.68^{ef}$ ± 0.14 | $32.64^{f}$ ± 1.1 | $1.72^{e}$ ± 0.1 | $7.01^{de}$ ± 0.65 |
| Asp | $81.25^{e}$ ± 1.28 | $0.18^{d}$ ± 0.03 | $1.71^{e}$ ± 0.26 | $38.82^{e}$ ± 3.5 | $2.22^{d}$ ± 0.1 | $8.02^{cd}$ ± 1.0 |
| GB+Asp | $57.5^{g}$ ± 1.75 | $0.14^{e}$ ± 0.02 | $1.49^{f}$ ± 0.10 | $25.34^{g}$ ± 1.2 | $1.24^{f}$ ± 0.3 | $3.67^{g}$ ± 0.6 |
| Ni + GB | $145^{c}$ ± 8.84 | $0.40^{c}$ ± 0.03 | $2.86^{c}$ ± 0.10 | $63.67^{c}$ ± 2.1 | $3.75^{b}$ ± 0.2 | $10.32^{bc}$ ± 2.0 |
| Ni + Asp | $208.75^{b}$ ± 9.12 | $0.43^{b}$ ±0.02 | $3.86^{b}$ ± 0.25 | $80.58^{b}$ ± 4 | $4.04^{b}$ ± 0.2 | $10.86^{b}$ ± 1.0 |
| Ni + GB + Asp | $93.75^{d}$ ± 2.34 | $0.34^{d}$ ± 0.02 | $2.16^{d}$ ± 0.05 | $61.26^{c}$ ± 3.2 | $2.91^{c}$ ± 0.15 | $5.71^{ef}$ ± 0.25 |

**Table 3.** Variations in the levels of proline, DNA and protein in the *P. typhoideum* radicles exposed to different combinations of nickel (Ni), aspirin (Asp) and glycinebetaine (GB). Each value represents mean (±SD) of five replicates. Values possessing different letters are statistically significant at 0.05% probability level.

| Treatments | Proline (mg $g^{-1}$ FM) | DNA (mg $g^{-1}$ FM) | Protein (μg $g^{-1}$ FM) |
|---|---|---|---|
| Control | $2.4^{h}$ ± 0.10 | $6.26^{c}$ ± 0.03 | $279.4^{bcd}$ ± 61.92 |
| Ni | $5.3^{d}$ ± 0.12 | $3.85^{f}$ ± 0.1 | $173.56^{d}$ ± 36.97 |
| GB | $2.8^{g}$ ± 0.07 | $7.19^{b}$ ± 0.3 | $366.34^{ab}$ ± 51.22 |
| Asp | $3.7^{f}$ ± 0.13 | $6.98^{b}$ ± 0.03 | $345.56^{bc}$ ± 65.48 |
| GB + Asp | $3.9^{e}$ ± 0.05 | $7.94^{a}$ ± 0.1 | $400.95^{a}$ ± 26.72 |
| Ni + GB | $5.7^{c}$ ± 0.04 | $4.92^{e}$ ± 0.01 | $251.68^{cd}$ ± 0.44 |
| Ni + Asp | $6.1^{b}$ ± 0.26 | $4.64^{e}$ ± 0.4 | $250.52^{cd}$ ± 35.19 |
| Ni + GB + Asp | $6.6^{a}$ ± 0.15 | $5.5^{d}$ ± 0.3 | $264.92^{bcd}$ ± 33.41 |

### *Proline and antioxidant enzymes*

Remarkable increase (120%) in proline content was discernible in Ni-stressed *P. typhoideum* radicles than that of control (Table 3). However, application of either Asp or GB along with Ni enhanced proline accumulation by 154% and 137% respectively, as compared to the control. Maximum (174%) proline was measured in both Asp and GB blended Ni-exposed *P. typhoideum* radicles. Activities of SOD, CAT, POD and APX were increased drastically (34, 175, 147 and 159%, respectively) by Ni in *P. typhoideum* radicles, compared to non-treated controls. Exogenous Asp and/or GB-induced only very small changes in the activities of tested enzymes (Fig. 1). These observations were in coherence with the electrophoretic profiles of tested antioxidants, which revealed two distinct isoforms each of SOD and CAT, three of POD, and five isoforms of APX, respectively. In general, all these isoforms were not only appeared, but also more pronounced in the Ni-stressed samples than of any other treatments, including control.

## Discussion

In the present study, *P. typhoideum* radicles subjected to deleterious amount of Ni revealed inhibited growth in terms of reduced length and DM accumulation, which might be

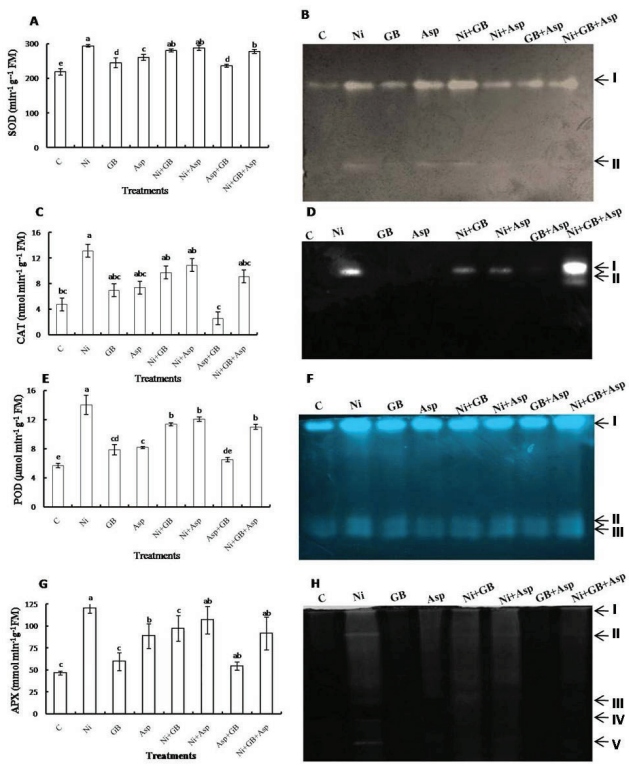


**Figure 1.** Spectrophotometric and Native-PAGE analyses of (A-B) superoxide dismutase (SOD), (C-D) catalase (CAT), (E-F) guaiacol peroxidase (POD) and (G-H) ascorbate peroxidase (APX) of *P. typhoideum* under nickel (Ni) stress alone or along with aspirin (Asp) and/or glycinebetaine (GB). Each bar represents mean (± SD) of five separate observations. Small letters correspond to significant difference at 0.05% level.

**Table 4.** Pearson's correlation coefficients of the studied parameters in the *P. typhoideum* radicles exposed to nickel (Ni), aspirin (Asp) and/or glycinebetaine (GB). Positive R and P < 0.05 meant the positive correlation (bold) between the two variables. Negative R and P < 0.05 meant the negative correlation (italic) between the two variables. P > 0.05 meant that there was no significant relationship between the two variables.

| | DM | TTC | MSI | $O_2^{\cdot-}$ | ·OH | $H_2O_2$ | MDA | 4-HNE | LOX | Proline | DNA | SOD | CAT | APX | POD |
|---|---|---|---|---|---|---|---|---|---|---|---|---|---|---|---|
| RL R | **0.895** | **0.896** | **0.918** | *-0.927* | *-0.909* | *-0.935* | *-0.966* | *-0.923* | *-0.858* | *-0.722* | **0.926** | -0.364 | -0.371 | *-0.842* | -0.457 |
| P | **0.003** | **0.003** | **0.001** | *0.001* | *0.002* | *0.001* | *0.000* | *0.001* | *0.006* | *0.043* | **0.001** | 0.376 | 0.366 | *0.009* | 0.254 |
| DM R | | 0.988 | **0.970** | *-0.798* | *-0.873* | *-0.797* | *-0.912* | *-0.938* | *-0.851* | -0.620 | **0.948** | -0.091 | -0.051 | *-0.808* | -0.146 |
| P | | **0.000** | **0.000** | *0.018* | *0.005* | *0.018* | *0.002* | *0.001* | *0.007* | 0.101 | **0.000** | 0.831 | 0.904 | *0.015* | 0.730 |
| TTC R | | | **0.989** | *-0.825* | *-0.926* | *-0.827* | *-0.938* | *-0.967* | *-0.838* | *-0.722* | **0.979** | -0.153 | -0.088 | *-0.762* | -0.211 |
| P | | | **0.000** | *0.012* | *0.001* | *0.011* | *0.001* | *0.000* | *0.009* | *0.043* | **0.000** | 0.717 | 0.835 | *0.028* | 0.616 |
| MSI R | | | | -0.856 | *-0.937* | *-0.863* | *-0.962* | *-0.978* | *-0.810* | *-0.784* | **0.984** | -0.238 | -0.145 | *-0.756* | -0.294 |
| P | | | | 0.007 | 0.001 | 0.006 | 0.000 | 0.000 | 0.015 | *0.021* | **0.000** | 0.570 | 0.731 | *0.030* | 0.479 |
| $O_2^{\cdot-}$ R | | | | | **0.924** | **0.998** | **0.953** | **0.917** | **0.898** | **0.792** | *-0.895* | 0.269 | 0.240 | 0.668 | 0.373 |
| P | | | | | **0.001** | **0.000** | **0.000** | **0.001** | **0.002** | **0.019** | *0.003* | 0.519 | 0.567 | 0.070 | 0.363 |
| ·OH R | | | | | | **0.931** | **0.969** | **0.966** | **0.841** | **0.873** | *-0.979* | 0.303 | 0.259 | 0.645 | 0.402 |
| P | | | | | | **0.001** | **0.000** | **0.000** | **0.009** | **0.005** | *0.000* | 0.466 | 0.535 | 0.084 | 0.324 |
| $H_2O_2$ R | | | | | | | 0.961 | 0.918 | 0.877 | **0.810** | *-0.902* | 0.300 | 0.271 | 0.662 | 0.408 |
| P | | | | | | | **0.000** | **0.001** | **0.004** | **0.015** | *0.002* | 0.471 | 0.517 | 0.074 | 0.316 |
| MDA R | | | | | | | | **0.968** | **0.854** | **0.815** | *-0.976* | 0.267 | 0.222 | **0.718** | 0.364 |
| P | | | | | | | | **0.000** | **0.007** | **0.014** | *0.000* | 0.523 | 0.597 | **0.045** | 0.375 |
| HNE R | | | | | | | | | **0.882** | **0.828** | *-0.987* | 0.284 | 0.197 | **0.756** | 0.344 |
| P | | | | | | | | | **0.004** | **0.011** | *0.000* | 0.496 | 0.640 | **0.030** | 0.403 |
| LOX R | | | | | | | | | | 0.563 | *-0.852* | 0.067 | 0.109 | **0.755** | 0.155 |
| P | | | | | | | | | | 0.146 | *0.007* | 0.876 | 0.796 | **0.030** | 0.713 |
| Proline R | | | | | | | | | | | *-0.813* | 0.560 | 0.378 | 0.448 | 0.599 |
| P | | | | | | | | | | | *0.014* | 0.149 | 0.356 | 0.265 | 0.116 |
| DNA R | | | | | | | | | | | | -0.250 | -0.198 | *-0.718* | -0.335 |
| P | | | | | | | | | | | | 0.550 | 0.639 | *0.045* | 0.418 |
| SOD R | | | | | | | | | | | | | **0.917** | 0.413 | **0.972** |
| P | | | | | | | | | | | | | **0.001** | 0.309 | **0.000** |
| CAT R | | | | | | | | | | | | | | 0.411 | **0.955** |
| P | | | | | | | | | | | | | | 0.312 | **0.000** |
| APX R | | | | | | | | | | | | | | | 0.411 |
| P | | | | | | | | | | | | | | | 0.311 |

4-HNE = 4-hydroxy-2-nonenal; APX = ascorbate peroxidase; CAT = catalase; DM = dry mass; $H_2O_2$ = hydrogen peroxide; LOX = lipoxygenase; MDA = malondialdehyde; MSI = membrane stability index; $O_2^{\cdot-}$ = superoxide; ·OH = hydroxyl radical; POD = guaiacol peroxidase; RL = radicle length, SOD = superoxide dismutase and TTC = 2,3,5-triphenyl tetrazolium chloride.

the consequence of Ni-imposed inhibition in photosynthesis, respiration and uptake of nutrients and water affecting energy metabolism, and rate of cell division and elongation (Yusuf et al. 2012). Our results are in coherence with the findings of Yusuf et al. (2012) and Siddiqui et al. (2013). However, Asp and/or GB caused improvement in growth, which may be due to enhanced rate of nutrient uptake, photosynthesis and overall metabolic activities (Zhen et al. 2010; Nusrat et al. 2014). Under abiotic stresses, addition of Asp and GB has been revealed to enhance expressions of genes responsive to ROS scavenging, photosynthesis, and energy utilization (Senaratna et al. 2000; Malekzadeh 2015). Radicles of *P. typhoideum* subjected to Ni accumulated considerable amount (5.6 μg $g^{-1}$ DM) of it, which later resulted in altered integrity of membranes and loss of tissue viability. Leakage of cellular constituents is a key indicator of membrane deterioration

that occurs due to peroxidation of PUFA fractions (Kaya et al. 2013). Exposure to Ni adversely affected MSI and tissue viability (Tables 1 and 4). However, exogenous Asp and GB maintained membrane integrity and thereby ionic balance inside the stressed cells (Senaratna et al. 2000; Nusrat et al. 2014). Our results approved the mitigation potential of both Asp and GB by measuring alleviation (65-70%) in the MSI and cell vitality, and reduced accumulation of Ni, in stressed radicles. Similar kind of Asp- and GB-induced modulation in the MSI and ion uptake system has previously been reported by Daneshmand et al. (2009) and Nusrat et al. (2014).

In general, ROS are produced as off-spins of various metabolic pathways operative in sub-cellular compartments of plants (Stanisavljevic et al. 2012). Many abiotic factors, including Ni exposure are designated to produce ROS in abundance (Yusuf et al. 2012; Siddiqui et al. 2013). In congruent, we have noted remarkable upsurge (206-112%) in ROS in Ni-exposed *P. typhoideum* and were quite low up on addition of Asp and/or GB. Exogenous GB protects RUBISCO, a $CO_2$ fixing enzyme, which minimizes ROS production under abiotic stresses (Malekzadeh 2015). On the other hand, Asp led to reduced turnover of ROS *via* enhanced activities of antioxidant enzymes in stressed plants (Daneshmand et al. 2009). Studies have proven that LOX plays crucial role in the catabolism of phospholipids by initiating a lipolytic cascade in the cellular membranes consequently MDA and 4-HNE production in stressed cells (Yadu et al. 2016). Our results exemplified high levels of MDA, 4-HNE and LOX in Ni-treated samples (Table 2). Similar rise in LOX mediated peroxidative products has also been reported by Kazemi et al. (2010). While, addition of Asp and GB demonstrated lower activity of LOX, consequently enhance stability of the membrane lipids (Daneshmand et al. 2009; Ali et al. 2015).

In stressed plants, LOX and ROS alter lipid composition of membranes (Yadu et al. 2017). A relationship among lipid peroxidation, ROS generation and Ni application has been well reported (Stanisavljevic et al. 2012). The PUFAs of membranes are highly vulnerable to ROS assault and give rise to cytotoxic products (MDA and 4-HNE), which interact with cellular macromolecules and adversely affects to the membranes (Gajewska et al. 2012). The results indicated an association of ROS with MDA (R = 0.961), 4-HNE (R = 0.933) and MSI (R = -0.885) (Table 4). On the contrary, Asp and GB stabilize the membrane lipid and reduced the levels of MDA and 4-HNE, which are well related with previous reports (Daneshmand et al. 2009; Lou et al. 2015).

Like lipids, proteins are also equally vulnerable to ROS by several mechanisms *viz*.; glycation, carbonylation, nitrosylation and hydroxylation (Chandrakar et al. 2016b). Nickel leads to depletion of protein bound thiols thereby making it non-functional. Oxidation of proteins in response to Ni resulted in reduced amount of active proteins (Negi et al. 2014). Our results for Ni-stressed *P. typhoideum* coincide well with this observation (Table 3). Conducted study revealed an inverse association (R = -0.754) between protein and ROS content. Exogenous application of Asp and GB stabilized the protein structure and increased the protein content (Zhen et al. 2010; Lou et al. 2015). Moreover, these compounds also reduced the rate of protein carbonylation, and increased the level of reduced glutathione (Ali et al. 2015). ROS promoted DNA damage has widely been shown to occur under abiotic stresses (Erturk et al. 2014; Chandrakar et al. 2017). ROS-imposed deleterious changes frequently results permanent deformity in the DNA strand *via* inactivating the repair systems (Erturk et al. 2014). In this study, considerable fall (38%) in the DNA content of Ni subjected *P. typhoideum* radicles was discernible, and was related inversely with ROS (R = -0.925) (Table 4). Content of DNA was raised in presence of Asp and/or GB, which suggests that they protect DNA either by up-regulating DNA polymerase activity or by direct scavenging of ROS in stressed cells.

Additionally, synthesis of proline has been shown as one of the strategies needed to tune the cell with stressed condition (Kazemi et al. 2010; Siddiqui et al. 2013). It stabilizes proteins and cell membranes, scavenges free radicals, functions as molecular chaperons, and enhances the activities of antioxidants (Yusuf et al. 2012). In this study, enhanced synthesis of proline was discernible after Ni, and Asp and/or GB addition in *P. typhoideum* radicles. Increased proline was largely shown to protect the plants from abiotic stress by scavenging ROS (Kaya et al. 2013).

In general, plants respond to oxidative condition by improving the activities of defensive enzymes (Daneshmand et al. 2009; Malekzadeh 2015). In this study, activities of SOD, CAT, POD and APX were enhanced in *P. typhoideum* under Ni-stress (Figs. 1A, C, E, G). It is known that these enzymes consume ROS as their substrate, therefore, with the rise of it, their activities also increased (Yusuf et al. 2012). Although, there was a rise in the antioxidants in Ni subjected *P. typhoideum*, but rise might not be sufficient to detoxify such a high amount of ROS, which caused oxidative condition inside the cells. Moreover, exogenous Asp and GB restored the antioxidants under varied abiotic stresses possibly due to lesser accrual of ROS (Daneshmand et al. 2009; Lou et al. 2015). Isoenzyme analyses of SOD, POD and APX revealed that isoforms of these enzymes appeared in the Native-PAGE gel, but their intensities varied in response to Ni (Figs. 1B, F, H). Interestingly, isoform(s) of CAT appeared only in the presence of Ni, which suggests the activation of enzymes to counteract the toxicity (Fig. 1D). Above observations were in coherence with their spectrophotometric results. Restoration in the enzyme activities in response to ROS scavenger, are in line with Mandal et al. (2013).

## Conclusions

The results of the present study revealed that exogenous Asp and/or GB prevented the *P. typhoideum* radicles against Ni-stress by improving biomass accumulation, viability, MSI, contents of protein, DNA and proline, restoring the activities of antioxidant enzymes, and controlling LOX and lipid peroxidation. We found that Asp and/or GB restored the activities/improved the isoforms of SOD, CAT, POD and APX, which are crucial to minimize Ni accumulation. Moreover, it is noteworthy that addition of Asp and/or GB inhibited the LOX, reduced the MDA and 4-HNE, and enhanced proline accumulation. However, information about the participation of Asp and GB in heavy metal uptake by varied plant species, and precise mechanisms of stress tolerance are limited, hence need to be studied further.

## Acknowledgements

The authors would like to thank the Department of Science & Technology, New Delhi, University Grants Commission, New Delhi, and Defense Research and Development Establishment, Gwalior, for awarding INSPIRE fellowship [No. DST/INSPIRE Fellowship/2013/791, dated 17. 01. 2014], Rajiv Gandhi National Fellowship [F1-17.1/2014-15/RGNF-2014-15-ST-CHH-86720] and Project Fellowship [DRDE/TC/05414/Proj/TASK-220/16 dated June 27, 2016] to Vibhuti Chandrakar, Roseline Xalxo and Bhumika Yadu, respectively. Authors are also grateful to Department of Science & Technology, New Delhi, for financial support through DST-FIST scheme (Sanction No. 2384/IFD/2014-15, dated 31. 07. 2014) sanctioned to the School of Studies in Biotechnology.

## References

Ali S, Chaudhary A, Rizwan M, Anwar HT, Adrees M, Farid M, Irshad MK, Hayat T, Anjum SA (2015) Alleviation of chromium toxicity by glycinebetaine is related to elevated antioxidant enzymes and suppressed chromium uptake and oxidative stress in wheat (*Triticum aestivum* L.). Environ Sci Pollut Res 22:10669-10678.

Bates LS, Walrow, RP, Teare ID (1973) Rapid determination of free proline for water stress studies. Plant Soil 39:205-208.

Bradford MM (1976) A rapid and sensitive method for the quantification of microgram quantities of protein utilizing the principle of protein-dye binding. Anal Biochem 72:248-254.

Chance M, Maehly AC (1955) Assay of catalases and peroxidases. Methods Enzymol 2:764-817.

Chandrakar V, Dubey A, Keshavkant S (2016a) Modulation of antioxidant enzymes by salicylic acid in arsenic exposed *Glycine max* L. J Soil Sci Plant Nutr 16:662-676.

Chandrakar V, Naithani SC, Keshavkant S (2016b) Arsenic-induced metabolic disturbances and their mitigation mechanisms in crop plants: A review. Biologia 71:367-377.

Chandrakar V, Yadu B, Meena RK, Dubey A, Keshavkant S (2017) Arsenic-induced genotoxic responses and their amelioration by diphenylene iodonium, 24-epibrassinolide and proline in *Glycine max* L. Plant Physiol Biochem 112:74-86.

Daneshmand F, Arvind MJ, Kalantari KM (2009) Effect of acetylsalicylic acid (aspirin) on salt and osmotic stress tolerance in *Solanum bulbocastanum in vitro*:enzymatic antioxidants. Am Eurasian J Agric Environ Sci 6:92-99.

Doyle JJ, Doyle JL (1987) A rapid DNA isolation procedure for small quantities of fresh leaf tissue. Phytochem Bull 19:11-15.

Erturk FA, Agar G, Arslan E, Nardemir G, Sahin Z (2014) Determination of genomic instability and DNA methylation effects of Cr on maize (*Zea mays* L.) using RAPD and CRED-RA analysis. Acta Physiol Plant 36:1529-1537.

Gajewska E, Bernat P, Długon J, Skłodowska M (2012) Effect of nickel on membrane integrity, lipid peroxidation and fatty acid composition in wheat seedlings. J Agro Crop Sci 198:286-294.

Hussain MB, Ali S, Azam A, Hina S (2013) Morphological, physiological and biochemical responses of plants to nickel stress. Afr J Agric Res 8:1596-1602.

Jafari SR, Arvin SMJ, Kalantari KM (2015) Response of cucumber (*Cucumis sativus* L.) seedlings to exogenous silicon and salicylic acid under osmotic stress. Acta Biol Szeged 59:25-33.

Kaya C, Sonmez O, Aydemir S, Dikilitas M (2013) Mitigation effects of glycinebetaine on oxidative stress and some key growth parameters of maize exposed to salt stress. Turk J Agric For 37:188-194.

Kazemi N, Khavari-Nejad RA, Fahimi H, Saadatmand S, Nejad-Sattari T (2010) Effects of exogenous salicylic acid and nitric oxide on lipid peroxidation and antioxidant enzyme activities in leaves of *Brassica napus* L. under nickel stress. Sci Hort 126:402-407.

Lakon G (1949) The topographical tetrazolium method for determining the germinating capacity of seeds. Plant Physiol 24:389-394.

Lou Y, Yang Y, Hu L, Liu H, Xu Q (2015) Exogenous glycinebetaine alleviates the detrimental effect of Cd stress on perennial ryegrass. Ecotoxicology 24:330-1340.

Malekzadeh P (2015) Influence of exogenous application of glycinebetaine on antioxidative system and growth of

salt-stressed soybean seedlings (*Glycine max* L.). Physiol Mol Biol Plants 21:225-232.

Mandal C, Ghosh N, Maiti S, Das K, Gupta S, Dey N, Adak MK (2013) Antioxidative responses of Salvinia (*Salvinia natans* L.) to aluminium stress and it's modulation by polyamine. Physiol Mol Biol Plants 19:91-103.

Marklund S, Marklund G (1974) Involvement of the superoxide anion radical in the autoxidation of pyrogallol and a convenient assay for superoxide dismutase. Eur J Biochem 47:469-474.

Mittler R, Zilinskas BA (1993) Detection of ascorbate peroxidase activity in native gels by inhibition of the ascorbate-dependent reduction of nitroblue tetrazolium. Anal Biochem 212:540-546.

Nakano Y, Asada K (1981) Hydrogen peroxide is scavenged by spinach chloroplasts. Plant Cell Physiol 22:867-880.

Negi A, Singh HP, Batish DR, Kohli RK (2014) $Ni^{+2}$-inhibited radicle growth in germinating wheat seeds involves alterations in sugar metabolism. Acta Physiol Plant 36:923-929.

Nusrat N, Shahbaz M, Perveen S (2014) Modulation in growth, photosynthetic efficiency, activity of antioxidants and mineral ions by foliar application of glycine betaine on pea (*Pisum sativum* L.) under salt stress. Acta Physiol Plant 36:2985-2998.

Ray S, Roy K, Sengupta C (2007) Evaluation of protective effects of water extract of *Spirulina platensis* on cisplatin-induced lipid peroxidation. Ind J Pharm Sci 69:378-383.

Sangeetha P, Das VN, Koratkar R, Suryaprabha P (1990) Increase in free radical generation and lipid peroxidation following chemotherapy in patients with cancer. Free Radic Biol Med 8:15-19.

Senaratna T, Touchell D, Bunn E, Dixon K (2000) Acetyl salicylic acid (aspirin) and salicylic acid induce multiple stress tolerance in bean and tomato plants. Plant Growth Regul 30:157-161.

Siddiqui MH, Al-Whaibi HM, Ali AM, Sakran MO, Basalah MYY, Khaishany AL (2013) Mitigation of nickel stress by the exogenous application of salicylic acid and nitric oxide in wheat. Aust J Crop Sci 7:1780-1788.

Srivastava, OP, Huystee RB (1949) An inter-relationship among peroxidase, IAA oxidase and polyphenol oxidase from peanut cells. Can J Bot 55:2630-2635.

Stanisavljevic N, Savic J, Jovanovic Z, Djukic JM, Radovic S, Vinterhalter D, Vinterhalter B (2012) Antioxidative related enzyme activity in *Alyssum markgrafii* shoot cultures as affected by nickel level. Acta Physiol Plant 34:1997-2006.

Velikova V, Yordanov I, Edreva A (2000) Oxidative stress and some antioxidant systems in acid rain treated bean:protective role of exogenous polyamine. Plant Sci 151:59-66.

Woodbury W, Spencer AK, Stahmann MA (1971) An improved procedure using ferricyanide for detecting catalase isozymes. Anal Biochem 44:301-305.

Yadu B, Chandrakar V, Keshavkant S (2016) Responses of plants towards fluoride: an overview of oxidative stress and defense mechanisms. Fluoride 49:293-302.

Yadu B, Chandrakar V, Meena RK, Keshavkant S (2017) Glycinebetaine reduces oxidative injury and enhances fluoride stress tolerance via improving antioxidant enzymes, proline and genomic template stability in *Cajanus cajan* L. South Afr J Bot 111:68-75.

Yusuf M, Fariduddin Q, Ahmad A (2012) 24-Epibrassinolide modulates growth, nodulation, antioxidant system and osmolyte in tolerant and sensitive varieties of *Vigna radiata* under different levels of nickel:A shotgun approach. Plant Physiol Biochem 57:143-153.

Zheljazkov VD, Nielson NE (1996) Effect of heavy metals on peppermint and cornmint. Plant Soil 178:59-66.

Zhen F, Fang L, Cheng-Shu Z, Huai-Rui S, Xian-Zhi S, Yongkweon Y (2010) Effects of acetylsalicylic acid and calcium chloride on photosynthetic apparatus and reactive oxygen-scavenging enzymes in chrysanthemum under low temperature stress with low light. Agr Sci China 9:1777-1786.

**Volume 61(2):173-178, 2017**
**Acta Biologica Szegediensis**
http://www2.sci.u-szeged.hu/ABS

**ARTICLE**

# The disappearance of three archaeophyte species in Hungary can be explained by their marked sensitivity to fertilizers

Károly Ecseri[1], István Dániel Mosonyi[2], Andrea Tilly-Mándy[2], Péter Honfi[2]*

[1]Neumann János University, Faculty of Horticulture and Rural Development, Department of Horticulture, Kecskemét, Hungary
[2]Szent István University, Faculty of Horticultural Science, Department of Floriculture and Dendrology, Budapest, Hungary

**ABSTRACT** The archaeophytes are the component of segetal plant communities, and ensure biodiversity in arable field margins. Unfortunately, the number of these species decreased in the last decades because of the changing structure of agricultural production and increasing chemical application. In this study, the fertilizer sensitivity of three archaeophyte species was characterized using germination test, outdoor observation and proline content measurement. *Papaver rhoeas* had the most favourable germination parameters with promptness indices (1.5-14.0) and germination rates (0.39-0.81) decreasing with the concentration of fertilizer. On the other hand, mean germination time (7.32-10.03 days) decreased with elevated fertilizer concentration. *Consolida regalis* was characterized by the weakest development in laboratory. Slow early development was detected in case of *Cyanus segetum* (promptness index: 0.25-1.75; mean germination time: 12-13 days). *Co. regalis* responded to fertilization with higher blooming intensity. The proline accumulation indicated pronounced salt sensitivity of *Cy. segetum* (0.49-0.54 mg/100 mg), which could be one reason of the disappearance of this species from fields under cultivation. Our results suggest that at least *Co. regalis* and *Cy. segetum* are highly sensitive to mineral fertilizers and hence natural protection techniques for example arable weed margins must be widely used to block the disappearance of those species.

**Acta Biol Szeged 61(2):173-178 (2017)**

**KEY WORDS**

cornflower
decoration value
larkspur
poppy
proline
salt stress

## Introduction

Archaeophytes are those species, which originally cannot be found in the flora of European area, but naturalized between Neolithic and the end of middle ages due to human influence. Survival of segetal species depends on the nature transformer activity of human beings. These are usually annual, ephemeral, pioneer species with high adaptation ability to arable field cereals (Preston et al. 2004; Williamson et al. 2008).

Many rare, endangered or extinct species can be found in the list of European archaeophytes since the development of agriculture poses a serious risk on their life conditions (Richner 2014). Fertilization has direct and indirect effects on arable field plants including archaeophytes. One of the most important challenges is the changing quantity and method of fertilization (Albrecht 1995; Šarić et al. 2011). Its direct effect is based on different nutrient uptake mechanisms: the bred grain cultivars are able to uptake quickly the mineral fertilizers, while segetal weed species prefer organic nutrients (Pyšek and Lepš 1991; Kleijn and van der Voort 1997). In addition, as an indirect effect, the increasing use of fertilizers results in the loss of plant diversity due to increased competition ability of crops (Pyšek and Lepš 1991; Meyer et al. 2013). Therefore, poor light competitors (e.g., *Co. regalis*) are disappearing and the stronger nitrophilous neophytes are spreading (Svensson and Wigren 1986; Albrecht 1995). Competitive species will have higher size due to limited light resource but their total biomass weight decrease (Kleijn and van der Voort 1997). The frequency of small and subordinate species decreases, and the number of species reduce over time (Schmitz et al. 2014). It depends on species whether direct or indirect effects will predominate (Pyšek and Lepš 1991).

The perennials of arable field border community uptake the remaining fertilizer that cannot be utilized by crops. This effect leads to stronger competition against annual archaeophytes, and structure changes (Stoate et al. 2001). Decrease of archaeophytes was observed in Germany between 1953 and 2000 (Baessler and Klotz 2006). The applied potassium

Submitted September 22, 2017; Accepted December 5, 2017
*Corresponding author. E-mail: honfi.peter@kertk.szie.hu

and nitrogen fertilizers caused significant reduction of anthropochorous species while the number of invasive weeds increased. The number of *Co. regalis* and *Papaver rhoeas* plants showed significant reduction between 1957 and 1979. The habitat-specific species (such as *Co. regalis*) were forced and the weed diversity decreased due to fertilizer application (Baessler and Klotz 2006).

The loss of archaeophytes was also observed in Denmark when comparing the 1967-1970 and 1987-1989 periods (Andreasen et al. 1996). The frequency of segetal species including *Cy. segetum*, *Co. regalis* and *P. rhoeas* also decreased in France from 1970s to 2000s (Fried et al. 2009).

Wassmuth et al. (2008) stated that *Cy. segetum* had higher biomass production in fertilized soil. This is a compensation mechanism caused by low number of individuals. However, this low number may cause population extinction (Bischoff and Mahn 2000). In the studies conducted by Mohammaddoust et al. (2008) the soil covering of *Cy. segetum* increased because of phosphorus application, while the nitrogen application had positive effect on dry biomass production. The germination rate of seeds decreased due to nitrogen application in contrast to phosphorus which improved germination. Optimal phosphorus level has positive effects on the appearance of species and improves soil fertility. On the other hand, potassium had no positive effects (Andreasen and Skovgaard 2009), its high level caused frequency reduction (Andreasen et al. 1991).

The aim of our investigation was to determine fertilizer sensitivity of three archaeophyte species (*Cy. segetum*, *Co. regalis,* and *P. rhoeas*) using laboratory examination and outdoor observations. The chosen species are easy to apply as indicator plants of archaeophytes because they are common, easy to determine at the early developmental stage, flexible but sensitive for environmental changes (Büchs 2003; Bellanger et al. 2012). The original (semi-natural) habitat of archaeophytes is the cereal fields and the border of arable crops. For the successful *in situ* protection of these species is necessary to identify the reasons of their disappearance. The problem of over-fertilization has already been known, but this observation often lacks statistical support (Wörz and Thiv 2015). Therefore, we wanted to identify and statistically confirm the destructive mechanisms of fertilizer application and give recommendation to reduce the chemical damage of segetal vegetation.

## Materials and Methods

### *Ex situ germination test*

Four replications of 25 seeds from each of the three species (*Cyanus segetum* Hill, *Consolida regalis* Gray, *Papaver rhoeas* L.) were used for germination test. *Cyanus* and *Consolida* seeds were placed in Petri dishes between two filter papers, while *P. rhoeas* seeds were placed on top of the filter papers. Applied fertilizer (N:P:K 6:12:24 + 8S - DC 42, TIMAC AGRO Düngemittelproduktions und Handels GmbH; mixed, spherical granulated form) were powdered and dissolved in distilled water. Treatments were carried out by adding 10 ml of 0.5; 1; 2 and 3 g/l the fertilizer solution. Control seeds were watered only with 10 ml distilled water. Germination tests were conducted under controlled conditions (10 hours dark period in 10 °C and 14 hours light period in 20 °C, 27.3 µmol/m$^2$s luminous photosynthetic photon flux). During the 14-20 days long examination period, germinated seeds containing two millimetres long radicles were removed. This was taken as a criterion of germination.

The following parameters were calculated:

Promptness index (PI): $PI = nd_2 \times (1.00) + nd_4 \times (0.75) + nd_6 \times (0.50) + nd_8 \times (0.25)$, where $nd_2$ $nd_4$ $nd_6$ $nd_8$ showed the number of seeds germinated on the 2nd 4th 6th and 8th day, respectively (Zafar et al. 2015),

Germination stress tolerance index (GSTI) expressed in %: GSTI = (PI of stressed seeds /PI of control seeds) × 100 (George 1967), where stressed seeds indicate fertilizer treated seeds,

Mean germination time (MGT) expressed in days: $MGT = (\sum ni \times ti)/\sum n$, where ni showed the number of seeds germinated on ti time, ti showed the number of days from start, n showed the number of germinated seeds at the end of the test,

Germination speed (GS): GS = 1/MGT × 100 (Hartmann et al. 1997), and

Germination rate (GR) = the number of germinated seeds until the end of the test / total number of planted seeds.

### *Outdoor experiments*

The experiment took place in the Experimental and Research Farm (Faculty of Horticultural Science, Budapest, Hungary) in Soroksár (47° 24' 1" N latitude, 19° 8' 37" E longitude and 115 m altitude). The soil was sandy and poor in humus, strongly infected by perennial weeds. The soil was rotated with cultivator on 23$^{th}$ September 2014. A total of 20 g/m$^2$ fertilizer (N:P:K 6:12:24 + 8S) was dispersed and rotated into the soil in 50% of the whole area. Plants were examined in separate parcels containing only the studied species; the size of parcels was 1.5×1.5 m. Two hundred seeds of all three species were sown three times (on 8$^{th}$, 14$^{th}$ and 21$^{st}$ of October). Seeds were covered with 2 cm soil and irrigated with 10 l of water. Size, phenological development and decoration value were determined weekly after germination from 21$^{st}$ of October to 14$^{th}$ of July (except the winter period from 24$^{th}$ of November to 14$^{th}$ of April).

Size parameters (horizontal sizes - width and length,

**Table 1.** Changes in the germination factors of two archaeophyte species exposed to different fertilizer (N:P:K 6:12:24 + 8S) treatments.

| Treatment | *PI* | *GSTI* (%) | *MGT* (day) | GS | GR |
|---|---|---|---|---|---|
| *C. segetum* | | | | | |
| control | $1.75^{a} \pm 0.52$ | -- | $12.06^{a} \pm 21.82$ | 8.29 | $0.52^{a} \pm 2.71$ |
| 0.5 g/l | $0.75^{a} \pm 0.38$ | 42.86 | $12.45^{a} \pm 33.42$ | 8.03 | $0.44^{ab} \pm 1.63$ |
| 1 g/l | $1.50^{a} \pm 0.48$ | 85.71 | $12.26^{a} \pm 8.71$ | 8.16 | $0.39^{ab} \pm 4.79$ |
| 2 g/l | $0.50^{a} \pm 0.25$ | 28.57 | $12.74^{a} \pm 16.18$ | 7.85 | $0.27^{bc} \pm 1.26$ |
| 3 g/l | $0.25^{a} \pm 0.13$ | 14.29 | $13.00^{b} \pm 8.05$ | 7.69 | $0.09^{c} \pm 1.50$ |
| *P. rhoeas* | | | | | |
| control | $14.00^{a} \pm 5.20$ | -- | $7.32^{a} \pm 62.64$ | 13.66 | $0.81^{a} \pm 2.50$ |
| 0.5 g/l | $10.00^{a} \pm 2.89$ | 71.43 | $8.30^{a} \pm 62.37$ | 12.05 | $0.72^{a} \pm 1.71$ |
| 1 g/l | $3.00^{a} \pm 1.19$ | 21.43 | $8.90^{a} \pm 67.45$ | 11.23 | $0.61^{ab} \pm 4.44$ |
| 2 g/l | $2.25^{a} \pm 1.13$ | 16.07 | $9.61^{a} \pm 43.90$ | 10.41 | $0.51^{b} \pm 1.71$ |
| 3 g/l | $1.50^{a} \pm 0.75$ | 10.71 | $10.03^{a} \pm 45.27$ | 9.97 | $0.39^{b} \pm 1.71$ |

GR: germination rate; GS: germination speed; GSTI: germination stress tolerance index; MGT: germination time; PI: promptness index. For each species, different letters within the same column indicate significantly different values at $p \leq 0.05$ according to the Tukey test. GSTI and GS data are derived from PI and MGT, respectively, and hence statistically not analysed.

vertical size - height) were measured by tape measure. Ranking was used to determine the phenological statement and ornamental value. The values represented the following categories:

5. Very decorative, full blooming, healthy wildflower.

4. Moderately decorative, begin or finish blooming, healthy wildflower.

3. Slightly decorative, decorated only by vegetative parts. Healthy plant.

2. No decoration value because of phenological stage, or some kind of stress (*e.g.*, sunshine, wind, insects or pathogen).

1. Plants could not be found in the area.

### *Proline content determination*

The proline content was measured according to Ábrahám et al. (2010). Leaves were collected from plants analysed in the outdoor experiment on 24th November 2014 and on 8th June 2015. Samples were stored at -20 °C until use. The samples (approx. 100 mg fresh weight) were ground with 3% sulfosalicylic acid (5 µl/mg fresh weight), and were centrifuged (15. 689 g, 5 min, 25 °C) using a 5418 R (Eppendorf, Hamburg, Germany). A total of 100 µl from the supernatant was mixed with the reaction mixture (100 µl 3% sulfosalicylic acid, 200 µl glacial acetic acid and 200 µl acidic ninhydrin). After 60 minutes of incubation at 96 °C, the reaction was terminated on ice. Then, 1 ml toluene was added to the reaction mixture and vortexed for 20 seconds. After the separation (5 minutes) the chromophore was removed into a fresh tube. Finally, the absorbance was measured at 520 nm using a GeneSys VIS-10 spectrophotometer (Thermo Fisher Scientific, Waltham, MA, USA). The proline content was calculated on fresh weight basis using a standard concentration curve.

### *Statistical evaluation*

Data presented for each species represent the mean values determined from 4 independent measurements. After tested for normal distribution and equality of variances, 1-way analysis of variance (ANOVA) was carried out and significant differences were calculated according to Tukey test, with $P \leq 0.05$ being considered significant in all analyses. Statistical analyses were carried out using the SPSS 20 software (IBM, New York, US).

## Results and Discussion

### *In vitro germination test*

Changes in the germination promptness index indicate that *P. rhoeas* is characterized by rapid development (Saeb et al. 2013), while the germination speed of *Cy. segetum* is slower than crop cultivars, but similar to the value of other *Centaurea* species (Turkoglu et al. 2009). This developmental response of archaeophytes to fertilizer effects might be in association with the disappearing of such plants from arable lands in Europe (Albrecht 1995; Svensson and Wigren 1986). The slowest development was shown in case of *Co. regalis*. This species has not germinated during the test period of 14-20 days. The stress tolerance index of examined species was low and decreased rapidly with increasing fertilizer concentra-

**Table 2.** Pairwise comparison of flower number depending on fertilizer application for three archaeophyte species.

| Species | Treatment | *N* | Average flower number in parcel |
|---|---|---|---|
| *P. rhoeas* | control | 33 | 0.705361[a] |
| *P. rhoeas* | fertilized | 33 | 0.759147[a] |
| *Cy. segetum* | control | 33 | 1.734274[a] |
| *Cy. segetum* | fertilized | 33 | 2.183164[ab] |
| *Co. regalis* | control | 33 | 3.529449[b] |
| *Co. regalis* | fertilized | 33 | 5.162685[c] |

N: number of examined plants. Different letters indicate significantly different values at $p \leq 0.05$ according to the Tukey test.

**Table 3.** Pairwise comparison of proline content depending on fertilizer treatment by three archaeophyte species – samples collected in November (mg/100 mg fresh weight).

| Species | Treatment | *N* | Average proline content |
|---|---|---|---|
| *P. rhoeas* | control | 5 | 0.47403020[a] |
| *P. rhoeas* | fertilized | 5 | 0.47569120[a] |
| *Co. regalis* | control | 5 | 0.47450840[a] |
| *Co. regalis* | fertilized | 5 | 0.47756320[a] |
| *Cy. segetum* | control | 5 | 0.48867940[a] |
| *Cy. segetum* | fertilized | 5 | 0.54261496[b] |

N: number of examined samples. Different letters indicate significantly different values at $p \leq 0.05$ according to the Tukey test.

tion (Table 1). GSTI values were 10-15% at 3 g/l fertilizer concentration that are considerably lower values than those of wheat cultivars (70-90%). For example, the salt tolerance index of three barley cultivars was 67.07-91.24% when 5 g/l NaCl was added into the medium (Goumi et al. 2014). The same index of sunflower cultivars ranged between 80% and 90% due to 5 g PEG added in 100 ml distilled water, but one cultivar had just 50% (Ahmad et al. 2009).

Comparing mean germination time (MGT), more pronounced sensitivity to 3 g/l fertilizer concentration was detected for *Cy. segetum*, as for the other two species ($SL < 0.05$). The germination rate of *P. rhoeas* was decreased by 3 g/l fertilizer solution to 39%, while *Cy. segetum* showed only 9% germination rate due to 3 g/l fertilizer treatment ($SL < 0.05$).

### *Outdoor experiments*

Differences were not shown in phenological development and plant size between treated and control parcels. Examining the covering shares a significant difference occurred for *Cy. segetum* ($SL < 0.001$): 39.27% in treated parcels, while 27.79% in control parcels. Significantly higher number of flowers was shown by *Co. regalis* (Tukey test $SL < 0.05$) when comparing fertilized and control parcels (Table 2).

The top of *P. rhoeas* blooming time (ornamental value 5) occurred in the third decade of June. Main blooming time of *Co. regalis* continued from the end of May until first decade of June. The number of blooming plants was 60-100% of all germinated seedlings in this period. Minor second decoration period could be observed in the last decade of June in treated parcels. *Cy. segetum* had the highest ornamental value (5) also from the end of May until the beginning of June. The blooming period of *Cy. segetum* was longer than those of *Co. regalis* and *P. rhoeas* blooming time. The number of flowering *Cy. segetum* individuals decreased continuously while the number of flower heads of the flowering individuals increased until the end of June. The decrease of individuals (Baessler and Klotz 2006; Fried et al. 2009) was not observed for *Consolida* and *Papaver* because of the short experimental period. However, positive effects of the fertilizer could be realized in the increased number of *Cyanus* plants (Wassmuth et al. 2008). Many studies confirmed that both herbaceous crops and trees become progressively more tolerant as the plants grow older with a salt-sensitive early-vegetative growth (emergence) stage and a less sensitive stage during flowering (Läuchli and Grattan 2007; Niinemets 2010). Regardless of the more abundant flowering of archeophytes, their number will be lowered by fertilizer induced stress effects in the most sensitive seedling stage, resulting in a definite loss of established plants. The treated *Cyanus* and *Consolida* plants were slightly and non-significantly higher than control that is associated with the bigger biomass weight due to fertilizer application (Bischoff and Mahn 2000).

### *Proline content determination*

A number of environmental stresses (*e.g.*, high salinity) cause proline accumulation (Ahmad et al. 1981; Kubala et al. 2015). This physiological response is hypothesized to be a consequence of the osmoprotective and osmolyte role of proline (Fougére et al. 1991). It is able to reduce the damage of oxidative stress and protect protein structures (Samuel et al. 2000). The determination of proline content may provide useful information on the actual physiological status and stress tolerance of plants (Ábrahám et al. 2010).

A significant difference was shown in samples of *Cy. segetum* (Table 3) in November. Proline content of fertilized stand was higher in comparison with the control ($SL < 0.01$). This difference was not observed in June (0.4537 mg/100 mg in treated parcels, 0.4545 mg/100 mg in control parcels). Such a difference was not shown by the other two species, but the values were similar. The effect of salt stress was decreased in comparison with two collecting times (paired samples test: $t = 4.504$, $SL < 0.001$). The proline content of the three examined species was higher than bred grain cultivars (Pyšek and Lepš 1991; Kleijn and van der Voort 1997). Ten times lower

fresh weight proline concentration (0.5 mg/g) was measured in tomato after daily complex nutrient application (Claussen 2005). Only treatments applied eleven times caused a similar value (3 mg/g) to our results (4.7-5.4 mg/g).

## Conclusions

The used parameters and analyses were useful to explain the disappearance of three archaeophyte species in Hungary due to their marked sensitivity to fertilizers.

*Co. regalis* had the weakest germination factors in laboratory tests. Germination rate of *P. rhoeas* and *Cy. segetum* was significantly decreased and rapid declining in germination stress tolerance index was observed due to fertilizer application in case of *P. rhoeas*. Furthermore, the slow early development may give an explanation for disappearing of archaeophytes (especially *Co. regalis* and partly *Cy. segetum*). Main blooming time continued from the end of May to the first decade of June; however, a significant second decoration period occurred at the end of June in fertilizer applied parcels. Nevertheless, the soil covering of *Co. regalis* was the least (8-10%). The applied fertilizer did not have any significant effect neither on blooming intensity nor on blooming period. Analysing proline concentration, higher salt sensitivity was determined for *Cy. segetum* seedlings, especially at the early stage of development. This sensitivity lowers the surviving and spreading opportunities of this species among crops. This stress factor can be prolonged under non-irrigated conditions, which is confirmed by the small variations in proline contents of samples collected from November to June.

## References


Ábrahám EC, Hourton-Cabassa C, Erdei L, Szabados L (2010) Methods for determination of proline in plants. In Sunkar R, ed., Plant Stress Tolerance. Methods and Protocols. Stillwater Humana Press, Oklahoma, 317-331.

Ahmad I, Wainwright SJ, Stewart GR (1981) The solute and water relations of *Agrostis stolonifera* ecotypes differing in their salt tolerance. New Phytol 87:615-629.

Ahmad S, Ahmad R, Ashraf MY, Ashraf M, Waraich EA (2009) Sunflower (*Helianthus annuus* L.) response to drought stress at germination and seedling growth stages. Pak J Bot 41:647-654.

Albrecht H (1995) Changes in the arable weed flora of Germany during the last five decades. In 9th European Weed Research Society Symposium "Challenges for Weed Science in a Changing Europe", 10-12 July 1995, Budapest, 41-48.

Andreasen C, Skovgaard IM (2009) Crop and soil factors of importance for the distribution of plant species on arable fields in Denmark. Agric Ecosyst Environ 133:61-67.

Andreasen C, Streibig JC, Haas H (1991) Soil properties affecting the distribution of 37 weed species in Danish fields. Weed Res 31:181-187.

Andreasen C, Stryhn H, Streibig JC (1996) Decline of the flora in Danish arable fields. J Appl Ecol 33:619-626.

Baessler C, Klotz S (2006) Effects of changes in agricultural land-use on landscape structure and arable weed vegetation over the last 50 years. Agric Ecosyst Environ 115:43-50.

Bellanger S, Guillemin JP, Bretagnolle V, Darmency H (2012) *Centaurea cyanus* as a biological indicator of segetal species richness in arable fields. Weed Res 52:551-563.

Bischoff A, Mahn EG (2000) The effects of nitrogen and diaspore availability on the regeneration of weed communities following extensification. Agric Ecosyst Environ 77:237-246.

Büchs W (2003) Biodiversity and agri-environmental indicators – general scopes and skills with special reference to the habitat level. Agric Ecosyst Environ 98:35-78.

Claussen W (2005) Proline as a measure of stress in tomato plants. Plant Sci 168:241-248.

Fougére F, Rudulier DL, Streeter JG (1991) Effects of salt stress on amino acid, organic acid, and carbohydrate composition of roots, bacteroids and cytosol of alfalfa (*Medicago sativa* L.). Plant Physiol 96:1228-1236.

Fried G, Petit S, Dessiant F, Reboud X (2009) Arable weed decline in Northern France: Crop edges as refugia for weed conservation? Biol Cons 142:238-243.

George DW (1967) High temperature seed dormancy in wheat (*Triticum aestivum* L.). Crop Sci 7:249-253.

Goumi YE, Fakiri M, Lamsaouri O, Benchekroun M (2014) Salt stress effect on seed germination and some physiological traits in three Moroccan barley (*Hordeum vulgare* L.) cultivars. J Mater Environ Sci 5:625-632.

Hartmann HT, Kester DE, Davies FT, Geneve RL (1997) Plant propagation. Principles and practices. Englewood Cliffs, New Jersey: Prentice-Hall.

Kleijn D, Van Der Voort LAC (1997) Conservation headlands for rare arable weeds: the effects of fertilizer application and light penetration on plant growth. Biol Conserv 81:57-67.

Kubala S, Wojtyla Ł, Quinet M, Lechowska K, Lutts S, Garnczarska M (2015) Enhanced expression of the proline synthesis gene P5CSA in relation to seed osmopriming improvement of *Brassica napus* germination under salinity stress. J Plant Physiol 183:1-12.

Läuchli A, Grattan S (2007) Plant growth and development under salinity stress. In Jenks MA, Hasegawa PM, Jain SM, eds., Advances in Molecular Breeding Toward Drought and Salt Tolerant Crops. Springer, Dordrecht,

1-32.
Meyer S, Wesche K, Krause B, Leuschner C (2013) Veränderungen in der Segetalflora in den letzten Jahrzehnten und mögliche Konsequenzen für Agrarvögel. [Changes in the segetal flora in recent decades and possible consequences for agrar birds] Agrarvögel - ökologische Bewertungsgrundlage für Biodiversitätsziele in Ackerbaugebieten, 1-2 March 2013, Kleinmachnow.
Mohammaddoust HR, Aleksander AA, Tulikov M, Hasanzadeh M, Saidi MR (2008) Effect of fertilizer application on density, dry matter and seed characteristics of garden cornflower (*Centaurea cyanus* L.) and corn spurry (*Spergula arvensis* L.). Pak J Weed Sci Res 14:73-80.
Niinemets Ü (2010) Responses of forest trees to single and multiple environmental stresses from seedlings to mature plants: Past stress history, stress interactions, tolerance and acclimation. Forest Ecol Manag 260:1623-1639.
Preston CD, Pearman DA, Hall AR (2004) Archaeophytes in Britain. Bot J Linn Soc 145:257-294.
Pyšek P, Lepš J (1991) Response of a weed community to nitrogen fertilization: a multivariate analysis. J Veg Sci 2:237-244.
Richner NA (2014) Changes in arable weed communities over the last 100 years. PhD Thesis. Universität Zürich, Germany.
Saeb H, Khayyat M, Zarezadeh A, Moradinezhad F, Samadzadeh A, Safaee M (2013) Effect of NaCl Stress on seed germination attributes of periwinkle (*Catharanthus roseus* L.) and corn poppy (*Papaver rhoeas* L.) plants. Plant Breed Seed Sci 67:115-123.
Samuel D, Kumar TKS, Ganesh G, Jayaraman G, Yang PW, Chang MM, Trivedi VD, Wang SL, Hwang KC, Chang DK, Yu C (2000) Proline inhibits aggregation during protein refolding. Protein Sci 9:344-352.
Šarić T, Ostojić Z, Stefanović L, Milanova SD, Kazinczi G, Tyšer L (2011) The changes of the composition of weed flora in Southeastern and Central Europe as affected by cropping practices. Herbologia 12:5-27.
Schmitz J, Hahn M, Bröhl CA (2014) Agrochemicals in field margins - An experimental field study to assess the impacts of pesticides and fertilizers on a natural plant community. Agric Ecosyst Environ 193:60-69.
Stoate C, Boatman ND, Borralho RJ, Rio Carvalho C, De Snoo GR, Eden P (2001) Ecological impacts of arable intensification in Europe. J Environ Manage 63:337-365.
Svensson R, Wigren M (1986) History and biology of *Consolida regalis* is Sweden. Sven Bot Tidskr 80:31-53.
Turkoglu N, Alp S, Cig A (2009) Effect of temperature on germination biology in *Centaurea* species. Afr J Agric Res 4: 259-261.
Wassmuth BE, Tscharntke T, Stoll P, Thies C (2008) Increasing the scale of intraspecific aggregation facilitates competitively weak plants. In Wassmuth BE, ed., Spatial Aggregations in Annual Wild Plant Communities: Competition, Performance, and Coexistence. Göttingen: Georg-August-Universität, Germany, 30-47.
Williamson M, Stout JC, Dehnen-Schmutz K, Milbau A, Hall AR (2008) A provisional list of Irish archaeophytes. Ir Nat J 29:30-35.
Wörz A, Thiv M (2015) The temporal dynamics of a regional flora – The effects of global and local impacts. Flora 217:99-108.
Zafar S, Ashraf MY, Niaz M, Kausar A, Hussain J (2015) Evaluation of wheat genotypes for salinity tolerance using physiological indices as screening tool. Pak J Bot 47:397-405.

**Volume 61(2):179-188, 2017**
**Acta Biologica Szegediensis**
http://www2.sci.u-szeged.hu/ABS

**ARTICLE**

# *In silico* study of *cis*-acting elements revealing the plastid gene involved in oxidative phosphorylation are responsive to abiotic stresses

Reza Shokri-Gharelo[1]*, Ali Bandehagh[1], Bizhan Mahmoudi[2], Pouya Moti-Noparvar[1]

[1]Department of Plant Breeding and Biotechnology, Faculty of Agriculture, University of Tabriz, Tabriz, Iran.
[2]Department of Animal Science, Ramin Agriculture and Natural Resources University, Ahvaz, Iran

**ABSTRACT** In order to study plastid gene response to abiotic stresses, the chloroplast genome of *Brassica nigra* and studied *cis*-acting elements were downloaded. All upstream regions of genes were determined and searched for the presence of known *cis*-acting elements. In these regions, 83 types of *cis*-acting elements were recognized. Unnamed elements (139 times), CAAT-box (96 times), and TATA-box (92 times) were in high frequency, whereas ATCC-motif, Box III, CE1, CE3, C-repeat/DRE, E2Fb, Gap-box, L-box, RY-element, and TGA-box occurred only one time. All of the *cis*-acting elements were grouped into seven categories, which 17% of *cis*-acting elements placed into abiotic and biotic-related elements. ARE (31 times) and LTR (21 times) elements were in high frequency. Among 42 genes with abiotic stress-related elements, 29 genes showed co-expression. Our results show that in response to anaerobic conditions and cold stress, chloroplast alters the genes-encoding proteins involved in complex I and V in oxidative phosphorylation pathway. This process, probably, is to reduce electron flow and convert NADPH and FADH forms to ATP form. These actions could decrease generating reactive oxygen species under stressful conditions. These findings could offer new insights on the strategies which chloroplasts take into account for preventing oxidative damage.
**Acta Biol Szeged 61(2):179-188 (2017)**

**KEY WORDS**

abiotic stress
*Brassica nigra*
chloroplast
gene regulatory network
genome
transcription factor

## Introduction

During evolution periods, plants have adapted molecular and cellular processes, which have enabled them to survive in constantly changing environments. Transcriptome analysis of plants have indicated that the expression of numerous genes is regulated by abiotic and biotic environmental stresses (Bray et al. 2000; Shinozaki et al. 2003). In such conditions, gene regulatory network is responsible to determine which sets of genes must be expressed, upregulated, downregulated or halted. Gene regulatory networks refer to a collection of molecules, which regulates a set of gene expression in a specific growth stage or in response to external stimuli. One of the important stages of gene expression regulation is at transcription level in which *cis*-acting elements and transcription factors (TF) mediate it. *Cis*-acting elements are strength (sequences) of DNA at the promoter region of a gene, which interact with transcription factors. TFs bound to *cis*-acting elements form the transcriptional initiation complex that activates RNA polymerase to start transcription process of specific genes. In this process, TFs act as molecular switchers to start transcription of the extraordinary gene. TFs themselves are activated in response to external stimuli such as salinity, drought, and temperature alterations and internal stimuli such as hormones (Yamaguchi-Shinozaki and Shinozaki 2005).

Many studies have focused on gene expression and regulatory networks of nucleus genes in response to various types of stimuli (Valliyodan and Nguyen 2006; Santos-Mendoza et al. 2008; Krasensky and Jonak 2012; Yoshida et al. 2014). The organelle genome, however, have been under less attention in the term of regulatory networks. Plastids are specific organelles responsible for photosynthesis and some important metabolic processes. They possess their own genetic material - found in plants and algal cells. It is believed that the origin of plastids in plant came back to an endosymbiotic relationship between plants and cyanobacteria a long time ago (McFadden and van Dooren 2004). The genome of chloroplast in higher plants are transcribed by two types of RNA polymerase, the nuclear-encoded RNA polymerase (NEP) and the plastid-encoded RNA polymerase (PEP). In *Arabidopsis*,

Submitted February 16, 2017; Accepted July 31, 2017
*Corresponding author. E-mail: shokri.gharelo@gmail.com

NEP is phage-type RNA polymerase encoded in three forms, which two forms of them are targeted to chloroplast (Hess and Börner 1999; Maréchal et al. 2009). PEP encoded by the genes *rpoA, rpoB, rpoC1,* and *rpoC2* that are located on the plastid genome. This type of RNA polymerase in higher plants has some features of bacterial RNA polymerase (Liere et al. 2011). Like its counterpart in bacteria, the PEP of *Arabidopsis* is regulated by sigma-like transcription factors (*i.e.* SIG1 to SIG6) that are encoded by the nuclear genome (Yu et al. 2014). The studies on different organisms such as *Nicotiana tabacum* (Suzuki et al. 2004), spinach (Melonek et al. 2012), mustard (Steiner et al. 2011), and *Arabidopsis* (Pfalz and Pfannschmidt 2013) have indicated association of other proteins with PEP core subunits. Proteomic and biochemical analysis have identified some relationships and interactions between some of these nucleus-encoded proteins with regulatory events in chloroplast. Functionally, these proteins could be categorized into DNA/RNA binding proteins, thioredoxin proteins, kinases, ribosome proteins and proteins with unknown function (Steiner et al. 2011). All these proteins make a complex regulatory network that is regulated in response to environmental stimuli and chloroplast gene expression.

It has been shown that the transcriptional activity of plastid genes is affected by exogenous and endogenous factors such as light, temperature, hormones, plastid type, and developmental stage of the plant (Kim and Mullet 1995; Liere et al. 2011). The interaction of regulatory factors with core subunits of RNA polymerases and/or *cis*-regulatory elements is obviously necessary to change the transcription activities. Many of studies have been conducted to identify and role determination of *cis*-acting elements in regulatory networks in plastids using experimental studies. One of the well-known example is the *rbcl* gene in maize, which encodes the large subunit of ribulose-1,5-bisphosphate carboxylase oxygenase. The upstream region of this gene acts as binding site for the chloroplast DNA-binding factor 1 (Lam et al. 1988). Another example for *cis*-acting element is -3 to -32 promoter region of the *rbcl* gene in tobacco. The light-induced DNA-binding protein binds specifically to this segment in response to light to initiate the transcription of *rbcl* in light-dependent manner (Kim et al. 2002). The involvement of such conserved motifs have also been characterized in response to other factors such as blue light-responsive promoter of *psbD* gene (Sexton et al. 1990), temperature stress (Sun and Guo 2016) and water deficit (Stockinger et al. 1997).

*In silico* study of *cis*-acting elements have widely carried out for nucleus genes such as sucrose transporter gene families in rice (Ibraheem et al. 2010), polyphenol oxidase gene (Mahmood et al. 2015), and ascorbate glutathione pathway genes (Pandey et al. 2015). However, it seems that there is no report for studying *cis*-acting regulatory element of chloroplast genome using *in silico* approaches.

In this study, we used simple *in silico* approaches to analyze putative *cis*-acting element of promoter regions in the chloroplast genome of *Brassica nigra,* which was recently sequenced using the latest sequencing and assembling technologies (Seol et al. 2015). *Brassica nigra* belongs to the genus *Brassica* from the family Brassicaceae. The species of the genus *Brassica* are widely cultivated as food supplement of people, especially to produce vegetable oil all around the world (Bandehagh et al. 2011; Gharelo Shokri et al. 2016). All known *cis*-regulatory elements in plants have been searched in the chloroplast complete genome. The occurrence, functional categorization, distribution and frequency of *cis*-regulatory elements were determined. This study could indicate, whether the results of studying through this way agree with previous findings. If the answer is yes, as will show in this study, it could answer the question that; which plastid genes might undergo differential expression in response to other less known crucial factors such as abiotic stresses.

## Materials and Methods

The whole genome of *Brassica nigra* chloroplast (NC_030450.1) was retrieved in FASTA format from National Center for Biotechnology Information (NCBI). Seol et al. (2015) generated this chloroplast genome sequence by *de novo* assembly using whole genome next generation sequences. The sequence consists of 153 633 bp and 114 genes including 80 protein-coding genes, 30 tRNA genes, and 4 rRNA genes.

Using the gene features recorded on NCBI, each gene sequence was separately extracted and saved in FASTA format. These sequences served as inputs on PlantPAN 2.0 (Chow et al. 2016), Promoter Prediction by Neural Network (Reese 2001), and PePPER (de Jong et al. 2012) to predict promoter regions and transcription starting sites (TSS) (Reese 2001). We searched possible promoter regions using the features of prokaryotes and eukaryotes, since chloroplast genome shows both features of prokaryote and eukaryote. A segment from 500 bp upstream and 45 bp downstream away from TSS was selected to detect known *cis*-regulatory elements (CRE) using PlantCARE, a database of plant promoters and their *cis*-acting regulatory elements (Lescot et al. 2002).

STRING 10.0 (http://string-db.org/) is an open source online bioinformatics tool that is used for studying co-expression of genes and gene ontology (GO) enrichment. The data setting was set as follows; minimum required interaction score: highest confidence (0.900), organism: *Arabidopsis thaliana* and disconnected node were hidden from the network. The results of GO enrichment illustrated as chart.

## Results

### Prediction of promoter regions and searching the cis-acting elements

The whole genome of the chloroplast (153 633 bp) was searched for occurrence of prokaryotic and eukaryotic promoters. Totally, 110 promoter regions including 50 eukaryotic and 60 prokaryotic promoters were identified. The average length of the promoter regions was 350 bp, although we selected 500 bp upstream and 20 bp downstream from TSS point. This was because of short length of upstream regions (<500 bp) for some predicted promoters. These regions were searched for presence of known *cis*-acting elements. The results indicated total 1125 known *cis*-acting elements in 83 types. Unnamed, CAAT-box and TATA-box sequences had the highest frequency with 139, 96 and 92 abundances, respectively. The *cis*-acting elements ATCC-motif, Box III, CE1, CE3, C-repeat/DRE, E2Fb, Gap-box, L-box, RY-element, and TGA-box occurred only one time.

### The functional categorization of the cis-acting elements

All recognized *cis*-acting elements had function for responding to internal and mostly to exogenous stimuli such as light, temperature, wounding and hormones (Table 1). Most of the *cis*-acting elements involved in light responsiveness. According to their functions, the *cis*-acting elements was grouped into seven categories: (A) light-responsive elements (40%), (B) abiotic and biotic-related elements (17%), (C) hormone-responsive elements (13%), (D) development-related elements (12%), (E) promoter-related elements (8%), (F) elements with unknown functions (6%), and (G) site-binding elements (4%). The *cis*-acting elements with a function in light responsiveness had the highest redundancy, but the *cis*-acting elements with a function as site-binding elements had the lowest frequency.

The *cis*-acting elements with annotation of light responsive element, *cis*-acting element involved in light responsiveness, part of a light responsive module and part of a conserved DNA module involved in light responsiveness were all placed

**Table 1.** The collection of the *cis*-acting elements at the promoter regions of the chloroplast genome of *B. nigra*.

| Motifs | Description | Position |
|---|---|---|
| CE1 | Cis-acting element associated to ABRE, involved in ABA responsiveness | -64 to-56 |
| TGA-box | Auxin-responsive element | -235 to-79 |
| AT-rich sequence | Binding site of AT-rich DNA binding protein (ATBP-1) | -437 to-426 |
| 5UTR Py-rich stretch | Cis-acting element conferring high transcription levels | -76 to-27 |
| CE3 | Cis-acting element involved in ABA and VP1 responsiveness | -142 to-133 |
| TC-rich repeats | Cis-acting element involved in defense and stress responsiveness | -373 to-262 |
| TATC-box | Cis-acting element involved in gibberellin-responsiveness | -54 to-48 |
| HSE | Cis-acting element involved in heat stress responsiveness | -463 to-445 |
| ACE | Cis-acting element involved in light responsiveness | -225 to-216 |
| LTR | Cis-acting element involved in low-temperature responsiveness | -195 to-190 |
| **TCA-element** | Cis-acting element involved in salicylic acid responsiveness | -448 to-331 |
| ABRE | Cis-acting element involved in the abscisic acid responsiveness | -137 to-57 |
| ATGCAAAT motif | Cis-acting regulatory element associated to the TGAGTCA motif | -166 to-159 |
| A-box | Cis-acting regulatory element associated with P- and L-box | -233 to-160 |
| ARE | Cis-acting regulatory element essential for the anaerobic induction | -487 to-131 |
| AuxRR-core | Cis-acting regulatory element involved in auxin responsiveness | -139 to-133 |
| Circadian | Cis-acting regulatory element involved in circadian control | -254 to-244 |
| G-box | Cis-acting regulatory element involved in light responsiveness | -252 to-63 |
| RY-element | Cis-acting regulatory element involved in seed-specific regulation | -129 to-58 |
| CGTCA-motif | Cis-acting regulatory element involved in the MeJA-responsiveness | -320 to-315 |
| TGACG-motif | Cis-acting regulatory element involved in the MeJA-responsiveness | -305 to-301 |
| O2-site | Cis-acting regulatory element involved in zein metabolism regulation | -240 to-89 |
| CAT-box | Cis-acting regulatory element related to meristem expression | -190 to-180 |
| CCGTCC-box | Cis-acting regulatory element related to meristem specific activation | -151 to-146 |
| Skn-1_motif | Cis-acting regulatory element required for endosperm expression | -98 to-92 |
| Box E | Cis-element for induction upon fungal elicitation | -197 to-187 |
| GCN4_motif | Cis-regulatory element involved in endosperm expression | -165 to-91 |
| CAAT-box | Common cis-acting element in promoter and enhancer regions | -286 to-69 |
| TATA-box | Core promoter element around -30 of transcription start | -125 to-25 |

in the group of light-responsive elements. The *cis*-acting elements, which were located in abiotic and biotic-related elements were responsive elements to wounding, pathogens, cold stress, high temperature, anaerobic conditions, and drought stress. In the third group, *cis*-acting elements had the function in response to endogenous hormones including methyl jasmonate, salicylic acid, gibberellin, abscisic acid, and ethylene. The development-related elements included *cis*-acting regulatory element related to meristem expression, *cis*-acting regulatory element related to meristem specific activation, *cis*-acting regulatory element involved in circadian control and MYB binding site involved in flavonoid biosynthetic genes regulation. The last two groups were common regulatory elements at promoter regions such as TATA-box and CAAT-box as well as motifs for binding of DNA-binding proteins (Table 1).

### *The frequency of the cis-acting elements*

Among 339 light-responsive elements, five *cis*-acting elements were predominant, including 47 G box, 28 Sp1, 27 Box 4, and 23 Box I. Totally, 154 abiotic and biotic stress-related elements among, which ARE was detected 31 times, LTR, 21 times, TC-rich repeats, 15 times and Box-W1, 14 times. The total frequency of hormone-responsive elements was 109 and predominant *cis*-acting elements were CGTCA-motif with frequency of 24, TGACG-motif, 22 and ABRE with frequency of 19. Total number of development-related elements was 116 of which, occurrence of Skn-1_motif was 26 times, MBS, 25 times and circadian, 21 times. TATA-box and CAAT-box with the frequency of 92 and 96 respectively, were dominant motifs in the promoter-related elements with total frequency of 217. In the group of elements with unknown functions, total frequency of all *cis*-acting elements was 181. Unnamed elements with frequency of 139 and AAGAA-motif with frequency of 30 were predominant. The latest group - site-binding elements - had total frequency of 11 (Figs. 1, 2).

### *Co-expression analysis of the plastid genes with abiotic stress-related cis-acting elements*

We analyzed protein-protein interaction (PPI) of the genes with ARE, LTR, and other abiotic stress-related *cis*-acting elements. The genes with the elements were atpF, atpI, cemA, clpP, locus_tag = AYB38_cgr001, locus_tag = AYB38_cgr002, locus_tag = AYB38_cgr007, ndhA, ndhB, ndhC, ndhG, ndhH, ndhI, ndhJ, ndhK, petB, psaA, psbA, psbB, psbC, rpl16, rpl2, rpl22, rpoB, rpoC1, rps12, rps12, rps16, rps2, rps7, rps7, trnA-UGC, trnA-UGC, trnG-UCC, trnI-GAU, trnI-GAU, trnI-GAU, ycf1, ycf1, ycf2, ycf2, and ycf3. Among forty-two genes, 29 genes indicated co-expression, 22 genes indicated interactions proved by experimental evidence, and 22 genes indicated co-occurrence (Fig. 3).

GO analysis set all genes into 15 biological processes. Single-organism process with 17 genes and photosynthetic electron transport in photosystem II with three genes had the highest and the lowest observed gene count. The genes were in four KEGG pathways including oxidative phosphorylation (pathway ID:00190), photosynthesis (pathway ID:00195), metabolic pathways (pathway ID:01100), and RNA polymerase (pathway ID:03020). The oxidative phosphorylation pathway had the highest gene count (Fig. 4).

## Discussion

In this study, we used simple *in silico* methods to survey *cis*-acting elements at promoter regions of the plastid genes. The results indicated light-responsive elements, hormone-responsive elements, and development-related elements as highly frequent elements through the chloroplast genome. All these element functions have previously proved for the chloroplast through experimental works. In *psbD* a 107 bp segment with three pairs of short, repeated sequences upstream of the core promoter -10/-35 is responsible for regulating of the gene expression at transcriptional level. It has been showed that removing these short sequences had leaded to none-responsiveness to light (Allison and Maliga 1995). The similar results for other plastid genes, *rbcS-3A* and *rbcS-3.6*, have also been reported (Cacchione et al. 1991).

The impact of different types of the plant hormones on chloroplast ultrastructure and pigment contents have been studied (Ouzounidou and Ilias 2005; Haisel et al. 2006; Polanská et al. 2007). In addition, researches have indicated that hormones such as methyl jasmonate, gibberellic acid, abscisic acid, and auxin changes chloroplast gene expression (Yamburenko et al. 2013; Zubo et al. 2011). In *Arabidopsis*, cytokinin signals the chloroplast development and function through the transcription factors ARR1, ARR10, and ARR12 (Rashotte et al. 2006). Brenner et al (2005) identified seven plastid genes (*PETA, PSBG, YCF10, YCF5, MATK, PSBA,* and *PSBI*), which their expression rapidly are induced by cytokinin. High portion of these genes, functions are categorized as transcriptional regulators that signals plastid genes. Some of the plastid genes expression such as most plastid sigma factor genes are regulated in different developmental stages. The plastid sigma factor genes seem to be differentially regulated by circadian rhythms during developmental stages (Oikawa et al. 2000; Ichikawa et al. 2004). The question was that how and which regulatory mechanisms govern changes of sigma factor gene expression. Answer was presence of the important factors AthSig2 and AthSig6. These factors bind to specific segment on the plastid genome, *cis*-acting elements, in response to the developmental and probably environmental

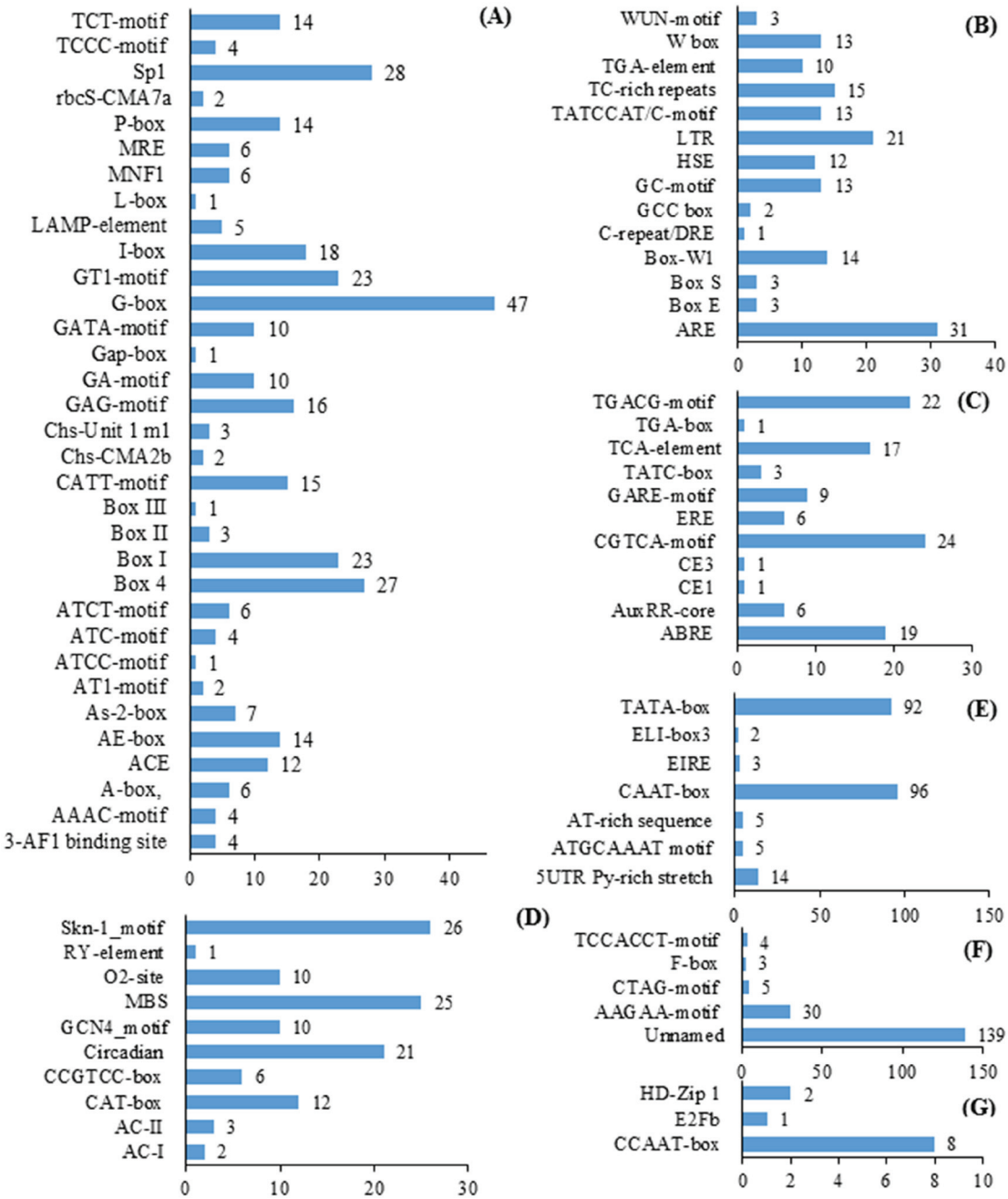


**Figure 1.** The frequency of the *cis*-acting elements. (A) light-responsive elements, (B) abiotic and biotic-related elements, (C) hormone-responsive elements, (D) development-related elements, (E) promoter-related elements, (F) elements with unknown functions, and (G) site-binding elements.

stresses and changes the affinity of PEP to bind on promoter regions (Lysenko 2007).

All these findings show the importance of *cis*-acting elements in regulatory networks in the chloroplast. Our findings also indicated occurrence of *cis*-acting elements with such functions and high frequency (Table 1; Fig. 2). Comparing our results with the results of experimental works, mentioned above, demonstrate the efficiency of this simple *in silico* approach. Therefore, our new findings could be reliable. However, experimental works are unavoidable requirements for final approval of results. It is found that ARE and LTR were high frequency *cis*-acting elements among abiotic and biotic-

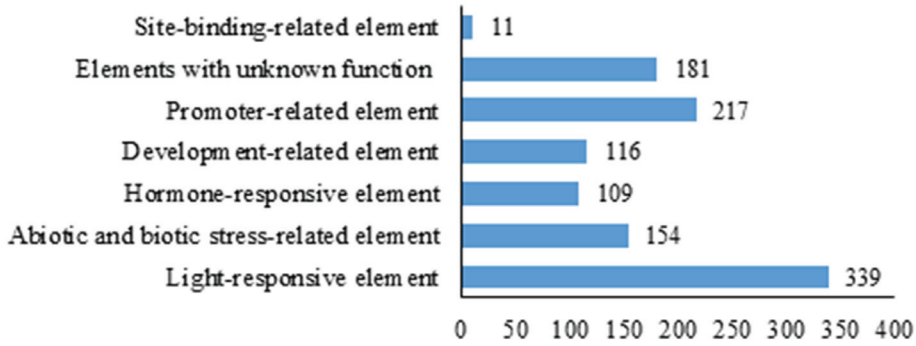


**Figure 2.** Total frequency of the *cis*-regulatory elements in each functional category. One gene can present in more than one category.

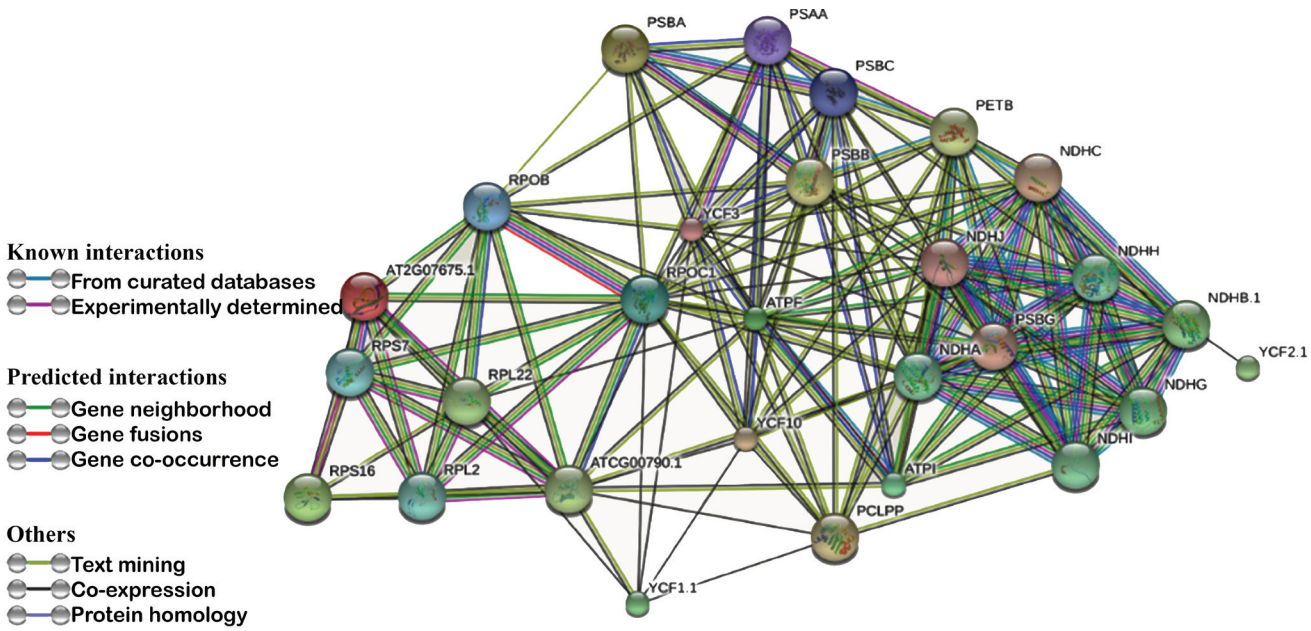


**Figure 3.** Protein-protein interaction of the plastid genes containing abiotic stress-related *cis*-acting elements. Black lines between nodes indicate co-expression.

related elements (Fig. 1). ARE acts as a *cis*-acting regulatory element essential for anaerobic induction and LTR acts as a *cis*-acting element involved in low temperature responsiveness. Other *cis*-acting elements, involved in dehydration and water deficit, occurred in a low frequency (Table 1). Van Veen et al. (2016) reported upregulation of chloroplast-encoded photosynthesis and redox-related genes under submerged plants and Robinson et al. (2008) reported expression changes of chloroplastic genes under low temperature conditions.

These factors also cause differential expression of many nuclear genes (Licausi et al. 2010; Qi et al. 2012; Shingaki-Wells et al. 2014; Chaudhary and Sharma 2015). The studies show that TFs constitute the major part of abiotic stress-responsive nuclear genes (Chen et al. 2012; Mizoi et al. 2012; Nakashima et al. 2012). On the other hand, over 95% of approximately 3000 proteins in plastid are encoded in the nuclear genome that significant portion of them is TFs for regulating the plastid DNA replication, division, and most of gene expression (Laloi et al. 2006). In addition, domain analysis of nuclear-encoded proteins association with PEP-complex in plastids have demonstrated presence of DNA-binding domains (Melonek et al. 2012). It is inferred that abiotic stresses including anaerobic conditions, low temperature, and water deficit (Table 1), are sensed by nucleus, then the nuclear gene expression profile is changed in response to these stimuli. The part of the nuclear expression-changed with

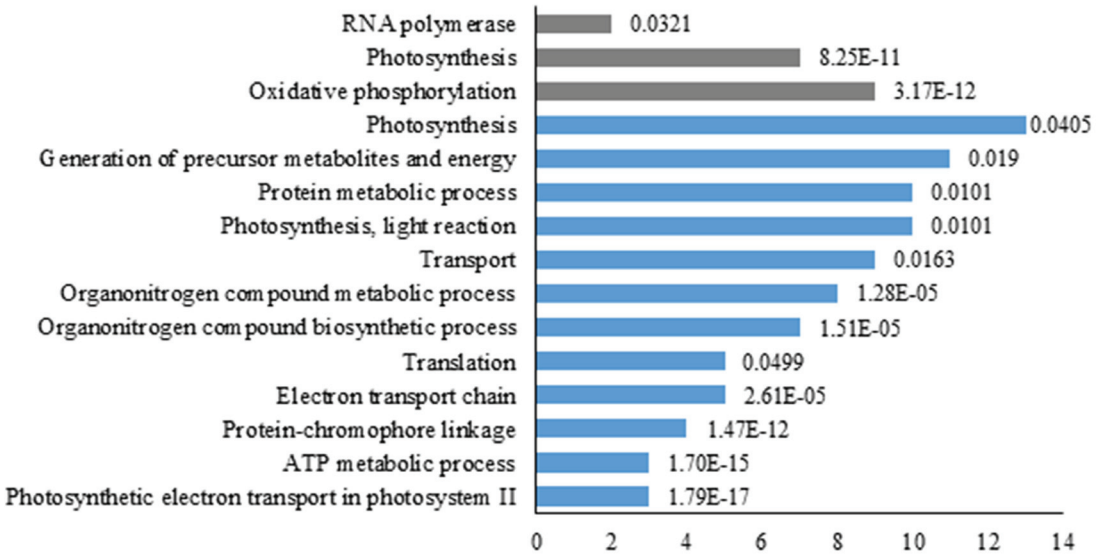


**Figure 4.** Functional enrichment (Biological Process) analysis of the genes with abiotic stress-related *cis*-acting elements. The bars indicate count in gene set. Data labels indicate false discovery rate. The gray bars indicate the count of genes in KEGG pathways.

TF activity might travel into the chloroplast and influence the plastid gene expression through binding these *cis*-acting elements.

In order, to evaluate the occurrence of abiotic stress-related *cis*-acting elements, we used STRING 10.0 to form protein-protein interaction network. All genes with abiotic stress-related *cis*-acting elements, specifically ARE- and LTR-containing genes, showed good connectivity (Fig. 3). STRING 10.0 calculates connectivity between proteins based on different evidences, in which one of them is co-expression of those protein-encoding genes. Almost all the genes showed co-expression (indicated as black lines between proteins in Fig. 3). Sharma (2015) found that genes co-expressed under osmotic stress share same regulatory motifs. He suggested that co-expressed genes with same motifs are under governing of a specific regulator system. Hudson and Quail (2003) in an attempt to identify promoter motifs in phytochrome A (phyA) -induced and phyA-repressed genes found that G-box and CACGTG-motif were abundant regulatory elements in these two sets of genes. This finding means that TFs induced in respond to an extraordinary stimulus, phyA here, bind to same and conserved sequences among genes responsive to that stimulus. There is another *in silico* and experimental studies such as regulatory elements that control the expression of the *Salmonella csrB* and *csrC* genes (Martínez et al. 2014), involving specific motifs in responsiveness of *Hippocampal* gene expression (Datson et al. 2011), genome-wide identification of DNA binding specificities for the *ApiAP2* family (Campbell et al. 2010), determining *cis*-regulatory elements specific for different types of reactive oxygen species (Petrov et al. 2012), and association of specific *cis*-regulatory elements with abiotic stresses (Bolívar et al. 2014), all indicate same conserved sequences in the upstream region of co-expressed genes in response to a particular stimulus. Therefore, from our results, it could be concluded that co-expression of the genes with abiotic stress-related *cis*-acting elements can represent that they are under same regulatory system in response to the abiotic stresses (Table 1; Fig. 1).

All GO terms were in relation with the functions of chloroplast in higher plants. In our results, single-organism process, single-organism metabolic process, and oxidation-reduction process were parent terms, which were divided into 12-child GO terms (*i.e.* photosynthesis, generation of precursor metabolites and energy, and protein metabolic process; blue bars in Fig. 4). In the case of KEGG pathways, the term metabolic pathway was parent term subdivided into 3-child GO terms including photosynthesis, oxidative phosphorylation, and RNA polymerase pathways (gray bars in Fig. 4). GO enrichment analysis provides terms for representing genes and gene products in living organisms (Shah et al. 2003). We used the term "Biological Process' and "KEGG pathways" to represent gene function and pathway.

According to our GO enrichment analysis (Fig. 4), significant count of genes had photosynthesis function involved in oxidative-phosphorylation pathway. This means that oxidative phosphorylation is more responsive to abiotic stress, taking place in the mitochondria and is linked to photophosphorylation events in the chloroplast (Buchanan et al. 2015). The chloroplast and mitochondria are involved in either the reduction of oxygen or the oxidation of water (Kristiansen et al. 2009). Therefore, the chloroplast and mitochondria are one of the main sources of reactive oxygen species (ROS) pro-

duction sites. Under normal conditions, antioxidant systems scavenger ROSs, prevent cell from being damaged. Under stressful conditions, however, the rate of ROS production is in a level that could harm these organelles and the cell thereupon (Gechev et al. 2006). Plants in order to avoid excessive production of ROSs, in the chloroplast, use variable systems including photorespiration, the cyclic electron flow through PSI or PSII, and the downregulation of 2 PSII quantum yield by the xanthophyll cycle and the proton gradient across the thylakoid membrane (Møller et al. 2007). Our results indicate that the genes involved in oxidative phosphorylation pathways encode two series of proteins: NADH dehydrogenase family protein in the complex I and ATP synthase in complex V. It seems that under abiotic stresses such as salinity, drought, and temperature, water absorption is impaired; a regulatory system controls these genes likely in order to decrease electron flow through regulation of NADH dehydrogenase-encoding genes and producing ATP through regulating ATP synthase-encoding genes. Theoretically, a low level of electron flow and conversion of equivalent equilibrium units in the forms of NADPH and FADH to ATP can be efficient and smart way to restrict electron transferring on oxygen molecules and therefor ROS production. However, this system needs to be confirmed by experimental works.

## Conclusions

Based on the role of *cis*-acting elements in regulating gene network in response to diverse types of stimuli, this study demonstrated that the chloroplast genome responds mainly to anaerobic and cold stresses among abiotic stress-responsive genes. In response to abiotic stress, it seems that the chloroplast genome mostly changes the genes involved in oxidative phosphorylation pathway through nuclear-encoded TFs. According to the function of these genes, the regulation is to decrease electron flow on electron transport chain and conversion of NADPH and FADH forms to ATP form in order to lower ROS production. Although, such *in silico* studies have previously been confirmed by experimental works, it is recommended that these genes expression should be studied under abiotic stresses by experimental methods such as RT-PCR.

## References

Allison LA, Maliga P (1995) Light-responsive and transcription-enhancing elements regulate the plastid psbD core promoter. EMBO J 14:3721.

Bandehagh A, Salekdeh GH, Toorchi M, Mohammadi A, Komatsu S (2011) Comparative proteomic analysis of canola leaves under salinity stress. Proteomics 11:1965-1975.

Bolívar JC, Machens F, Brill Y, Romanov A, Bülow L, Hehl R (2014) '*In silico* expression analysis', a novel PathoPlant web tool to identify abiotic and biotic stress conditions associated with specific cis-regulatory sequences. Database 2014:bau030.

Bray EA, Bailey-Serres J, Weretilnyk E (2000) Responses to abiotic stresses. Biochem Mol Biol Plants 1158:e1203.

Brenner WG, Romanov GA, Köllmer I, Bürkle L, Schmülling T (2005) Immediate-early and delayed cytokinin response genes of *Arabidopsis thaliana* identified by genome-wide expression profiling reveal novel cytokinin-sensitive processes and suggest cytokinin action through transcriptional cascades. Plant Cell J 44:314-333.

Buchanan BB, Gruissem W, Jones RL (2015) Biochemistry and Molecular Biology of Plants, 2nd ed. John Wiley & Sons.

Cacchione S, Savino M, Tufillaro A (1991) Different superstructural features of the light responsive elements of the pea genes *rbcS-3A* and *rbcS-3.6*. FEBS Lett 289:244-248.

Campbell TL, De Silva EK, Olszewski KL, Elemento O, Llinás M (2010) Identification and genome-wide prediction of DNA binding specificities for the ApiAP2 family of regulators from the malaria parasite. PLoS Pathog 6:e1001165.

Chaudhary S, Sharma PC B (2015) DeepSAGE based differential gene expression analysis under cold and freeze strees in seabuckthorn (*Hippophae rhamnoides* L.). PloS ONE 10:e0121982.

Chen L, Song Y, Li S, Zhang L, Zou C, Yu D (2012) The role of WRKY transcription factors in plant abiotic stresses. BBA-Gene Reg Mech 1819:120-128.

Chow CN, Zheng HQ, Wu NY, Chien CH, Huang HD (2016) PlantPAN 2.0: an update of plant promoter analysis navigator for reconstructing transcriptional regulatory networks in plants. Nucleic acids research 44:1154-1160.

Datson N, Polman J, de Jonge R, van Boheemen P, van Maanen E (2011) Specific regulatory motifs predict glucocorticoid responsiveness of hippocampal gene expression. J Endocrinol 152:3749-3757.

de Jong A, Pietersma H, Cordes M, Kuipers OP, Kok J (2012) PePPER: a webserver for prediction of prokaryote promoter elements and regulons. BMC genomics 13:299.

Gechev TS, van Breusegem F, Stone JM, Denev I, Laloi C (2006) Reactive oxygen species as signals that modulate plant stress responses and programmed cell death. BioEssays 28:1091-1101.

Gharelo Shokri R, Bandehagh A, Tourchi M, Farajzadeh D (2016) Canola 2-dimensional proteom profile under osmotic stress and inoculation with *Pseudomonas fluorescens* FY32. PCBMB 17:257-266.

Haisel D, Pospíšilová J, Synková H, Schnablová R, Baťková P (2006) Effects of abscisic acid or benzyladenine on pigment contents, chlorophyll fluorescence, and chloroplast ultrastructure during water stress and after rehydration. Photosynthetica 44:606-614.

Hess WR, Börner T (1999) Organellar RNA polymerases of higher plants. Int Rev Cytol 190:1-59.

Hudson ME, Quail PH (2003) Identification of promoter motifs involved in the network of phytochrome A-regulated gene expression by combined analysis of genomic sequence and microarray data. Plant Physiol 133:1605-1616.

Ibraheem O, Botha CE, Bradley G (2010) *In silico* analysis of cis-acting regulatory elements in 5′ regulatory regions of sucrose transporter gene families in rice (*Oryza sativa* Japonica) and *Arabidopsis thaliana*. Comput Biol Chem 34:268-283.

Ichikawa K, Sugita M, Imaizumi T, Wada M, Aoki S (2004) Differential expression on a daily basis of plastid sigma factor genes from the moss Physcomitrella patens. Regulatory interactions among PpSig5, the circadian clock, and blue light signaling mediated by cryptochromes. Plant Physiol 136:4285-4298.

Kim JW, Park JK, Kim BH, Lee J-S, Sim WS (2002) Molecular analysis of the accumulation of the transcripts of the large subunit gene of ribulose-1,5-bisphosphate carboxylase/oxygenase by light. Mol Cell Biol 14:281-287.

Kim M, Mullet JE (1995) Identification of a sequence-specific DNA binding factor required for transcription of the barley chloroplast blue light-responsive psbD-psbC promoter. Plant J 7:1445-1457.

Krasensky J, Jonak C (2012) Drought, salt, and temperature stress-induced metabolic rearrangements and regulatory networks. J Exp Bot 63:1593-1608.

Kristiansen KA, Jensen PE, Møller IM, Schulz A (2009) Monitoring reactive oxygen species formation and localisation in living cells by use of the fluorescent probe CM-H2DCFDA and confocal laser microscopy. Physiol Plant 136:369-383.

Laloi C, Przybyla D, Apel K (2006) A genetic approach towards elucidating the biological activity of different reactive oxygen species in *Arabidopsis thaliana*. J Exp Bot 57:1719-1724.

Lam E, Hanley-Bowdoin L, Chua N (1988) Characterization of a chloroplast sequence-specific DNA binding factor. J Biol Chem 263:8288-8293.

Lescot M, Déhais P, Thijs G, Marchal K, Moreau Y (2002) PlantCARE, a database of plant cis-acting regulatory elements and a portal to tools for in silico analysis of promoter sequences. Nucleic Acids Res 30:325-327.

Licausi F, Van Dongen JT, Giuntoli B, Novi G, Santaniello A (2010) HRE1 and HRE2, two hypoxia-inducible ethylene response factors, affect anaerobic responses in *Arabidopsis thaliana*. Plant Cell J 62:302-315.

Liere K, Weihe A, Börner T (2011) The transcription machineries of plant mitochondria and chloroplasts: composition, function, and regulation. J Plant Physiol 168:1345-1360.

Lysenko EA (2007) Plant sigma factors and their role in plastid transcription. Plant Cell Rep 26:845-859.

Mahmood T, Rehman MU, Aziz E, Ali I, Shinwari ZK (2015) *In silico* analysis, mapping of regulatory elements and corresponding dna-protein interaction in polyphenol oxidase gene promoter from different rice varieties. Pak J Bot 47:2321-2327.

Maréchal A, Parent JS, Véronneau-Lafortune F, Joyeux A, Lang BF, Brisson N (2009) Whirly proteins maintain plastid genome stability in *Arabidopsis*. Proc Natl Acad Sci USA 106:14693-14698.

Martínez LC, Martínez-Flores I, Salgado H, Fernández-Mora M, Medina-Rivera A (2014) *In silico* identification and experimental characterization of regulatory elements controlling the expression of the *Salmonella* csrB and csrC genes. J Bacteriol 196:325-336.

McFadden GI, van Dooren GG (2004) Evolution: red algal genome affirms a common origin of all plastids. Curr Biol 14:R514-R516.

Melonek J, Matros A, Trösch M, Mock H-P, Krupinska K (2012) The core of chloroplast nucleoids contains architectural SWIB domain proteins. Plant J 24:3060-3073.

Mizoi J, Shinozaki K, Yamaguchi-Shinozaki K (2012) AP2/ERF family transcription factors in plant abiotic stress responses. BBA-Gene Reg Mecha 1819:86-96.

Møller IM, Jensen PE, Hansson A (2007) Oxidative modifications to cellular components in plants. Annu. Rev. Plant Biol. 58:459-481.

Nakashima K, Takasaki H, Mizoi J, Shinozaki K, Yamaguchi-Shinozaki K (2012) NAC transcription factors in plant abiotic stress responses. BBA-Gene Reg Mech 1819:97-103.

Oikawa K, Fujiwara M, Nakazato E, Tanaka K, Takahashi H (2000) Characterization of two plastid σ factors, SigA1 and SigA2, that mainly function in matured chloroplasts in *Nicotiana tabacum*. Gene 261:221-228.

Ouzounidou G, Ilias I (2005) Hormone-induced protection of sunflower photosynthetic apparatus against copper toxicity. Biol Plant 49:223.

Pandey S, Subramanaym Reddy C, Yaqoob U, Negi Y, Arora S (2015) *In silico* Analysis of cis acting regulatory elements CAREs in upstream regions of ascorbate glutathione pathway genes from *Oryza sativa*. Biochem Physiol 4:2.

Petrov V, Vermeirssen V, de Clercq I, Van Breusegem F, Minkov I (2012) Identification of cis-regulatory elements specific for different types of reactive oxygen species in *Arabidopsis thaliana*. Gene 499:52-60.

Pfalz J, Pfannschmidt T (2013) Essential nucleoid proteins in early chloroplast development. Trends Plant Sci 18:186-194.

Polanská L, Vičánková A, Nováková M, Malbeck J, Dobrev PI (2007) Altered cytokinin metabolism affects cytokinin, auxin, and abscisic acid contents in leaves and chloroplasts, and chloroplast ultrastructure in transgenic tobacco. J Exp Bot 58:637-649.

Qi XH, Xu XW, Lin XJ, Zhang WJ, Chen XH (2012) Identification of differentially expressed genes in cucumber (*Cucumis sativus* L.) root under waterlogging stress by digital gene expression profile. Genomics 99:160-168.

Rashotte AM, Mason MG, Hutchison CE, Ferreira FJ, Schaller GE, Kieber JJ (2006) A subset of *Arabidopsis* AP2 transcription factors mediates cytokinin responses in concert with a two-component pathway. Proc Natl Acad Sci USA 03:11081-11085.

Reese MG (2001) Application of a time-delay neural network to promoter annotation in the *Drosophila melanogaster* genome. Comput Chem 26:51-56.

Robinson SJ, Parkin IA (2008) Differential SAGE analysis in *Arabidopsis* uncovers increased transcriptome complexity in response to low temperature. BMC Genomics 9:434.

Santos-Mendoza M, Dubreucq B, Baud S, Parcy F, Caboche M, Lepiniec L (2008) Deciphering gene regulatory networks that control seed development and maturation in *Arabidopsis*. Plant Cell J 54:608-620.

Seol Y-J, Kim K, Kang SH, Perumal S, Lee J, Kim CK (2015) The complete chloroplast genome of two *Brassica* species, *Brassica nigra* and *B. oleracea*. MDN 1-2.

Sexton TB, Christopher DA, Mullet J (1990) Light-induced switch in barley psbD-psbC promoter utilization: a novel mechanism regulating chloroplast gene expression. EMBO J 9:4485.

Shah N, King D, Shah P, Fedoroff NV (2003) A tool-kit for cDNA microarray and promoter analysis. Bioinformatics 19:1846-1848.

Sharma A (2015) *In silico* identification of regulatory motifs in co-expressed genes under osmotic stress representing their co-regulation. Plant Gene 1:29-34.

Shingaki WR, Millar AH, Whelan J, Narsai R (2014) What happens to plant mitochondria under low oxygen? An omics review of the responses to low oxygen and reoxygenation. Plant Cell Environ 37:2260-2277.

Shinozaki K, Yamaguchi-Shinozaki K, Seki M (2003) Regulatory network of gene expression in the drought and cold stress responses. Curr Opin Plant Biol 6:410-417.

Steiner S, Schröter Y, Pfalz J, Pfannschmidt T (2011) Identification of essential subunits in the plastid-encoded RNA polymerase complex reveals building blocks for proper plastid development. Plant Physiol 157:1043-1055.

Stockinger EJ, Gilmour SJ, Thomashow MF (1997) *Arabidopsis thaliana* CBF1 encodes an AP2 domain-containing transcriptional activator that binds to the C-repeat/DRE, a cis-acting DNA regulatory element that stimulates transcription in response to low temperature and water deficit. Proc Natl Acad Sci USA 94:1035-1040.

Sun AZ, Guo FQ (2016) Chloroplast retrograde regulation of heat stress responses in plants. Front Plant Sci 7.

Suzuki JY, Jimmy Ytterberg A, Beardslee TA, Allison LA, Wijk KJ, Maliga P (2004) Affinity purification of the tobacco plastid RNA polymerase and in vitro reconstitution of the holoenzyme. Plant Cell J 40:164-172.

Valliyodan B, Nguyen HT (2006) Understanding regulatory networks and engineering for enhanced drought tolerance in plants. Curr Opin Plant Biol 9:189-195.

van Veen H, Vashisht D, Akman M, Girke T, Mustroph A (2016) Transcriptomes of eight *Arabidopsis thaliana* accessions reveal core conserved, genotype-and organ-specific responses to flooding stress. Plant Physiol 172(2):668-689.

Yamaguchi-Shinozaki K, Shinozaki K (2005) Organization of cis-acting regulatory elements in osmotic-and cold-stress-responsive promoters. Trends Plant Sci 10:88-94.

Yamburenko MV, Zubo YO, Vanková R, Kusnetsov VV, Kulaeva ON, Börner T (2013) Abscisic acid represses the transcription of chloroplast genes. J Exp Bot 64:4491-4502.

Yoshida T, Mogami J, Yamaguchi-Shinozaki K (2014) ABA-dependent and ABA-independent signaling in response to osmotic stress in plants. Curr Opin Plant Biol 21:133-139.

Yu Q-B, Huang C, Yang ZN (2014) Nuclear-encoded factors associated with the chloroplast transcription machinery of higher plants. Front Plant Sci 5:316.

Zubo YO, Yamburenko MV, Kusnetsov VV, Börner T (2011) Methyl jasmonate, gibberellic acid, and auxin affect transcription and transcript accumulation of chloroplast genes in barley. J Plant Physiol 168:1335-1344.

**Volume 61(2):189-195, 2017**
**Acta Biologica Szegediensis**
http://www2.sci.u-szeged.hu/ABS

**ARTICLE**

# Growth, secondary metabolites production, antioxidative and antimicrobial activity of mint under the influence of plant growth regulators

Adisa Parić[1]*, Erna Karalija[1], Jasmina Čakar[2]

[1]University of Sarajevo, Faculty of Sciences, Department of Biology, Sarajevo, Bosnia and Herzegovina
[2]University of Sarajevo, Institute for Genetic Engineering and Biotechnology, Sarajevo, Bosnia and Herzegovina

**ABSTRACT** The effects of plant growth regulators on *Mentha piperita* explants cultured *in vitro* were studied for the purpose of analyse growth, secondary metabolite production, antioxidant and antimicrobial activities in micropropagated plants. The basal medium was experimentally supplemented with the auxin, indole-3-butyric acid (IBA) and the cytokinin, N6-benzyladenine (BAP) individually and in combination. Treatment with BAP and IBA resulted in an increased shoot and root number. The production of phenolic compounds was affected by the addition of the highest concentration of BAP, while antioxidant and antimicrobial activities were affected by several BAP and IBA treatments. Our results demonstrate that the application of growth regulators increases growth and secondary metabolite productions in the medicinal herb *M. piperita*.
**Acta Biol Szeged 61(2):189-195 (2017)**

**KEY WORDS**

antimicrobial activity mint
antioxidants
secondary metabolites

## Introduction

Oxygen free radicals induce damage due to membrane peroxidation, which leads to tissue damage. The consequences include peroxidation of lipids, oxidation of proteins, enzyme inhibition, activation of programmed cell death pathway and finally to death of the cells (Mittler 2002). In order to minimize damage induced by free radicals, plants have a number of mechanisms, such as the antioxidants. Many aromatic and medicinal plants contain chemical compounds showing antioxidant properties (Gautam et al. 2012). The most abundant is family Lamiaceae with numerous species that are used as spice and medicinal herb. One of them is mint (*Mentha piperita* L.) that is used in the traditional medicine to relieve the symptoms of vomiting, indigestion, stomach and menstrual cramps and parasitosis (Baliga and Rao 2010; Kavina et al. 2011). It is also known for its carminative, stimulant, antispasmodic, antiseptic, anti-inflammatory, antibacterial and antifungal activities (Guedon and Pasquier 1994; Sean et al. 2004).

Flavonoids and phenolic acids are the major classes of phenolic compounds, whose antioxidant activity is described in a number, of papers (Nenadis et al. 2004). In addition to antioxidant activity, many phenolic compounds have been shown to exert anticancer or antimutagenic activity (Tapiero et al. 2002; Awale et al. 2005). *In vitro* culture techniques today present an effective alternative tool for the production, of secondary metabolites, with even higher secondary metabolites production than the intact plants (Parr 1989; Rao and Ravishankar 2002). Plant growth regulators are crucial factors in growth and secondary metabolite biosynthesis in plant tissue cultures. For example, they noticed that the auxins and cytokinins influences both growth index and rosmarinic acid accumulation in *Coleus blumei* (Qian et al. 2009) or cardiac glycosides production in *Digitalis lanata* (Palazon et al. 1994). Alterations in the type and concentration of auxin or cytokinin as well as the auxin/cytokinin ratio have strong effects on both growth and metabolite formation in plants (Rao and Ravishankar 2002). Auxin/cytokinin ratio appears to be the primary factor controlling growth and morphology, while the effects on secondary metabolite formation varied and depended on plant species (Sharafzadeh and Zare 2001; Scravoni et al. 2006). The effects of some plant growth regulators on secondary metabolite production have been already studied and confirmed (Shukla and Farooqi 1990; Stoeva and Iliev 1997; Sharafzadeh and Zare 2001; Farooqi et al. 2003; Arikat et al. 2004).

The aim of this study was to analyze the effect of different concentration of a cytokinin, N6-benzyladenine purine (BAP) alone or in combination with an auxin, indole-3-butyric acid

Submitted August 9, 2017; Accepted November 20, 2017
*Corresponding author. E-mail: adisa.p@pmf.unsa.ba

(IBA) on the growth, biochemical changes and secondary metabolites production of *Mentha piperita* L. cultures *in vitro*.

## Materials and Methods

### Plant materials and treatments

Commercially purchased seeds of *M. piperita* L. (Sjemenarna, Ljubljana, Slovenia) were surface-sterilized and germinated on a MS basal medium (Murashige and Skoog 1962). Shoot multiplication was investigated by culturing epicotyls at different level (0.0, 0.1, 0.5, 1.0, 2.0 and 4.0 mg/L) of N6-benzyladenine (BAP) alone (BH; B0.1; B0.5; B1; B2; B4) or in combination with 0.1 mg/L indole-3-butyric acid (IBA; BI0.1; BI0.5; BI1; BI2; BI4). The pH of all media was adjusted to 5.8 with 1 M KOH or 1 M HCl before autoclaving at 121 °C for 20 min. All cultures were incubated at 24 ± 1 °C under cool white fluorescent lights (40 μmol $m^{-2}s^{-1}$) and with the 16 h light photoperiod. The plants were collected on thirty days after treatment and used for the analysis of growth parameters, photosynthetic pigments and secondary metabolite content, antioxidant and antimicrobial activity.

### Growth parameters and photosynthetic pigments

Number of shoots and roots per explant was recorded after 30 days of cultivation. Extraction of photosynthetic pigments followed the method described by Porra et al. (1989). Quantification was done by spectrophotometric determination of the absorbance at 663 nm (chlorophyll a), 646 nm (chlorophyll b) and 440 nm (carotenoids) according to Porra et al. (1989) and Holm (1954). The concentrations of photosynthetic pigments were expressed as mg of pigments per g fresh weight (mg/g FW).

### Secondary metabolite analysis

#### *Sample preparation*

Aerial parts of *in vitro* cultivated mint were air dried and grounded in a mixer. A portion of the finely powdered material was extracted three times with 70% methanol during a 24 h period at 4 °C. After removal of methanol all extracts were evaporated to dryness and then dissolved in absolute ethanol to make 1% (w/v) solutions.

#### *Determination of total phenol content*

Total phenolic compound contents were determined by the Folin-Ciocalteu method (Pal et al. 2009). Phenols were determined by spectrophotometric readings at 765 nm. The standard curve was prepared using catechine as standard. Total phenol values are expressed in terms of catechine equivalent (mg/g of dry mass - DM).

#### *Determination of total flavonoid content*

Colorimetric aluminium chloride method was used for flavonoid determination (Waterhouse 2001). Solution of plant extract was mixed with 95% ethanol, 10% aluminium chloride, 1 M sodium acetate and distilled water. After incubation at room temperature for 30 min absorbance was measured at 415 nm at Shimadzu UV/Vis mini-1240 spectrophotometer. Total flavonoid contents were calculated as quercetin from a calibration curve and expressed as quercetin equivalent (mg/g DM).

#### *Flavanols determination*

Flavanols determination was based on the method of Gadzovska et al. (2007) and calibration curve of quercetin. Flavanol contents were expressed as quercetin equivalent (mg/g DM).

#### *Determination of antioxidant activity by the FTC (ferric thiocyanate) method*

The inhibitory capacity of extracts was tested against oxidation of linoleic acid by FTC method according to Larrauri et al. (1996). The absorbance was measured spectrophotometrically at 500 nm. Butylated hydroxytoluene (BHT) and butylated hydroxyanisole (BHA) used as positive control. The percent inhibition of linoleic acid peroxidation was calculated as: (%) inhibition = 100 - [(absorbance increase of sample/absorbance increase of control) × 100].

#### *Antimicrobial bioassay*

Antibacterial activity was determined by the disc diffusion method according to the Taylor et al. (1995). Two Gram-positive (*Enterococcus faecalis* ATCC 19433and *Bacillus subtilis* ATCC 6633), two Gram-negative (*Salmonella abony* NCTC 6017 and *Escherichia coli* ATCC 8397) bacterial species and two fungal strains (*Candida albicans* ATCC 10231 and *Aspergillus brasiliensis* ATCC 16404) were used. All tested microorganisms were inoculated into respective medium in concentration of $2.0 \times 10^6$ colony forming units (cfu/mL). Mueller-Hinton and Sabouraud agar (15 mL), sterilized in a flask and cooled to 45-50 °C, was distributed to sterilized Petri dishes with a diameter of 9 cm. A volume of 10 mL of the sample was injected onto the inoculated discs. The Petri dishes were kept at 4 °C for 2 h, and then incubated at 37 °C

**Table 1.** Effect of BAP on adventitious shoot and root formation, photosynthetic pigment, total phenolic, total flavonoid, flavanol contents and antioxidative activity of *Mentha piperita*.

| Treatment | Number of shoots per explant | Number of roots per explant | Chlorophyll a (mg/g FW) | Chlorophyll b (mg/g FW) | Total chlorophyll | Carotenoids (mg/g FW) | Total phenolics (mg/g DW) | Total flavonoids (mg/g DW) | Flavanols (mg/g DW) | Antioxidative activity (% of inhibition) |
|---|---|---|---|---|---|---|---|---|---|---|
| BH | 2.467$^{b}$ | 3.158$^{b}$ | 0.2089$^{c}$ | 0.0600$^{b}$ | 0.2689$^{b,c}$ | 0.0736$^{c}$ | 185.63$^{b}$ | 70.29$^{a}$ | 0.026$^{a}$ | 7.69$^{d}$ |
| B 0.1 | 3.189$^{b}$ | 5.278$^{a}$ | 0.3710$^{a}$ | 0.1065$^{a}$ | 0.4775$^{a}$ | 0.1066$^{a}$ | 173.63$^{c}$ | 75.30$^{a}$ | 0.025$^{a}$ | 56.64$^{a}$ |
| B 0.5 | 4.167$^{a}$ | 5.394$^{a}$ | 0.2639$^{b}$ | 0.0748$^{a,b}$ | 0.3387$^{b}$ | 0.0875$^{b}$ | 51.40$^{d}$ | 63.07$^{a}$ | 0.018$^{b}$ | 36.27$^{b}$ |
| B 1 | 2.500$^{b}$ | 3.563$^{b,c}$ | 0.1631$^{c,d}$ | 0.0515$^{b}$ | 0.2146$^{c,d}$ | 0.0657$^{c}$ | 189.13$^{b}$ | 24.59$^{c}$ | 0.013$^{c}$ | 26.67$^{c}$ |
| B 2 | 4.167$^{a}$ | 3.542$^{b}$ | 0.1402$^{d}$ | 0.0558$^{b}$ | 0.1959$^{c,d}$ | 0.0541$^{d}$ | 181.27$^{b}$ | 69.25$^{a}$ | 0.014$^{c}$ | 39.15$^{b}$ |
| B 4 | 1.400$^{b}$ | 1.600$^{c}$ | 0.0923$^{e}$ | 0.0619$^{b}$ | 0.1543$^{d}$ | 0.0508$^{d}$ | 221.13$^{a}$ | 35.35$^{b}$ | 0.001$^{d}$ | 8.67$^{d}$ |
| BHA | | | | | | | | | | 56.50$^{b}$ |
| BHT | | | | | | | | | | 61.91$^{a}$ |

Values are mean (±SD) of three replicates. Treatments not sharing the same letter within one column differ significantly employing parametric (Newman-Keuls) and non-parametric for No of roots and shoots (Kruskal-Walis analysis) tests.
BH-without plant growth regulators; B 0.1-0.1 mg/L BAP; B 0.5-0.5 mg/L BAP; B 1-1 mg/L BAP; B 2-2 mg/L BAP; BHA-butylated hydroxyanisol; BHT-butylated hydroxytoluene.

for 24 h. The diameters of the inhibition zones were measured in mm. Controls were set up with equivalent quantities of methanol. The developing inhibition zones were compared with those of reference discs. Antibiotic chloramphenicol (5 mg/mL) and kanamycin (5 mg/mL) were used as reference.

### *Statistical analysis*

Experimental results were represented as the mean value of the three replicates with standard deviation (SD). The data was analyzed using SPSS 15.0 by employing parametric (Newman-Keuls) and non-parametric (Kruskal-Walis analysis) tests. All statistically significant differences were evaluated at $p<0.05$.

## Results and Discussion

### *Growth parameters and pigment contents*

Epicotyls of *M. piperita* inoculated on MS medium supplemented with different concentrations of growth regulators were suitable material for shoot and root induction (Tables 1, 2), with the exception of treatment BI4 (4 mg/L BAP in combination with 0.1 mg/L IBA), which induced necrosis of tissue. Thus, this treatment was not used for further analysis. BAP alone increased the number of shoots comparing to the control. The highest number of shoots (4.167 shoots per explant) was obtained with B0.5 and B2 treatments. However, the shoot number decreased when the highest BAP concentration (4 mg/L) was used for the induction of shoots compared to control, but the changes were not significant (from 1.4 to 2.5). The addition of IBA into the medium considerably enhanced the multiple shoots induction. The maximum induction of multiple shoots (6.490 and 6.241) was achieved from medium BI0.5 and BI2, respectively.

Remarkable improvement was observed when the IBA + BAP combination was used with significant positive correlation between the number of shoots and the plant growth regulator concentration at a level of 5%. Very similar situation was recorded for number of roots. The best rooting response, however, was observed on medium BI0.5, where 8.608 roots were formed per explant. Similarly, the addition of IBA into the medium significantly improved the root induction (treatments BI0.1 and BI0.5). This was expected since the application of auxins enhanced rooting in most species (Benkova and Hejatko 2009; Fukaki and Tasaka 2009). Usually, BAP and kinetin have been reported to be good plant growth regulators for shoot induction from axillary buds and nodal segments when cultured on MS medium (Rech and Pires 1986; Sunandakumari et al. 2004). However, in some plant species, including *M. spicata*, *M. arvensis,* and *Lavandula viridis*, a combination of cytokinin and auxin in the medium was more effective (Hirata et al. 1990; Kukreja et al. 1991; Dias et al. 2002).

Some hormonal treatments stimulated significant increases in the chlorophyll a and total chlorophyll contents (Tables 1, 2). The highest chlorophyll a content (0.3710) was obtained in treatment B0.1 followed by BI2 (0.2989), B0.5 (0.2639) and BI0.5 (0.2556). Similar situation was found in total chlorophyll content. Higher concentrations of BAP alone decreased chlorophyll b and carotenoids content (Table 1), while the addition of IBA induced the opposite effect (Table 2), where the highest concentration of BAP (2 mg/L) in combination with IBA increased the level of photosynthetic pigments (BI2 treatment). It was not possible to find a direct link between concentrations of plant growth regulators used

**Table 2.** Effect of BAP and IBA on adventitious shoot and root formation, photosynthetic pigment, total phenolic, total flavonoid, flavanol contents and antioxidative activity of *Mentha piperita*.

| Treatment | Number of shoots per explant | Number of roots per explant | Chlorophyll a (mg/g FW) | Chlorophyll b (mg/g FW) | Total chlorophylls | Carotenoids (mg/g FW) | Total phenolics (mg/g DW) | Total flavonoids (mg/g DW) | Flavanols (mg/g DW) | Antioxidative activity (% of inhibition) |
|---|---|---|---|---|---|---|---|---|---|---|
| BH | 2.467$^{b}$ | 3.158$^{c}$ | 0.2089$^{c}$ | 0.0600$^{b}$ | 0.2689$^{b.c}$ | 0.0736$^{d}$ | 185.63$^{a}$ | 70.29$^{b.c}$ | 0.026$^{c}$ | 7.69$^{d}$ |
| BI 0.1 | 3.967$^{a.b}$ | 7.400$^{a.b}$ | 0.2175$^{b.c}$ | 0.0700$^{a.b}$ | 0.2875$^{b.c}$ | 0.0731$^{d}$ | 168.99$^{b}$ | 121.42$^{a}$ | 0.046$^{a}$ | 23.14$^{c}$ |
| BI 0.5 | 6.490$^{a}$ | 8.608$^{a}$ | 0.2556$^{a.b}$ | 0.0834$^{a.b}$ | 0.3390$^{b}$ | 0.0868$^{b}$ | 61.19$^{d}$ | 57.00$^{c}$ | 0.019$^{d}$ | 24.20$^{c}$ |
| BI 1 | 4.211$^{a.b}$ | 6.278$^{a.b.c}$ | 0.1692$^{d}$ | 0.0569$^{b}$ | 0.2261$^{c}$ | 0.0619$^{c}$ | 143.40$^{c}$ | 58.63$^{c}$ | 0.033$^{b}$ | 63.33$^{a}$ |
| BI 2 | 6.241$^{a}$ | 4.481$^{b.c}$ | 0.2989$^{a}$ | 0.1029$^{a}$ | 0.4018$^{a}$ | 0.0979$^{a}$ | 167.60$^{b}$ | 77.06$^{b}$ | 0.033$^{b}$ | 50.82$^{b}$ |
| BHA | | | | | | | | | | 56.50$^{b}$ |
| BHT | | | | | | | | | | 61.91$^{a}$ |

Values are mean of three replicates. Treatments not sharing the same letter within one column differ significantly employing parametric (Newman-Keuls) and non-parametric for No of roots and shoots (Kruskal-Walis analysis) tests.
BH-without plant growth regulators; BI 0.1-0.1 mg/L BAP + 0.1 mg/L IBA; BI0.5-0.5 mg/L BAP + 0.1 mg/L IBA; BI1-1 mg/L BAP + 0.1 mg/L IBA; BI2-2 mg/L BAP + 0.1 mg/L IBA; BHA-butylated hydroxyanisol; BHT-butylated hydroxytoluene.

and the content of photosynthetic pigments (Edelman and Hanson 1971; Karalija and Parić 2011; Karalija et al. 2016). Cytokinins as well as auxins can improve concentration of photosynthetic pigments (Verma and Sen 2008; Parsaeimehr et al. 2010; Vamil et al. 2010). Changes in the chlorophyll content, caused by plant growth regulators could be related to growth rate, primary and secondary metabolic activities (Lichtenthaler 1987) as shown in treatments B0.5, BI0.5 and BI2.

### Phenolic content and antioxidative properties

Application of BAP alone in highest concentration significantly increased production of total phenolics and all other treatments induced similar or decreased total phenolics contents. Addition of IBA in the medium decreased total phenolics content.

Among all applied treatments only BI0.1 increased flavonoid contents. Flavanols content also varied depending of treatment. A 2-fold increase on BI0.1 treatment was observed (Tables 1,2).

The effects of plant growth regulators on secondary metabolite production in *in vitro* culture systems are highly variable (Khan et al. 2008; Santoro et al. 2013), depending of the plant species. For example, BAP and IBA stimulated the production of total phenolics and flavonoids in *Thymus vulgaris* and *Origanum vulgare*, but decreased it in *Ocimum basilicum* (Karalija and Parić 2011; Karalija et al. 2016). On the other hand, BAP alone increased the total yield of essential oils and its components (menthone, menthol, pulegone, and menthofuran) in *M. piperita*, while the combination of BAP and IBA did not significantly change the production of plant secondary compounds (Santoro et al. 2013).

A single plant hormone may regulate a wide range of physiological and growth processes, or a particular process may be regulated by the action of many plant hormones (Santoro et al. 2013). Chemical changes were evident in some cases, but not in others. BAP applied alone increased total phenolics content only in highest concentration (Tables 1, 2). All combinations of BAP and IBA decreased the production of phenolic compounds when compared to control.

In the present study, the antioxidant activity of *M. piperita* extracts were determined by peroxidation of linoleic acid using the ferric thiocyanate method (FTC) and significant differences between various treatments were determined (Tables 1, 2). It was found that all the treatments were significantly different comparing to control (BH). A 6-fold increase of antioxidant activity was noticed in treatment BI1 (63.33), which was more effective than two positive probes, followed by B0.1 (56.64) and BI2 (50.82). These results indicate that these extracts can significantly inhibit the peroxidation of linoleic acid and reduce the formation of hydroperoxide, thus implying that antioxidative activity of *M. piperita* could be successfully improved by hormone type/ratio manipulation. Antioxidant activities from aromatic plants are mainly associated with the active compounds present in their tissues. But, since it is a complex mixture of various molecules this can be due to the high percentage of main constituents, but also to the synergistic and antagonistic effect between these main constituents and other constituents that can be present in small quantities (Ćavar et al. 2012). To the best of our knowledge, this is the first report of effect of plant growth regulators on antioxidative activities of *M. piperita* using FTC method, but antioxidant activity of *M. piperita* essential oils, using other methods of determination has previously been reported (Mimica-Dukic et al. 2003; Derwich et al. 2011).

### Antimicrobial activity

Results obtained in the present study revealed that the dif-

**Table 3.** Effect of BAP alone or in combination with IBA on antimicrobial activity of different *M. piperita* extracts.

| Treatment | *E. coli* | *S. abony* | *E. faecalis* | *B. spizizenii* | *A. brasiliensis* | *C. albicans* |
|---|---|---|---|---|---|---|
| BH | - | - | - | - | - | - |
| B 0.1 | - | - | - | - | 11.3 | 11.7 |
| B 0.5 | 14.0 | 13.0 | - | - | 14.0 | 11.0 |
| B 1 | - | - | - | - | 12.7 | 11.0 |
| B 2 | - | - | - | - | 12.7 | 9.5 |
| B 4 | - | - | - | - | 12.0 | 9.7 |
| BI 0.1 | 10.3 | - | - | - | 13.3 | 10.0 |
| BI 0.5 | 9.3 | - | - | - | 12.0 | - |
| BI 1 | 9.0 | - | - | - | 14.3 | 10.7 |
| BI 2 | - | - | - | - | 14.7 | 10.5 |
| Standards | | | | | | |
| Amphothericin B | 20.0 | | | | | |
| Chloramphenicol | 17.7 | | | | | |
| Nystatin | 17.0 | | | | | |

Values are mean inhibition zone (mm) ± SD of three replicates. (-) No zone of inhibition.
BH-without plant growth regulators; B 0.1-0.1 mg/L BAP; B 0.5-0.5 mg/L BAP; B 1-1 mg/L BAP; B 2-2 mg/L BAP; BI 0.1-0.1 mg/L BAP + 0.1 mg/L IBA; BI0.5-0.5 mg/L BAP + 0.1 mg/L IBA; BI1-1 mg/L BAP + 0.1 mg/L IBA; BI2-2 mg/L BAP + 0.1 mg/L IBA.

ferent tested plants extracts possess potential antibacterial activity against *E. coli* and antifungal activity against *A. brasiliensis* and *C. albicans* (Table 3). The antimicrobial activities of the all extracts showed no inhibition activity against Gram-positive strains tested (*E. faecalis*, *B. spizizenii*). Both fungi, *A. brasiliensis* and *C. albicans* appeared to be sensitive to the all tested extracts and only the Gram-negative *E. coli* was sensitive to some of them (B0.5, BI0.1, BI0.5, and BI1). The extracts of B0.5 treatments were active against Gram-negative *S. abony*. *A. brasiliensis* and *C. albicans* appeared to be the most sensitive strains followed by Gram-negative *E. coli*. Our results indicate that plant growth regulators can enhance antimicrobial activity since control plants, showed no activity against tested microbial strains. Similar results were obtained, by other authors, who reported antimicrobial activity of different *Mentha* species (oils) (Abdel Moneim et al. 2011; Basheer and Abdullah 2013). Numerous studies have confirmed that plant growth regulators in medium can affect the antibacterial properties of plants (Gibbons 2004; Pitta-Alvarez et al. 2008; Karalija et al. 2016).

## Conclusions

IBA and BAP alter secondary metabolite production in sterile cultures by changing both primary and secondary metabolism of plants. This study showed that application of plant growth regulators is a good option for stimulating secondary metabolites production, but selection of the right plant hormone and its optimal concentrations are crucial for increasing secondary metabolite production and bioactivity of plant extracts.

## References

Abdel Moneim ES, Sitana EA, Awad M, Abdel R (2011) Phytochemical analysis of local spearmint (*Mentha spicata*) leaves and detection of the antimicrobial activity of its oil. J Microbiol Res 1(1):1-4.

Arikat NA, Jawad FM, Karam NS, Shibli RA (2004) Micropropagation and accumulation of essential oils in wild sage (*Salvia fruticosa* Mill.). Sci Hortic 100:193-202.

Awale S, Shrestha SP, Tezuka Y, Ueda J, Matsushige K, Kadota S (2005) Neoflavonoids and related constituents from Nepalese propolis and their nitric oxide production inhibitory activity. J Nat Prod 68:858-864.

Baliga MS, Rao S (2010) Radioprotective potential of mint: A brief review. J Cancer Res Ther 6:255-262.

Basheer AA, Abdullah AA (2013) Antimicrobial activity of the aqueous extract of mint plant. SJCM 2(3):110-113.

Benkova E, Hejatko J (2009) Hormone interactions at the root apical meristem. Plant Mol Biol l69:383-396.

Ćavar S, Maksimović M, Vidic D, Parić A (2012) Chemical composition and antioxidant and antimicrobial activity of essential oil of *Artemisia annua* L. from Bosnia. Ind Crops Prod 37:479-485.

Derwich E, Chabir R, Taouil R, Senhaji O (2011) *In vitro* antioxidant activity and GC/MS studies on the leaves of *Mentha piperita* (Lamiaceae) from Morocco. IJPSDR 3(2):130-136.

Dias MC, Almeida R, Romano A (2002) Rapid clonal multiplication of *Lavandula viridis* L'Hér through in vitro axillary shoot proliferation. Plant Cell Tissue Organ Cult 68:99-102.

Edelman J, Hanson AD (1971) Sucrose suppression of chlorophyll synthesis in carrot callus culture. Planta 98:150-156.

Farooqi AHA, Khan A, Sharma S (2003) Effect of kinetin and chlormequat chloride on growth, leaf abscission and essential oil yield in *Mentha arvensis*. Ind Perf 47(4):359-363.

Fukaki H, Tasaka M (2009) Hormone interactions during lateral root formation. Plant Mol Biol l69:437-449.

Gadzovska S, Maury S, Delaunay A, Spasenoski M, Joseph C, Hagège D (2007) Jasmonic acid elicitation of *Hypericum perforatum* L. cell suspensions and effects on the production of phenylpropanoids and naphtodianthrones. Plant Cell Tiss Organ Cult 89:1-13.

Gautam MK, Gangwar M, Singh A, Rao CV, Goel RK (2012) *In vitro* antioxidant properties of *Murraya paniculata* Linn. leaves extract. Inventi Rapid: Ethnopharm 2012:1-3.

Gibbons S (2004) Anti-staphylococcal plant natural products. Nat Prod Rep 21:263-277.

Guedon DJ, Pasquier BP (1994) Analysis and distribution of flavonoid glycosides and rosmarinic acid in 40 *Mentha piperita* clones. J Agric Food Chem 42:679-684.

Hirata T, Murakami S, Ogihara K, Singa T (1990) Volatile monoterpenoid constituents of the plantlets of *Mentha spicata* produced by shoot tip culture. Phytochemistry 29:493-496.

Holm G (1954) Chlorophyll mutations in barley. Acta Agric Scand 4:457-471.

Karalija E, Neimarlija D, Cakar J, Paric A (2016) Elicitation of biomass and secondary metabolite production, antioxidative and antimicrobial potential of basil and oregano induced by BA and IBA application. EJMP 14(4):1-11.

Karalija E, Parić A (2011) The effect of BA and IBA on the secondary metabolite production by shoot culture of *Thymus vulgaris* L. Biol Nyssana 2(1):29-35.

Kavina J, Gopi R, Panneerselvam R (2011) Traditional and nontraditional plant growth regulators alter the growth and photosynthetic pigments in *Mentha piperita* Linn. IJES 1:124-134.

Khan T, Krupadanam D, Anwar SY (2008) The role of phytohormone on the production of berberine in the calli cultures of an endangered medicinal plant, turmeric (*Coscinium fenestratum* I.). AJB 7(18):244-3246.

Kukreja AK, Dhawanop, Mathur AK, Ahuja PS, Mandal S (1991) Screening and evaluation of agronomically useful somaclonal variations in Japanese mint (*Mentha arvensis* L.). Euphytica 53:183-191.

Larrauri JA, Gosimni I, Martín-Carrón N, Rupérez P, Saura-Calixto F (1996) Measurement of health-promoting properties in fruit dietary fibres, antioxidant capacity, fermentability, and glucose retardation index. J Sci Food Agric 71:515-519.

Lichtenthaler HK (1987) Chlorophylls and carotenoids, the pigments of photosynthetic biomembranes. In Douce R, Packer L, eds, Methods in Enzymology. Academic Press, New York, 350-382.

Mimica-Dukic N, Bozin B, Sokovic M, Mihajlovic B, Matavulj M (2003) Antimicrobial and antioxidant activities of three *Mentha* species essential oils. Planta Med 69:413-419.

Mittler R (2002) Oxidative stress, antioxidants and stress tolerance. Trends Plant Sci 7(9):405-410.

Murashige T, Skoog FA (1962) Revised medium for rapid growth and bioassay with tobacco tissue culture. Physiol Plant 29:247-255.

Nenadis N, Wang LF, Tsimidou M, Zhang HY (2004) Estimation of scavenging activity of phenolic compounds using the $ABTS^{+}$ assay. J Agric Food Chem 52:4669-3674.

Palazon J, Bonfil M, Cusido RM, Pinol MT, Morales M (1994) Effects of auxin and phenobarbital on morphogenesis and production of digitoxin in *Digitalis* callus. Plant Cell Physiol 36:247-252.

Pal RS, Ariharasivakumar G, Girhepunje K, Ashutosh U (2009) *In vitro* antioxidative activity of phenolic and flavonoid compounds extracted from seeds of A*brus precatorius*. Int J Pharm Pharm Sci 1:136-140.

Parr AJ (1989) The production of secondary metabolites by plant cell cultures. J Biotech 10:1-26.

Parsaeimehr A, Sargsyan E, Javidnia K (2010) A comparative study of the antibacterial, antifungal and antioxidant activity and total content of phenolic compounds of cell cultures and wild plants of three endemic species of ephedra. Molecules 15(3):1668-1678.

Pitta-Alvarez SI, Medina-Bolivar F, Alvarez MA, Scambatto AA, Marconi PL (2008) *In vitro* shoot culture and antimicrobial activity of *Berberis buxifolia* Lam. In vitro Cell Dev Biol Plant 44:502-507.

Porra R, Thompson W, Kriedemann P (1989) Determination of accurate extinction coefficients and simultaneous equations for assaying chlorophylls a and b extracted with four different solvents: verification of the concentration of chlorophyll standards by atomic absorption. J Biochem Mol Biol Biophys 975:384-394.

Qian J, Guiping L, Xiujun L, Xincai H, Hongmei L (2009) Influence of growth regulators and sucrose concentrations on growth and rosmarinic acid production in calli and suspension cultures of *Coleus blumei*. Nat Prod Res 23(2):127-137.

Rao SR, Ravishankar GA (2002) Plant cell cultures: chemical factories of secondary metabolites. Biotechnol Adv 20:101-153.

Rech EL, Pires MJP (1986) Tissue culture propagation of *Mentha* sp. by use of axillary buds. Plant Cell Rep 5:17-18.

Santoro MV, Nievas F, Zygadlo J, Giordano W, Banchio E

(2013) Effects of growth regulators on biomass and the production of secondary metabolites in peppermint (*Mentha piperita* L.) *in vitro*. AJPS 4:49-55.

Scravoni J, Vasconcellos MC, Valmorbida J, Ferri AF, Marques MOM, Ono EO, Rodrigues JD (2006) Rendimento e composicao química do oleo essencial de *Mentha piperita* L. submetida a aplicacoes de giberelina e citocinina. Rev Bras Pl Med 8:40-43.

Sean S, Lee DDS, Wu Zang MD, Yiming Li DDS (2004) The antimicrobial potential of 14 natural herbal dentifrices. J Am Dent Assoc 135:1133-1141.

Sharafzadeh S, Zare M (2001) Influence of growth regulators on growth and secondary metabolites of some medicinal plants from Lamiaceae family. Adv Environ Biol 5(8):2296-2302.

Shukla YN, Farooqi AHA (1990) Utilization of plant growth regulators in aromatic plant production. Curr Res Med Arom Plants 12:152-157.

Stoeva T, Iliev L (1997) Influence of some phenylurea cytokinins on spearmint essential oil composition. Bulg J Plant Physiol 23(3-4):66-71.

Sunandakumari C, Martin KP, Chithra M, Sini S, Madhusoodanan PV (2004) Rapid axillary bud proliferation and *ex vitro* rooting of herbal spice, *Mentha piperita* L. Ind J Biotechnol 3:108-112.

Tapiero H, Tew KD, Ba N, Mathé G (2002) Polyphenols: do they play a role in the prevention of human pathologies? Biomed Pharmacother 56:200-207.

Taylor RSL, Manandhar NP, Hudson JB, Towers GHN (1995) Screening of selected medicinal plants of Nepal for antimicrobial activities. J Ethnopharmacol 546:153-159.

Vamil R, Aniat-ul-Haq Agnihotri RK (2010) Plant growth regulators as effective tool for germination and seedling growth for *Bambusa arundinaceae*. RJAS 1(3):233-236.

Verma P, Sen NL (2008) The impact of plant growth regulators on growth and biochemical constituents of coriander (*Coriandrum sativum* L.). J Herbs Spices Med Plants 14(3/4):144-153.

Waterhouse AL (2001) Determination of total phenolics. In Wrolstad RE, Acree TE, An H, Decker EA, Penner MH, Reid DS, Schwartz SJ, Shoemaker CF, Sporns P, eds, Current Protocols in Food Analytical Chemistry. John Wiley & Sons, New York.